



รายงานวิจัยฉบับสมบูรณ์

โครงการ พลศาสตร์ของโครงสร้างเนื่องจากกลุ่มของยานพาหนะเคลื่อนที่ บนพื้นผิวแบบสุ่ม

โดย นายปฤษทัศว์ ศีตะปันย์ และคณะ

พฤศจิกายน 2548

รายงานวิจัยฉบับสมบูรณ์

โครงการ พลศาสตร์ของโครงสร้างเนื่องจากกลุ่มของยานพาหนะเคลื่อนที่ บนพื้นผิวแบบสุ่ม

คณะผู้วิจัย

สังกัด

1. นายปฤษทัศว์ ศีตะปันย์

มหาวิทยาลัยนเรศวร

2. ศาสตราจารย์สมชาย ชูชีพสกุล มหาวิทยาลัยเทคโนโลยีพระจอมเกล้ำธนบุรี

สนับสนุนโดยทบวงมหาวิทยาลัย และสำนักงานกองทุนสนับสนุนการวิจัย

(ความเห็นในรายงานนี้เป็นของผู้วิจัย ทบวงฯ และสกว. ไม่จำเป็นต้องเห็นด้วยเสมอไป)

Table of Contents

Table of Cor	ntents	ii
List of Table	es	iv
List of Figur	res	V
Abstract (Th	ai)	viii
Abstract (En	Abstract (English)	
Executive Su	ummary	xi
Chapter 1	Introduction	
	1.1 Significance and Motivation	1
	1.2 Objectives	2
	1.3 Literature Review	3
	1.4 Conclusions from Literatures	9
	References	9
Chapter 2	Random Roughness and Interface Models for Multi-Axle Moving	
	Vehicles	
	2.1 Introduction	13
	2.2 Filtered White Noise and Existence of Derivatives of Filter	red
	Processes	13
	2.3 Roughness Models	18
	2.3.1 Dimensioned Spatial Process	18
	2.3.2 Dimensioned Temporal Process	21
	2.3.3 Nondimensionalization of $h_d(t_d)$ and $W_d(t_d)$	23
	2.3.4 Nondimensionalization of Time	25
	2.3.5 Modeling Actual Roughness	28
	2.4 Interface Models	29

	2.5 Modeling Lags	36
	2.6 Conclusions	40
	References	40
Chapter 3	Dynamic Responses of A Two-Span Beam Subjected to High	Speed
	2DOF Sprung Vehicles	
	3.1 Introduction	43
	3.2 Coupled vehicle-structure system equations in state space	43
	3.3 Parametric study and results	47
	3.3.1 Effect of span passage rate	47
	3.3.2 Effect of axle arrival rate	48
	3.3.3 Effect of number of axles (interfaces)	52
	3.3.4 Effect of fundamental frequencies of vehicle	56
	3.4 Conclusions	56
	References	57
Chapter 4	Conclusions	58
Outputs		60
Appendix		61

List of Tables

Table 3.1 Vehicle axle arrival rate and span passage rate for high speed	48
Table 3.2 The maximum beam responses when f_a is in resonance with f_1 for two different suspension configurations	52
Table 3.3 The maximum beam responses when f_a is in resonance with f_2 for two different suspension configurations	53

List of Figures

Figure 2.1 : Square of the Absolute Value of the Transfer Function between h_d and W_d for the First Order Filter given by Equation 2.1	15
Figure 2.2 : Square of the Absolute Value of the Transfer Function between \dot{h}_d/r_f and W_d in Equation 2.1	15
Figure 2.3 : Square of the Absolute Value of the Transfer Function between h_d and W_d for the Second Order Filter given by Equation 2.6	17
Figure 2.4 : PSD and Autocovariance of $h_d(x_d)$ in Dimensioned Spatial Domain	19
Figure 2.5 : Spatial Autocorrelation Function of $h_d(x_d)$	20
Figure 2.6 : PSD and Autocovariance of Temporal Process $h_d(t_d)$	21
Figure 2.7 : Temporal Autocorrelation Function of $h_d(t_d)$	23
Figure 2.8 : PSD and Autocovariance of Nondimensional $h(t_d)$	24
Figure 2.9 : PSD and Autocovariance of Nondimensional $h(t)$ in Nondimensional Time Domain	26
Figure 2.10 : Autocorrelation Function of Nondimensional Process $h(t)$ with a Nondimensional Time Lag	27

Figure 2.11: Modeling Actual Roughness	28
Figure 2.12: SDOF System with Linear Spring Interface with Elastic Beam	30
Figure 2.13: SDOF System with Parallel Spring and Dashpot Interface Elements with Elastic Beam	32
Figure 2.14: SDOF System with Rigid Mass and Parallel Spring and Dashpot as Interface Elements with Elastic Beam	34
Figure 3.1 : Models of coupled vehicle structure system: a. two of 2DOF vehicle model, b. eight of 2DOF vehicle model	45
Figure 3.2: Time history of expected values and variances of displacement at midspan	49
Figure 3.3: Time history of expected values and variances of moment at midspan	50
Figure 3.4: Time history of expected values and variances of moment at interior support	50
Figure 3.5: Time history of expected values and variances of shear at 0.95L	51
Figure 3.6: Time history of expected values and variances of beam acceleration at midspan	51
Figure 3.7 : Time history of expected values and variances of displacement at midspan	53

Figure 3.8: Time history of expected values and variances of	
moment at midspan	54
Figure 3.9: Time history of expected values and variances of	
moment at interior support	54
Figure 3.10 : Time history of expected values and variances of shear at 0.95L	55
Figure 3.11: Time history of expected values and variances of	
beam acceleration at midspan	55

บทคัดย่อ

ในปัจจุบัน ความสนใจของการขนส่งภาคพื้นดินด้วยความเร็วสูงมีมากขึ้น การศึกษาระบบยานพาหนะ-โครงสร้างที่ ความเร็ว 240 ถึง 480 กิโลเมตรต่อชั่วโมงจึงมีความจำเป็น แบบจำลองของระบบที่พิจารณาในงานวิจัยนี้ประกอบด้วย แบบจำลองยานพาหนะที่มีการรับการกระเทือนแบบแพสซีฟ และมีหลายเพลา แบบจำลองความขรุขระพื้นผิวแบบสุ่ม และแบบจำลองโครงสร้างยืดหยุ่นเชิงเส้น งานวิจัยนี้นำเสนอแนวคิดในการสร้างแบบจำลองระบบ การวิเคราะห์ ระบบ และการออกแบบระบบ

แบบจำลองของกลุ่มยานพาหนะแบบ 2DOF ที่มีความเร็วคงที่และมีระยะระหว่างเพลาคงที่ถูกนำมาใช้ใน งานนี้ และมีการพิจารณายานพาหนะควบคู่ไปกับโครงสร้างที่ตำแหน่งของเพลา จุดเชื่อมต่อระหว่างยานพาหนะและ โครงสร้างเป็นตัวกำหนด การปรากฏของเทอมพาราเมตริกซ์ในเมตริกซ์ของระบบ ถ้ามวล-สปริง-ตัวหน่วงเป็น ตัวเชื่อมทุกเมตริกซ์ของระบบจะมีเทอมพาราเมตริกซ์ ถ้าสปริงเป็นตัวเชื่อมเทอมพาราเมตริกซ์จะเกิดขึ้นเฉพาะใน สตีฟเนสเมตริกซ์

ความขรุขระพื้นผิวถูกจำลองขึ้นด้วยสเตชันนารีแรนดอมโพรเซส แบบจำลองมาคอฟเวกเตอร์ที่มีจุดเชื่อมต่อ หลายจุดจะถูกสร้างขึ้น คานสองช่วงถูกใช้เป็นแบบจำลองโครงสร้างโดยมีความถี่ธรรมชาติ รูปร่างโหมด และค่า ความหน่วงเป็นตัวกำหนด ตัวแปรต่าง ๆ ในระบบจะถูกทำเป็นตัวแปรไร้หน่วย และสมการการเคลื่อนที่ของระบบ ควบคู่ยานพาหนะ-โครงสร้างจะถูกเขียนในสเตทฟอร์ม สมการจะถูกแยกออกเป็น 2 สมการ สมการแรกคือ สมการ เวกเตอร์ของค่าเฉลี่ย อีกสมการหนึ่งคือ สมการแมตริกซ์ของค่าความแปรปรวน สมการเวกเตอร์ของค่าเฉลี่ยจะมีเทอม พาราเมตริกซ์และมีตัวแปรแบบกำหนดได้ สมการเมตริกซ์ความแปรปรวนจะมีเทอมพาราเมตริกซ์และมีตัวแปรแบบ สุ่ม ผลตอบสนองของโครงสร้างจะถูกหารด้วยค่าสูงสุดของผลตอบสนองสถิตสาสตร์ ดังนั้น ค่าเฉลี่ยและค่าความ แปรปรวนจะมีเพลเดอร์กำลังขยายพลสาสตร์จะถูกคำนวณขึ้น

ผลของพารามิเตอร์ต่าง ๆ ที่มีต่อค่าเฉลี่ยและค่าความแปรปรวนของผลตอบสนองจะถูกศึกษาขึ้น อัตราใน การข้ามช่วงคานและอัตราการมาถึงของเพลาเป็นตัวแปรสองตัวที่มีผลต่อผลตอบสนองมาก ที่ความเร็วสูงอัตราการ มาถึงของเพลาอาจเท่ากับความถี่พื้นฐานของโครงสร้างและจะก่อให้เกิดค่าเฉลี่ยของผลตอบสนองที่มีค่าสูง ผลของ จำนวนของเพลาจะมีการศึกษาด้วย ผลของความแตกต่างของความขรุขระพื้นผิวที่มีต่อผลตอบสนองของระบบควบคู่ ยานพาหนะ-โครงสร้างที่มีความเร็วสูงได้ถูกนำเสนอ

Abstract

In recent years, interest in high speed ground transportation has encouraged the study of vehicle-guideway systems that can operate at 240 to 480 kph (150 to 300 mph). The system considered here consists of a multiple axle, passive suspension vehicle model, random surface roughness model and a linear elastic structure model. This research provides insights on system modeling, system analysis and system design.

A series of 2DOF vehicle model with a constant velocity are used and a fixed wheelbase or distance between axles. The vehicle is coupled with the structure at the spatial positions of the axles. The interface between the vehicle and the structure determines the appearance of parametric terms in system matrices. If a mass-spring-dashpot interface is used, then all the system matrices are parametric. If a spring interface is used, then only the stiffness matrix is parametric.

Surface roughness is modeled as a stationary spatial random process. A Markov vector model that includes multiple interface points is formulated.

A two-span beam is used as a structure model. It is defined in the modal domain by natural frequencies, mode shapes and damping values. All vehicle, roughness and structure parameters are nondimensionalized and the equations of motion of the vehicle-guideway coupled system are written in state form. Then, by taking expectations, stochastic state equation is decoupled into two matrix equations. One is for the evolutionary mean vector and the other is for the evolutionary covariance matrix. The matrix equation for the evolutionary mean vector has parametric and deterministic additive excitation. The equation for the evolutionary covariance matrix has parametric and random additive excitation. Structural responses are normalized by maximum static responses, so the evolutionary means and variances of dynamic amplification factors are computed.

Effects of parameters on mean and variance responses are studied. The nondimensional span passage rate and the nondimensional axle arrival rate are two parameters that affect responses significantly. At very high velocities, the axle arrival rate can be equal to fundamental frequencies of the structure, causing large mean values of responses. Effects of the number of axles are also studied. Effects of different surface

roughnesses, including those corresponding to current surface roughness specifications, on the responses of the high speed vehicle-guideway coupled system are presented.

Executive Summary

Dynamics of high speed vehicle-guideway coupled systems is an important problem for future ground transportation systems. The system considered here consists of a multiple axle, passive suspension vehicle model, random surface roughness model and a linear elastic structure model. This research provides insights on system modeling, system analysis and system design.

A series of 2DOF vehicles were used as models. A distance between axles, a socalled wheelbase, was fixed to be equal for all axles. The vehicle-structure interface model determines the appearance of parametric excitation in system matrices. If an unsprung mass-dashpot-spring is used, all matrices have parametric terms. If a spring is used, then only the stiffness matrix contains parametric terms.

Linear filter equations are used to incorporate roughness into the system state equations. The roughness process and perhaps its derivatives should have a finite variance. The interface model determines the order or number of filters required. If a mass-spring-dashpot is used as interface, three first order linear filters are needed for the first and second derivatives of roughness processes to exist and have finite variance. If a spring is used, only one first order linear filter is sufficient.

Multiple axle vehicles have a kinematic filtering effect on system excitation. Multiple interface points are taken into account by adding a first order filter to model an excitation with lag. The filter equations are excited by correlated white noises in order to have an appropriate zero-time-lag cross-correlation between any two roughness processes.

High speed vehicles will operate on multiple-span, elevated guideways. A two-span beams, used a structure model herein, is a possible choice. The formulation presented uses a modal domain model of the structure. Mode shapes of a two-span symmetric beam are either antisymmetric or symmetric.

Nondimensional parameters of the system are defined. They are wheelbase-to-span length ratio (ℓ/L) , vehicle-to-guideway mass ratio $(M/\overline{m}L)$, nondimensional velocities such as span passage rate (f_v) and axle arrival rate (f_a) , suspension parameters (f_k) and f_c , and modal damping ratio (ξ) .

A matrix first order linear stochastic differential equation was formed and, taking expectations, two deterministic first order equations are obtained: evolutionary mean vector equation and evolutionary covariance matrix equation. The first has parametric and deterministic additive excitation. The second equation has parametric and random additive excitation.

Effects of a sudden change of surface, smooth and rigid to rough and flexible, were also studied. Amplification of the beam responses varies for different types of responses. Such surface change does not affect the expected values of beam responses significantly. The sudden change affects variance of vehicle responses substantially. Variances of vehicle responses overshoot after a surface change then decay to stationary values. Vehicle damping affects this phenomenon; vehicle variances spike higher if a vehicle is highly damped.

There are two important parameters that have strong effects on evolutionary mean and variance responses. One is the nondimensional span passage rate, f_{ν} . Variances of beam responses become larger with increasing f_{ν} . Expected values of beam responses tend to increase also, in most cases, but they also depend on ℓ/L . The other significant parameter is the axle arrival rate, f_a . At high speed, for reasonable values of ℓ/L and $M/\overline{m}L$, the axle arrival rate, f_a , can match the first or even second natural frequency of the beam. Therefore, the moment at the interior support which is dominated by the secondmode shape (first symmetric mode shape), may be significantly amplified. Expected values of dynamic amplification of beam responses can be up to 1.40. Moreover, variances of beam responses seem to have large contribution to the RMS responses if current surface roughness specifications are used. Roughness can cause standard deviations of dynamic amplification up to 0.20. It is found that one specific value of a nondimensional parameter may cause a maximum in one responses while a different value may cause a maximum in another response.

CHAPTER 1

INTRODUCTION

1.1 Significance and Motivation

High speed rail (HSR) with speed between 200 and 350 km/h has a crucial role to transport people. It has been of increasing interest nowadays and has great advantages for third world countries. China's largest city, Shanghai, is going to launch the first commercial maglev train of the world. With the power of electromagnetic levitation, magnetic levitated (maglev) vehicle can convey passengers up to the speed of 430 km/h. Using German technology maglev line of 30 km at a cost of \$1.2 billion has been in service since summer 2003. It can carry passengers from Shanghai's financial district to its international airport in eight minutes, while a car usually takes from 45 minutes to 1 hour. Maglev supporters expect that the Shanghai's maglev project would lead to other HSR projects worldwide. In Thailand, the plan of building HSR was started in 1995 when the National Economic and Social Development Board (NESDB) hired Wilbur Smith Associates to do a feasibility study of HSR interconnecting the second Bangkok international airport (Suvarnabhumi) and Rayong. However, recently the Ministry of Transport has planned to provide budget of 18.5 million baths in 2004 for a feasibility study of 260 km-HSR from Bangkok to Nakhon Ratchasima. Hence, it is important to provide some aspects of system-modeling, -analysis, and -design for Thai engineers.

Engineers have traditionally studied vehicle and structure systems separately. Civil engineers might consider a vehicle load as a moving point load because it is the easiest way to analyze a structure. It is applicable if the inertia of the vehicle is small [31, 32, 38]. Today it is possible to analyze models that capture the interaction between a vehicle and a structure. System excitations may be either deterministic or random. Normally the weight of the cars is considered deterministic. Random excitation may come from surface irregularities. Surface irregularities in turn affect ride quality and structural response.

The principal objective of this research is to quantify the effects of vehicle and structure parameters on the dynamic behavior of vehicle-structure coupled systems.

The goal is to provide guidelines for structural design by nondeterministic approach. By modeling vehicle-structure coupled system, parametric excitation, deterministic excitation and random excitation can be taken into account. Results from system analysis are statistical moments of the system. One is the evolutionary mean vector and the other is the evolutionary covariance matrix.

In this research nondimensional parameters are introduced, thus formulations can be simply applied to any unit systems. Responses are presented in terms of dynamic amplification factor (DAF) which is defined as dynamic response divided by maximum static response. The concepts can be applied to any systems, i.e., carbridge, train-railway, high speed rail system and magnetic levitated vehicle depending on range of velocities and interface between vehicle and structure.

It is essential for designers to know about system responses at resonant condition, especially at high speed. Excessive vibration imposes a great danger. It may lead to disastrous accident. Parameters involving in how resonant condition occurs are span crossing rate, axle arrival rate [34], fundamental frequencies of vehicle and structure, damping properties of vehicle and structure, and mass ratio.

1.2 Objectives

- To study dynamic behaviors of vehicle-structure coupled system, particularly an interaction force and amplitude of responses at resonant condition.
- To study effects of vehicle parameters such as vehicle velocities, number of axles, axle-arrangement and mass of vehicle to mean values and variances of structural responses.

Vehicle velocities – At high speed, axle arrival rate can cause resonance at the higher modal frequency and it can strongly amplify structural response corresponding to that modal frequency such as negative bending moment at the interior support [34]. At lower speed, especially when wheelbase to span ratio is less than 0.5, the same phenomena occurs. Hence, it is interesting to investigate how it affects amplitude of responses.

Number of axles – When more axles (interface points) are added to the vehicle, load configuration is changed from two-point load to eight-point load (maglev can have up to eight magnetic pads). Maximum response may be lower since

it approaches a uniform load. However, how many interface points is optimal is still questionable.

Axle-arrangement and mass ratio – This parameter can be studied as follow:

<u>Truck</u> – Typical truck weight 20 to 40 ton crossing bridge with speed 50-80 km/h, i.e., at a bridge across the Chaopraya river in Nakhon Sawan vibration is sensible while trucks traverse it.

<u>Train</u> – Normally a train has two parts, locomotives at the front and at the end, and carriages in the middle. Locomotives usually are much heavier than carriages. Different mass distribution in train can affect structural responses.

<u>Intercity rapid transit</u> – Configuration of this kind of vehicle normally is three or four bogies. It travels with speed higher than the other two previously mentioned cases. This system was partly investigated [34]. Only two parameters, span crossing rate and axle arrival rate were studied. Other vehicle parameters that can affect amplitude of structural responses will be studied.

 To study effects of surface roughness to mean values and variances of system responses. By the nature of surface roughness it does not have a dominant peak. It has, however, an additional amplification to system responses. At low speed it affects mainly to passenger ride comfort. It may not be as crucial to the structure. At high speed surface roughness must be considered in the design.

1.3 Literature Review

Since the 1960s, extensive research on coupled vehicle-structure systems has been done in the United States and Europe. Early studies of beam-vehicle system dynamics concentrated on a simply supported beam traversed by a simple vehicle model [1, 9, 39]. Investigations arising out of AASHTO road test [10] expanded studies to three span continuous beams with more complicated vehicle models. More recently, orthotropic plate theory has been applied to dynamic analyses by Marchesiello, et al. [26]. Most of these studies have used simple vehicle models and equations of motion have been solved by numerical integration. Many researchers, Lin and Trethewey [24], Henchi, et al. [16, 17] and Hino, et al. [18] used the finite element method to model and analyze structures. Several others employed Fourier series and Fourier transforms [37]. The state space approach was also used by many groups including Harrison and Hammond [11, 12, 13, 14], Yadav [41] and Narayanan

, et al. [28]. In general, vehicle-structure interaction is significant. Law, et al [4, 19, 20, 21, 44] tried to obtain the real interaction force when a vehicle traverses a structure and studied moving force identification both experimentally and analytically using both time domain and frequency domain approaches. The modal properties of the bridge were measured by impulse tests with an instrumented hammer [10] and compared with a simple mathematical model. Of course the real interaction force is not constant, it is affected by surface roughness, vehicle suspension and stiffness of the structure. Other work on identifying interaction force can be found in references [5, 25]. A few papers related to analysis of roughness-vehicle-structure coupled systems are briefly reviewed here:

Marchesiello, et al. [26] used a seven-DOF vehicle model, including pitch, roll and heave motions for an analysis of dynamic interaction of multi-span continuous bridges modeled by isotropic plates with MDOF vehicles moving at constant speed. Modal superposition was adopted and vehicle-bridge interaction was computed. Bridge surface irregularities were modeled as an ergodic stationary Gaussian random process with cut-off spatial frequencies. A technique to implement flexural and torsional modes of structure was presented. Contribution of torsional modes on displacement at midspan and the importance of surface roughness and vehicle speed were pointed out. A three span continuous bridge was analyzed by finite element method as an example. The result showed that the dynamic amplification factor was very sensitive to the damping of the vehicle suspension and to the roughness of the road. At the center of the bridge, dynamic amplification factor of beam deflection can increase from 1.05 to 1.35, when roughness was included for relatively low suspension damping. They found that for a realistic range of velocities, the span crossing frequency (velocity divided by span length) does not cause resonance in beam structures.

Smith, Gilchrist and Wormley [36] develop analyses to determine the dynamic performance of vehicles interacting with single and multiple span structures. They used a two-dimensional rigid body vehicle that is capable of heave and pitch motion and used the modal analysis technique to derive the finite multiple-span guideway-vehicle model. Studies indicated that the largest dynamic amplification factor occurs at vehicle crossing frequencies (also called nondimensional velocity) $v_c \sim 2$ ($v_c = v/\ell_s f$, v is vehicle speed, f is natural frequency, ℓ_s is span length). This basic

observation is made by Timoshenko, et al. [39], Biggs [1] and Fryba [9], and it appears in many other references [8, 36]. For $v_c < 1$ guideway damping has very little influence to the responses. For larger values of $v_c > 1$ guideway dynamics become important for all of case studies. So for high-speed (150-300 mph) systems a dynamic analysis is required. They note that: 1) For advanced transportation systems, which must provide good ride quality, the complete vehicle-guideway system must be considered in design. 2) Improvements in both guideway design and vehicle performance influence the overall system material requirements and economic feasibility significantly.

Doran and Mingori [8] examined two approaches for analysis of vehicle-guideway systems. The first approach was based on a combined analytical and numerical study of the exact governing equations (fully coupled equations). The second approach was based on the analytical solution of a set of approximate governing equations (partially coupled equations). This approach takes advantage of the fact that a requirement for acceptable vehicle acceleration is a small fraction of g to reduce complications of the governing equation. This study showed that if ride comfort constraints were satisfied (maximum vertical acceleration < 0.1 g), maximum accelerations based on partially coupled equations agree closely with those based on fully coupled equations. Note that in this work vehicle was modeled as SDOF and only a simply supported beam was considered. For high-speed and more complex vehicle/guideway coupled systems using partially coupled equations may not be sufficient.

Cai, Chen, Rote and Coffey [3] studied dynamic interactions between a maglev vehicle and guideway. The vehice model, two suspensions and two masses (primary and secondary), was used. Their results showed that dynamic interaction of vehicle and guideway had little influence on the secondary suspension at the given parameter. The effect on guideway displacement was smaller for $v/v_c = 0.25$ than for $v/v_c = 0.5$, however the acceleration of the primary suspension was greater for $v/v_c = 0.25$ than for $v/v_c = 0.5$. With other parameters fixed, the ratio of vehicle mass to guideway mass had less influence on vehicle than on guideway displacement. Only guideway displacements were computed, other important responses such as moment were not included.

Henchi, Fafard, Dhatt and Talbot [16] presented an exact dynamic stiffness formulation using finite element approximation to study the dynamic behavior of multispan beams under moving loads. The modal technique was used with an FFT algorithm to obtain the dynamic responses of continuous bridges. Three examples were considered: free vibrations of a multispan beam, a single span beam under a convoy of moving loads and the three span beam under a moving force. In this work vehicle/structure interaction was not considered. In later work [17] they presented an algorithm to solve the coupled dynamic system using a modal superposition method for the bridge and the physical components for the vehicles. The vehicles were modeled as a linear discrete mass-spring-damper system. The road roughness was also taken into account through the power spectral density. The numerical examples studied 2D and 3D vehicles traveling on a bridge modeled from simple supported beam and plate. The results obtained from the proposed formulation (using the central difference method and inverse of pseudo-static mass matrix) were in agreement with those reported in the past work [2, 15]. Several of simple numerical examples were used to test efficiency of the algorithm, there was no parametric study.

Some aspects of vehicle-structure and surface roughness modeling are presented in [33]. Surface roughness can have deterministic or stochastic (random process) models. The stochastic model may be either stationary or non-stationary and it may be formulated in a time or frequency domain. Several models are defined for the interface between a multi-car vehicle and structure. A Markov vector model that includes multiple interface points is formulated.

In [34, 35] one-car and three-car systems with a constant velocity and a fixed wheelbase are used as vehicle models. The vehicle is coupled with the structure at the spatial positions of the axles. A series of two-span beams is used as a structure model. It is defined in the modal domain by natural frequencies, mode shapes and damping values. Effects of parameters on mean and variance responses are studied. The nondimensional span passage rate and the nondimensional axle arrival rate are two parameters that affect responses significantly. At very high velocities, the axle arrival rate can be equal to fundamental frequencies of the structure, causing large mean values of responses. Other parameters are still needed to be explored.

Liang, Zhu and Cai [23] presented dynamic analysis of the vehicle-subgrade model of a vertical coupled system. The interactions between the vehicle running quality and the subgrade design parameters were investigated. They used the six-

DOF, two at the center of mass and one at each wheel as a vehicle model. Quadrangle finite elements were used to model track and subgrade. Modal analysis and the Newmark- β method were performed. Elastic deformation of base surface was computed for various subgrade design parameters. It was found that if the foundation stiffness was given in, the range De \geq 10 MPa, the elastic deformations of base structure were in the range of 1.2-3.7 mm.

Yau, We and Yang [42] studied impact response of bridges with elastic bearings to moving point loads. Elastic bearings were often adopted as base isolators in bridge engineering to prevent the damage from severe earthquake. The span length of the beam was assumed to be no greater than twice the interval between two consecutive moving loads. It was found that the resonance response for the damped beam remained practically constant regardless of the number of moving loads passed the beam unlike the undamped case. It was concluded that the elastic bearing may increase the response of the beam under most resonance conditions. The more flexible the elastic bearings, the larger the response of the beam is.

Degrande and Schillemans [6] presented the experimental data of the high-speed train track between Brussels and Paris, free field vibrations and track response were measured during the passage of a Thalys high-speed train at speeds varying between 223 and 314 km/h. This data set can be used for the validation of numerical prediction models for train-induced vibrations.

Verichev and Metrikine [40] examined the stability of vibration of a bogic uniformly moving along a Timoshenko beam on viscoelastic foundation. The bogic was modeled by a spring and a dashpot connected in parallel. They showed that when the velocity of the bogic exceeds the minimum phase velocity of waves in the beam, the vibration of the system may become unstable (the amplitude of vibrations grow exponentially in time). They also found that the stability of the model depended on the damping in the supports and the mass of the bogic bar was the least influential factor.

Zheng and Fan presented the derivation of the governing equations for the stability of vibration of a train-and-rail coupling system. The train consists of a convoy of two-axle wagons. Each axle was modeled as a mass-spring-damper vibration unit. The rail was an infinite long Euler beam rested on a viscoelastic foundation. The equations were solved by Fourier and Laplace transforms. It was

found that the total mass was the critical parameter (unlike in [40]). Various variables were found influencing the critical mass to different extent. Amongst them, the effects of axle, total number of axles were investigated. Furthermore, the governing equations reveal the existence of negative damping in the coupled system. A stiffer foundation can diminish the negative damping and reduce the danger of instability.

Michaltsos [27] examined the influence of loads moving with variable speeds on the dynamic behavior of a single-span beam. Three cases were considered. Firstly, the concentrated load, moving with time-varying velocity, secondly the vehicle (with wheelbase), moving also with time-varying velocity and lastly, the influence of light damping on the above case of a moving vehicle. He concluded that the effect of a variable speed was significant for deflections of the bridge. The acceleration tends to induce larger deflection than the deceleration. Regarding of type of model, the loading by a two-axle model is more accurate than that by a single-axle model. Single-axle model may be more favorable in the case of long span bridge. The last conclusion was the influence of external damping can be neglected.

Lei and Noda [22] formulated a dynamic model for the vehicle and track coupling system by means of finite element method. Also the track vertical profile was included in this model. Analyses for the coupling system were performed in time and frequency domains. The system was solved by the iterative scheme and the conventional Hertz formula. The interaction force, the acceleration of vehicle and rail were obtained for various speeds and various irregularity. It is very good presentation for system modeling. However, the results and conclusions obtained from this literature and preliminary, it does not provide much insight.

Demic, Lukic and Milic [7] attempted to develop criteria for ride comfort improvement. An investigation of the human body behavior under random vibration was reported. The results showed that humans are very sensitive to vertical random vibration of frequencies below 1 Hz, and are least sensitive of frequencies above 5 Hz. Moreover, humans are more sensitive to random multi-directional vibration than to one-directional vibration.

Paddan and Griffin [29, 30] measured the vibration in 100 different vehicles. They tried to model a comprehensive comparison of the evaluation methods in BS 6841 and ISO 2631. For most measurements, the vertical axis on the seat gave the greatest acceleration magnitude. Evaluations of vibration in accord with ISO 2631 (using the most severe axis) gave lower values than those in accord with BS 6841. It

is because of a combination of different frequency weighting, different axis multiplier (for horizontal vibration) and the use of one versus for axes in the calculation.

1.4 Conclusions from Literatures

- Only a few studies have concentrated on analyses of dynamic of coupling system with random surface.
- None of them discussed about reliability of the system.
- None of them used the more systematic method, i.e. response surface methodology, for making decision about significance of parameters.
- There are many types of vehicle models to choose for the analysis of a roughness-vehicle-structure coupled system. The selection depends on physical nature of the system.

References

- 1. Biggs, J.M. Introduction to Structural Dynamics. McGraw-Hill, 1964.
- 2. Boudjelal, T., Fafard, M., and Gakwaya, A. Modeling of damping and its applications to dynamic bridge-vehicle interaction. In *Proceedings of the EURODYN' 96, Structural Dynamics* (1996), pp. 767-774.
- 3. Cai, Y., Chen, S.S., Rote, D.M., and Coffey, H.T. Vehicle/guideway interaction for high speed vehicles on a flexible guideway. *J. of Sound and Vibration* 175, 5 (1994), 625-646.
- 4. Chan, T.H.T., Yu, L., and Law, S.S. Comparative studies on moving force identification from bridge strains in laboratory. *J. of Sound and Vibration* 235 (2000), 87-104.
- 5. Cho, D.S., and Lee, W.K. Modal interactions of a randomly excited hinged-clamped beam. *J. of sound and Vibration* 237 (2001), 377-393.
- 6. Degrande, G., and Schillemans, L. Free field vibrations during the passage of a Thalys high-speed train at variable speed. *J. of Sound and Vibration* 247 (2001), 131-144.
- 7. Demic, M., Lukic, J., and Milic, Z. Some aspects of the investigation of random vibration influence on ride comfort. *J. of Sound and Vibration* 253 (2002), 109-129.

- 8. Doran, A.L., and Mingori, D.L. Periodic motion of vehicles on flexible guideways. *J. of Dynamic Systems, Measurement and Control* (1977), 268-276.
- 9. Fryba, L. Vibration of Solids and Structures under Moving Loads. Groninggen: Noordhoff International Publishing, 1972.
- 10. Green, M.F., and Cebon, D. Dynamic response of highway bridges to heavy vehicle loads: Theory and experimental validation. *J. of Sound and Vibration* 170 (1994), 51-78.
- 11. Hammond, J.K., and Harrison, R.F. Nonstationary response of vehicles on rough ground-state space approach. *J. of Dynamic Systems, Measurement and Control* 103 (1981), 245-250.
- 12. Harrison, R.F., and Hammond, J.K. Analysis of the nonstationary response of vehicles with multiple wheels. *J. of Dynamic Systems, Measurement and Control* 108 (1986), 69-73.
- 13. Harrison, R.F., and Hammond, J.K. Evolutionary (frequency/time) spectral analysis of the response of vehicles moving on rough ground by using covariance equivalent modeling. *J. of Sound and Vibration* 107 (1986), 29-38.
- 14. Harrison, R.F., and Hammond, J.K. Approixmation, time domain, non-stationary analysis of stochastically excited, non-linear systems with particular reference to themotion of vehicles on rough ground. *J. of Sound and Vibration* 105 (1986), 361-371.
- 15. Henchi, K. Dynamic Analysis of Bridges Under Moving Vehicles by a Finite Element Method. PhD thesis, Conpiegne University of Technology, France, 1995.
- Henchi, K., Fafard, M., Dhatt, G., and Talbot, M. Dynamic behaviour of multi-span beams under moving loads. *J. of Sound and Vibration* 199 (1997), 33-50.
- 17. Henchi, K., Fafard, M., Dhatt, G., and Talbot, M. An efficient algorithm for dynamic analysis of bridges under moving vehicles using a coupled modal and physical components approach. *J. of Sound and Vibration* 212 (1998), 663-683.

- 18. Hino, J., Yoshimura, T., Konishi, K., and Ananthanarayana, N. A finite element method prediction of the vibration of a bridge subjected to a moving vehicle load. *J. of Sound and Vibration* 96 (1984), 45-53.
- 19. Law, S.S., Chan, T.H.T., and Zeng, Q.H. Moving force identification: A time domain method. *J. of Sound and Vibration* 210 (1997), 1-22.
- 20. Law, S.S., and Zhu, X. Study on different beam models in moving force identification. *J. of Sound and Vibration*234 (2000), 661-679.
- 21. Law, S.S., Chan, T.H.T., Zhu, Q.X., and Zeng,Q.H. Regularization in moving force identification. *J. of Engineering Mechanics* (Feb 2001), 136-148.
- 22. Lei,X., and Noda, N.A. analyses of dynamic response of vehicle and track coupling system with random irregularity of track vertical profile. *J. of Sound and Vibration* 258 (2002), 147-165.
- 23. Liang, B., Zhu, D., and Cai, Y. Dynmaic analysi of the vehicle-subgrade model of a vertical coupled system. *J. of Sound and Vibration* 245 (2001), 79-92.
- 24. Lin, Y.H., and Trethewey, M.W. Finite element analysis of elastic beams subjected to moving dynamic loads. *J. of Sound and Vibration* 236 (2000), 61-87.
- 25. Liu, C. Vehicle-road interaction, evolution of road profiles and present service ability index. *Road Material and Pavement Design* 1 (2000), 35-51.
- 26. Marchesiello, S., Fasana, A., Garibaldi, L., and Piombo, B.A.D. dynamics of multi-span continuous straight bridges subject to mdof moving vehicle excitation. *J. of Sound and Vibration* 224 (1999), 541-561.
- 27. Michaltsos, G.T. Dynamics behavior of single-span beam subjected to loads moving with variable speeds. *J. of Sound and Vibration* 258 (2002), 359-372.
- 28. Narayanan, S., and Raju, G.V. Stochastic optimal control of nonstationary response of a sdof vehicle model. *J. of Sound and Vibration* 141 (1990), 449-463.
- 29. Paddan, G.S., and Griffin, M.J. Evaluation of whole-body vibration in vehicles. *J. of Sound and Vibration* 253 (2002), 195-213.
- 30. Paddan, G.S., and Griffin, M.J. Effects of seating on exposures to whole-body vibration in vehicles. *J. of Sound and Vibration* 253 (2002), 215-241.
- 31. Pesterev, A.V., and Bergman, L.A. Response of elastic continuum carrying moving linear oscillator. *J. of Engineering Mechanics* (Aug 1997), 878-889.

- 32. Sadiku,S., and Leipholz, E. On the dynamics of elastic systems with moving concentrated masses. *Ingenieur-Archiv* 57 (1987), 223-242.
- 33. Seetapan, P. and Gasparini, D.A. Random roughness and interface models for multi-axle moving vehicles. In *Proceedings of great Lakes Civil Engineering Graduate Student Research Symposium* (2001), p. 138.
- 34. Seetapan, P. Dynamics of hgh speed vehicles traversing structures with random surfaces. Ph.D. thesis, Caes Western Reserve University, USA, 2001.
- 35. Seetapan P. and Gasparini D.A. Dynamic of bridge for very high speed vehicle. In *Proceedings of the EURODYN'02*, *Structural Dynamics*, Munich, Germany (2002).
- 36. Smith, C.C., Gilchrist, A.J., and Wormley, D.N. Multiple and continuous span elevated guideway-vehicle dynamic performance. *J. of Dynamic Systems, Measurement and Control* (1975), 30-40.
- 37. Smith, C.C., and Wormley, D.N. Response of continuous periodic supported guideway beams to traveling vehicle loads. *J. of Dynamic Systems, Measurement and Control*(1975), 21-29.
- 38. Stanisic, M. On a new theory of the dynamic behavior of the structures carrying moving masses. *Ingenieur-Archiv* 55 (1985), 176-185.
- 39. Timoshenko, S., Young, D.H., and Weaver, W. *Vibration Problems in Engineering*. Wiley, 1974.
- 40. Verichev, S.N., and Metrikine, A.V. Instability of a bogie moving on a flexibly supported Timoshenko beam. *J. of Sound and Vibration* 253 (2002), 653-668.
- 41. Yadav, D., and Nigam, N.C. Ground induced nostationary response of vehicles. *J. of Sound and Vibration* 61 (1978), 117-126.
- 42. Yau, J.D., Wu, Y.S., and Yang, Y.B. Impact response of bridges with elastic bearings to moving loads. *J. of Sound and Vibration* 248 (2001), 9-30.
- 43. Zheng, D.Y., and Fan, S.C. Instability of vibration of a moving-train-and-rail coupling system. *J. of Sound and Vibration* 255 (2002), 243-259.
- 44. Zhu, X., and Law, S.S. Identification of vehicle axle loads from bridge dynamic responses. *J. of Sound and Vibration* 236 (2000), 705-724.

CHAPTER 2

RANDOM ROUGHNESS AND INTERFACE MODELS FOR MULTI-AXLE MOVING VEHICLES

2.1 Introduction

Vehicle-structure models and interface models have been studied for a long time [4,7,18]. Some aspects of surface roughness modeling [7,20,25] and interface models are discussed in this chapter. Surface roughness can have deterministic or stochastic (random process) models [10,11]. Stochastic models may be either stationary or nonstationary and may be formulated in a time or frequency domain [1,15,16]. Moreover, there are several interface points between a multi-car vehicle and a structure. A Markov vector model that includes multiple interface points is formulated in this Chapter.

2.2 Filtered White Noise and Existence of Derivatives of Filtered Processes

To incorporate roughness processes into the vehicle-structure model, the system state equations may be augmented by shaping filter equations [12]. The filters may be either low-pass or high-pass, first order or higher order. In general, filter transfer functions are expressed in terms of wavenumber, r (the inverse of wavelength, λ), and one or more filter parameters. Some common filters and their transfer functions are as follow:

A first order filter is given by the equation:

$$\frac{\dot{h}_d}{r_f} + h_d = W_d \tag{2.1}$$

the transfer function between W_d and h_d , H(r), is:

$$H(r) = \frac{1}{1 + (r/r_f)i} \tag{2.2}$$

and the square of the absolute value is:

$$|H(r)|^2 = \frac{1}{1 + (r/r_f)^2}$$
 (2.3)

Returning to Equation 2.1, the transfer function between W_d and $\frac{\dot{h}_d}{r_f}$ is:

$$H(r) = \frac{\left(r/r_f\right)}{1 + \left(r/r_f\right)i} \tag{2.4}$$

and the square of the absolute value is:

$$|H(r)|^2 = \frac{(r/r_f)^2}{1 + (r/r_f)^2}$$
 (2.5)

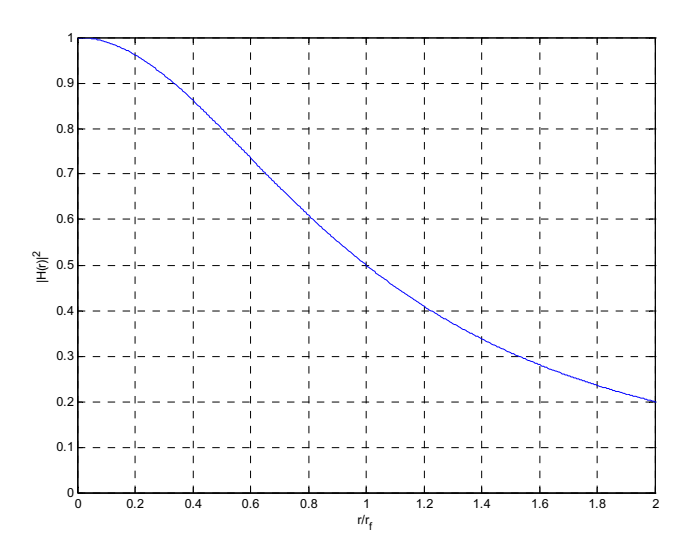


Figure 2.1 : Square of the Absolute Value of the Transfer Function between h_d and W_d for the First Order Filter given by Equation 2.1

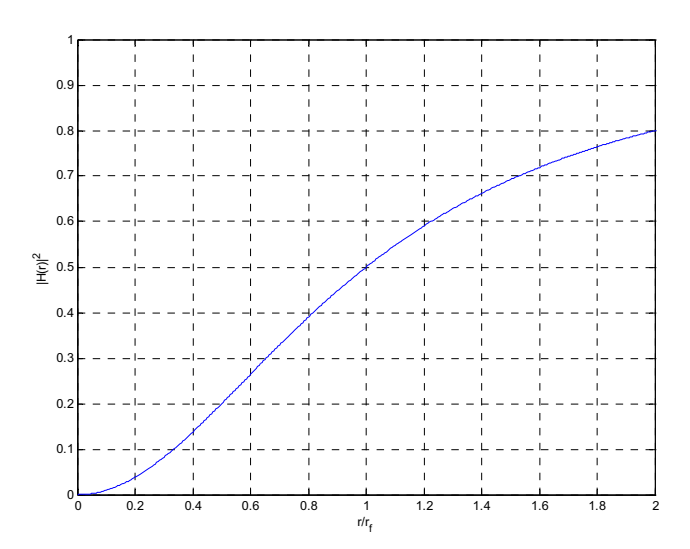


Figure 2.2 : Square of the Absolute Value of the Transfer Function between \dot{h}_d/r_f and W_d in Equation 2.1

Figure 2.1 shows that if W_d is white noise, its high wavenumber components are filtered out and h_d has only low wavenumber content. r_f is the wavenumber at which the square

of the absolute value of the transfer function is equal to 0.5. Figure 2.2 shows that if W_d is white noise, the response \dot{h}_d/r_f retains the high wavenumber content.

A second order filter may be defined by:

$$\frac{\ddot{h}_{d}}{r_{f}^{2}} + \frac{2\xi_{f}}{r_{f}}\dot{h}_{d} + h_{d} = W_{d}$$
 (2.6)

The transfer function between W_d and h_d , H(r), is:

$$H(r) = \frac{1}{1 - (r/r_f)^2 + (2\xi_f r/r_f)i}$$
 (2.7)

and the square of the absolute value is:

$$|H(r)|^2 = \frac{1}{\left(1 - \left(r/r_f\right)^2\right)^2 + \left(2\xi_f r/r_f\right)^2}$$
 (2.8)

Figure 2.3 shows $|H(r)|^2$ of Equation 2.8. At $r/r_f = 1$, $|H(r)|^2 = 1/(2\xi)^2$. For high values of ξ_f the peak shifts from $r/r_f = 1$ toward the low wavenumber range.

If W_d is viewed as white noise and $h_d(x_d)$ as a surface roughness the Power Spectral Density (PSD) of h_d , $S_{h_dh_d}(r)$, can be obtained from the following basic stationary input-output equation, (Note that in this work all PSD's are two-sided PSD's):

$$S_{h,h}(r) = |H(r)|^2 S_0$$
 (2.9)

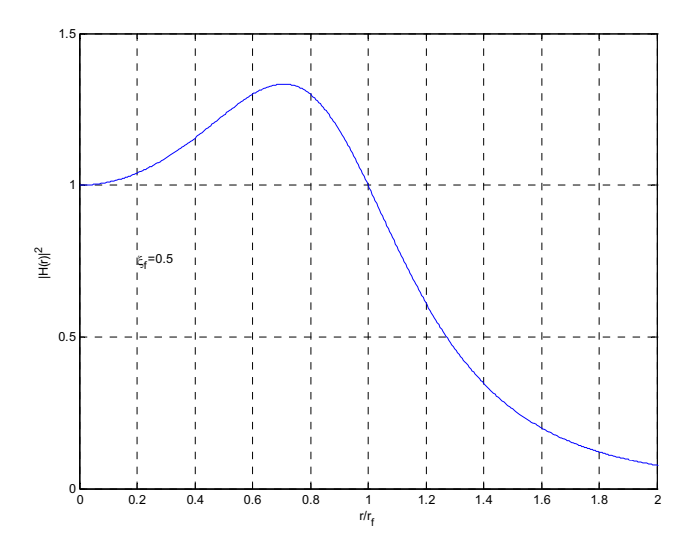


Figure 2.3 : Square of the Absolute Value of the Transfer Function between h_d and W_d for the Second Order Filter given by Equation 2.6

in which S_0 is the intensity of the white noise process, W_d , and the variance of the roughness process, $h_d(x_d)$, is found from the integral of its PSD:

$$\sigma_{h_d h_d}^2 \left(r \right) = \int_{-\infty}^{\infty} \left| H \left(r \right) \right|^2 S_0 dr \tag{2.10}$$

The variance of the first derivative of the process is:

$$\sigma_{\kappa_d \kappa_d}^2(r) = \int_{-\infty}^{\infty} r^2 \left| H(r) \right|^2 S_0 dr \qquad (2.11)$$

and the variance of the second derivative of the process is:

$$\sigma_{h_0^2 h_0^2}^2(r) = \int_{-\infty}^{\infty} r^4 |H(r)|^2 S_0 dr$$
 (2.12)

Because these integrals are functions of r^m/r^n , for a finite variance m must be less than n. Therefore the derivative process from Equation 2.1 does not exist, whereas the derivative process from Equation 2.6 does. The importance of the existence of derivative processes is explained in Section 2.4, which discusses various vehicle-structure interface models.

2.3 Roughness Models

The system equations of motion are herein solved in the time domain. Since roughness is a spatial function and has a dimension of length, it must be transformed from the spatial domain to the time domain and then nondimensionalized. The procedure is as follows:

2.3.1 Dimensioned Spatial Process

Here, surface roughness is modeled as the output of a first order filter driven by white noise and expressed in a real spatial domain by the following linear ordinary differential equation:

$$\Delta_c \frac{dh_d(x_d)}{dx_d} + h_d(x_d) = W_d(x_d)$$
 (2.13)

in which $W_d(x_d)$ is a zero mean Gaussian white noise with dimension of $(length)^1$, $\Delta_c = 1/r_f$ is a correlation distance, $h_d(x_d)$ is a real, spatial, zero mean roughness process with dimension of $(length)^1$, S_0 is the white noise intensity with dimension of $(length)^3$ and the subscript d refers to a dimensioned quantity.

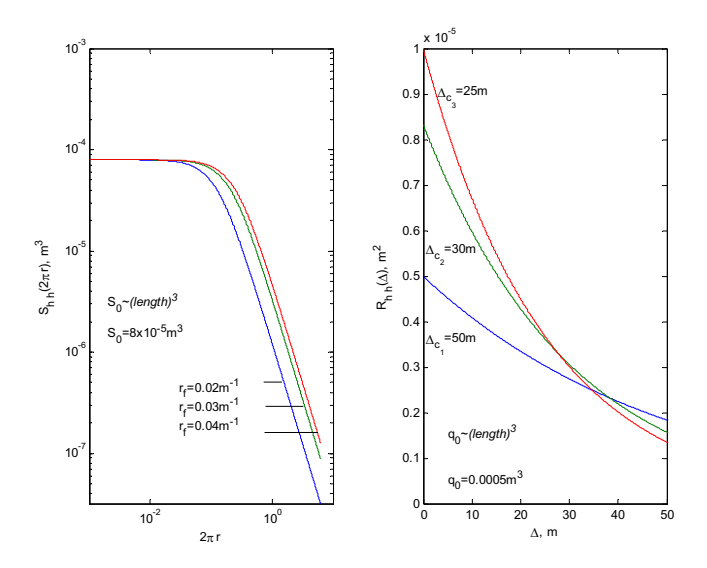


Figure 2.4 : PSD and Autocovariance of $h_d(x_d)$ in Dimensioned Spatial Domain Let $S_0 = 8x10^{-5}m^3$ and $r_f = 0.02,0.03$ and $0.04~{\rm m}^{-1}$. Figure 2.4 shows that if $r_f = 1/\Delta_c$ increases, the PSD of $h_d(x_d)$, given by Equations 2.3 and 2.9, expands to the right which adds power. In other words, the surface has more high wavenumber roughness. Because the white noise and roughness have $(length)^1$ dimension, their autocovariances have dimensions of $(length)^2$. The autocovariance of $W_d(x_d)$ is a Dirac delta function. The stationary autocovariance of the zero mean process $h_d(x_d)$ given by Equation 2.13, which is the Fourier transform of $S_{h_dh_d}(2\pi r)$, is as follows:

$$COV\left[h_d\left(x_d\right)h_d\left(x_d+\Delta\right)\right] = R_{h_dh_d}\left(\Delta\right) = \frac{q_0}{2\Delta_c} \exp\left[-\frac{|\Delta|}{\Delta_c}\right]$$
 (2.14)

in which Δ is a spatial lag, q_0 is the strength of the white process, $W_d(x_d)$, which is related to the intensity as follows:

$$q_0 = 2\pi S_0 (2.15)$$

The variance of $h_d(x_d)$ is:

$$VAR\left[h_d\left(x_d\right)\right] = R_{h_d h_d}\left(0\right) = \frac{q_0}{2\Delta_c}$$
(2.16)

Equation 2.16 implies that the variance, $R_{h_d h_d}(0)$, decreases as Δ_c increases.

The stationary autocorrelation function of $h_d\left(x_d\right)$, $\rho_{h_dh_d}\left(\Delta\right)$, is defined as:

$$\rho_{h_d h_d} \left(\Delta \right) = \frac{COV \left[h_d \left(x_d \right) h_d \left(x_d + \Delta \right) \right]}{VAR \left[h_d \left(x_d \right) \right]} = \exp \left[-\frac{\left| \Delta \right|}{\Delta_c} \right]$$
 (2.17)

The correlation distance, Δ_c , is then the spatial lag at which $\rho_{h_dh_d}(\Delta) = e^{-1}$.

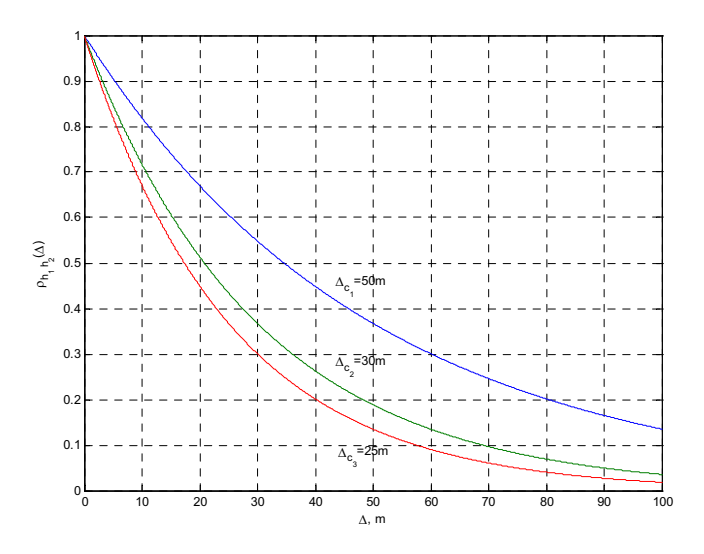


Figure 2.5 : Spatial Autocorrelation Function of $h_d(x_d)$

Figure 2.5 shows the decay rate of the autocorrelation. For high r_f or low Δ_c the autocorrelation decays faster because it is a decaying exponential function of $|\Delta|/\Delta_c$.

2.3.2 Dimensioned Temporal Process

Denote the constant velocity of a vehicle as V. Let $x_d = Vt_d$ and $dx_d = Vdt_d$, then the spatial process $h_d(x_d)$ is transformed to a temporal random process defined by the equation:

$$\frac{\Delta_c}{V}\dot{h}_d(t_d) + h_d(t_d) = W_d(t_d)$$
 (2.18)

in which $h_d(t_d)$ is a temporal roughness process with dimension of $(length)^1$, $W_d(t_d)$ is a temporal white noise process with dimension of $(length)^1$. From the fact that the variance of the process must be the same after transforming to the time domain, the intensity and strength of the white noise are scaled to $S_1 = S_0/V$ and $q_1 = q_0/V$ and their dimensions are $(length)^2(time)^1$. The PSD and stationary autocovariance of $h_d(t_d)$ are shown in Figure 2.6.

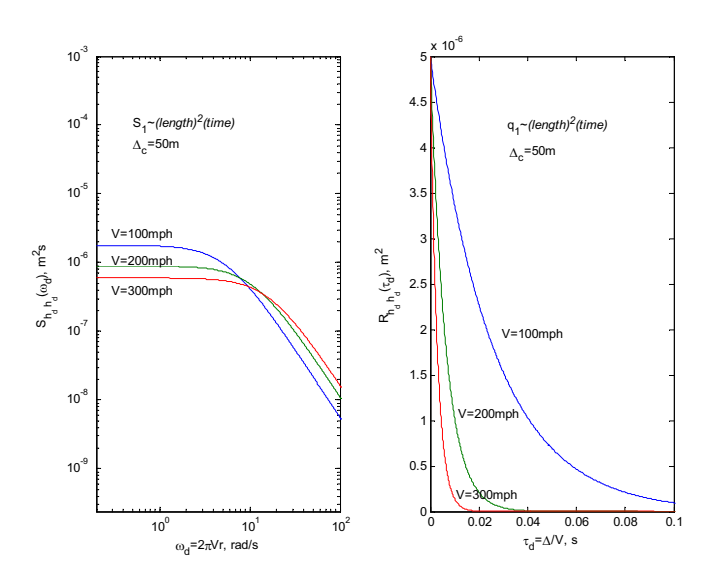


Figure 2.6 : PSD and Autocovariance of Temporal Process $h_d\left(t_d\right)$

The stationary autocovariance of $h_d(t_d)$ is:

$$COV\left[h_d\left(t_d\right)h_d\left(t_d + \tau_d\right)\right] = \frac{q_1}{2\left(\Delta_c/V\right)} \exp\left[-\frac{|\tau_d|}{\left(\Delta_c/V\right)}\right]$$
(2.19)

in which τ_d is a time lag.

And the variance of $h_d(t_d)$ is:

$$VAR\left[h_d\left(t_d\right)\right] = \frac{q_1}{2\left(\Delta_c/V\right)} = \frac{q_0}{2\Delta_c}$$
(2.20)

The velocity that is used in transforming to the time domain affects the characteristics of the PSD and covariance function. Let $\Delta_c = 50$ m, at higher velocities the power in the low frequency range is lower but the power in the high frequency range is higher. The autocovariance function decays very fast for high velocities as shown in Figure 2.6. The stationary autocorrelation function of $h_a(t_d)$ is:

$$\rho_{h_d h_d} \left(\tau_d \right) = \exp \left[-\frac{\left| \tau_d \right|}{\Delta_c / V} \right] \tag{2.21}$$

Define τ_{d_c} as the lag at which $\rho_{h_d h_d}(\tau_{d_c}) = e^{-1}$. From Equation 2.21, τ_{d_c} is:

$$\tau_{d_c} = \frac{\Delta_c}{V} \tag{2.22}$$

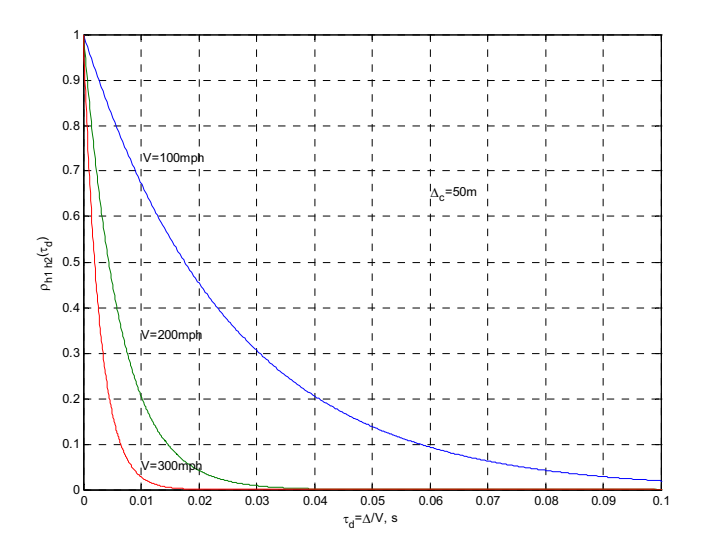


Figure 2.7 : Temporal Autocorrelation Function of $h_d\left(t_d\right)$

Figure 2.7 shows that the process becomes uncorrelated more quickly for higher velocities.

2.3.3 Nondimensionalization of $h_d(t_d)$ and $W_d(t_d)$

The processes $h_d(t_d)$ and $W_d(t_d)$ may be nondimensionalized as $h(t_d) = h_d(t_d)/L$ and $W(t_d) = W_d(t_d)/L$ in which L is a span length. Thus, the filter equation (Equation 2.18) is changed (the subscript d is dropped) to:

$$\frac{\Delta_c}{V}\dot{h}(t_d) + h(t_d) = W(t_d) \tag{2.23}$$

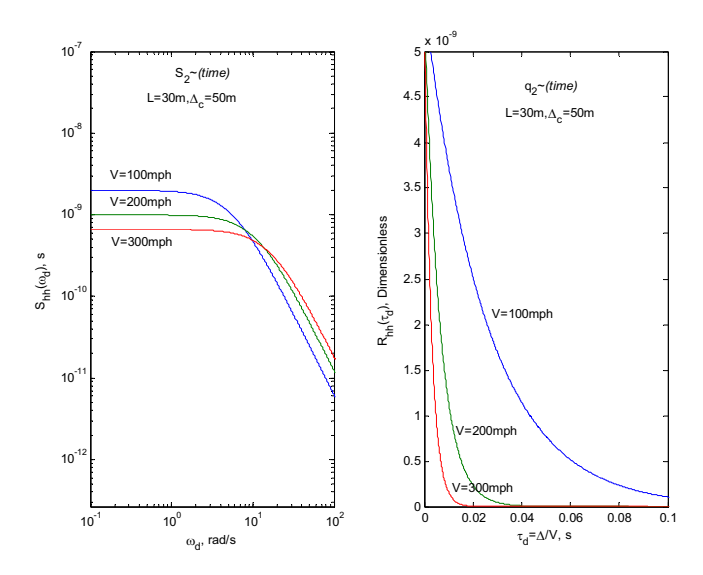


Figure 2.8 : PSD and Autocovariance of Nondimensional $h(t_d)$

Note that the strength, q_2 , of the nondimensional temporal white noise is related to the strength in the spatial domain by $q_2=q_0/(VL^2)$. The stationary autocovariance and variance can also be written as

$$COV\left[h(t_d)h(t_d + \Delta_d)\right] = \frac{q_2}{2(\Delta_c/V)} \exp\left[-\frac{|\tau_d|}{(\Delta_c/V)}\right]$$
(2.24)

and

$$VAR\left[h(t_d)\right] = \frac{q_2}{2(\Delta_c/V)} = \frac{q_0}{2VL^2} \frac{V}{\Delta_c} = \frac{q_0}{2\Delta_c L^2}$$
(2.25)

The PSD and autocovariance function of the nondimensionalized process $h(t_d)$ are shown in Figure 2.8.The stationary autocorrelation function of $h(t_d)$ is:

$$\rho_{hh}(\tau_d) = \exp\left[-\frac{|\tau_d|}{\Delta_c/V}\right]$$
 (2.26)

The autocorrelation time remains:

$$\tau_{d_c} = \frac{\Delta_c}{V} \tag{2.27}$$

2.3.4 Nondimensionalization of Time

Define nondimensional time, t, by:

$$t = \frac{t_d}{L/V} = \frac{V}{L}t_d \tag{2.28}$$

$$\tau = \frac{V}{L}\tau_d \tag{2.29}$$

in which t is time nondimensionalized by the time required to cross a span, L, with a velocity, V, and τ is a nondimensional time lag. The filter equation is now written as:

$$\frac{\Delta_c}{L}\dot{h}(t) + h(t) = W(t) \tag{2.30}$$

in which \dot{h} now denotes differentiation with respect to nondimensional time.

Assuming that the span length of a guideway is 30 m, the values of the parameter Δ_c/L corresponding to the assumed wave numbers, r_f in Section 2.3.1 (Figure 2.4) are 1.7, 1.0

and 0.8 respectively. The PSD and autocovariance of the nondimensional process h(t) in nondimensional time are shown in Figure 2.9:

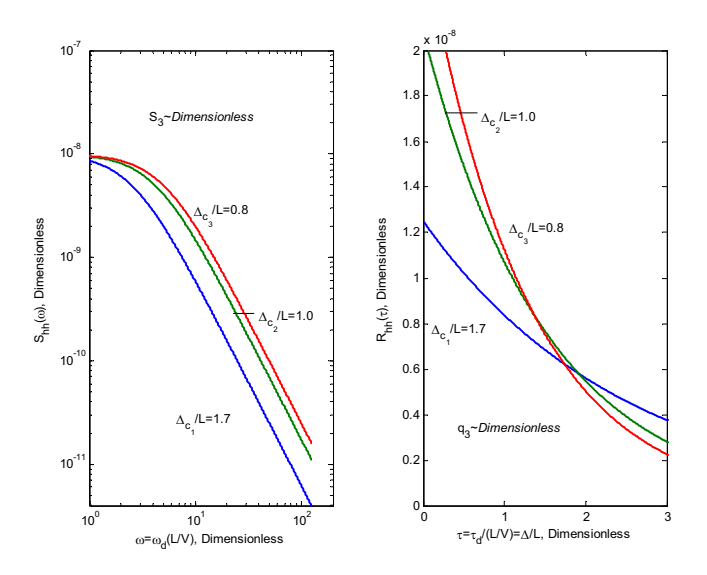


Figure 2.9 : PSD and Autocovariance of Nondimensional h(t) in Nondimensional Time Domain

Denote the nondimensional intensity and strength of the nondimensional white process in nondimensional time as $S_3 = S_0/L^3$ and $q_3 = q_0/L^3$. The autocovariance and variance of h(t) are:

$$COV\left[h(t)h(t+\tau)\right] = \frac{q_3}{2(\Delta_c/L)} \exp\left[-\frac{|\tau|}{(\Delta_c/L)}\right]$$
 (2.31)

and

$$VAR\left[h(t)\right] = \frac{q_3}{2(\Delta_c/L)} = \frac{q_0}{2\Delta_c L^2} = \frac{\left(q_0/L^3\right)}{2(\Delta_c/L)}$$
(2.32)

The autocorrelation function and the nondimensional correlation time of h(t) are:

$$\rho_{hh}(\tau) = \exp\left[-\frac{|\tau|}{\Delta_c/L}\right] \tag{2.33}$$

and

$$\tau_c = \frac{\Delta_c}{L} \tag{2.34}$$

Note that the autocovariances in Figure 2.9 cross. This is an effect of nondimensionalization. However, the autocorrelations in Figure 2.10 do not cross. At a particular τ the correlation function is lower if Δ_c/L is smaller.

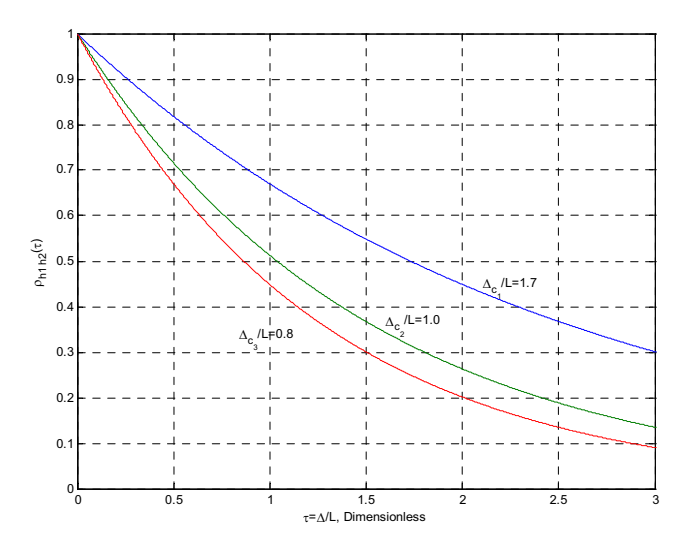


Figure 2.10 : Autocorrelation Function of Nondimensional Process h(t) with a Nondimensional Time Lag

The parameters q_0/L^3 and Δ_c/L may be adjusted to fit the roughness model to real data.

2.3.5 Modeling Actual Roughness

Shaping filter parameters (strength and Δ_c) may be chosen so that the PSD of the filter response matches a target PSD such as the U.S. DOT rail specification.

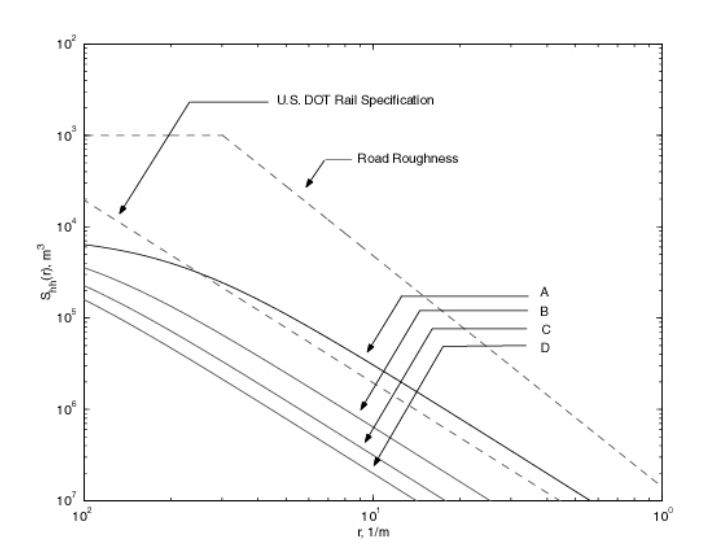


Figure 2.11: Modeling Actual Roughness

Figure 2.11 shows the U.S. DOT target PSD and four PSD's of filter response, determined using the following parameters:

For L = 30 m and $S_0 = 8 \times 10^{-5} \text{ m}^3$,

PSD A: $S_0/L^3 = 3 \times 10^{-9}$, $\Delta_c/L = 1.67$,

PSD B: $S_0/L^3 = 3x10^{-9}$, $\Delta_c/L = 3.33$,

PSD C: $S_0/L^3 = 3 \times 10^{-9}$, $\Delta_c/L = 5.33$,

PSD D: $S_0/L^3 = 3 \times 10^{-9}$, $\Delta_c/L = 6.67$.

PSD A is the better fit to the U.S. DOT rail specification. From now on these PSD's, labeled A,B,C and D, are used to study effects of roughness on responses.

2.4 Interface Models

Interface models can be linear or nonlinear. Common nonlinear models consider loss-of-contact [2, 27] or nonlinear elastic springs [19]. A mass or dashpot or spring or any parallel combination can be used as interface elements [21]. Only linear interface elements are considered here. The three basic cases of a linear spring interface, a parallel spring and dashpot interface and a rigid mass with a spring and dashpot in parallel are analyzed next to understand the nature of the coupling and requirements for roughness models. The displacement, $v_d^t(x_d, t_d)$, at a contact point, x_d , depends on the vertical displacement of the beam, $v_d(x_d, t_d)$, and the irregularity, $h_d(x_d)$:

$$v_d^t(x_d, t_d) = v_d(x_d, t_d) + h_d(x_d)$$
 (2.35)

in which the vertical displacement of the beam can be written in terms of modal coordinates and mode shapes, $v_d(x_d, t_d) = \sum_{i=1}^n \phi_i(x_d) y_i(t_d)$. The total temporal derivatives of the displacement at a contact point [21, 23, 26] are obtained as:

$$\dot{v}_{d}^{t}(x_{d}, t_{d}) = \sum_{i=1}^{n} \phi_{i}(x_{d}) \dot{y}_{i}(t_{d}) + \dot{x}_{d} \sum_{i=1}^{n} \phi_{i}^{t}(x_{d}) y_{i}(t_{d}) + \dot{x}_{d} h_{d}^{t}(x_{d})$$
(2.36)

$$\ddot{v}'_{d}(x_{d},t_{d}) = \sum_{i=1}^{n} \phi_{i}(x_{d}) \ddot{y}_{i}(t_{d}) + 2\dot{x}_{d} \sum_{i=1}^{n} \phi'_{i}(x_{d}) \dot{y}_{i}(t_{d}) + \dot{x}_{d}^{2} \sum_{i=1}^{n} \phi''_{i}(x_{d}) y_{i}(t_{d}) + \ddot{x}_{d}^{2} \sum_{i=1}^{n} \phi''_{i}(x_{d}) y_{i}(t_{d}) + \ddot{x}_{d}^{2} h''_{d}(x_{d}) + \ddot{x}_{d} h'_{d}(x_{d})$$

$$(2.37)$$

Assuming that a vehicle is traversing with a constant velocity, then . $\dot{x}_d = V$ and $\ddot{x}_d = 0$.

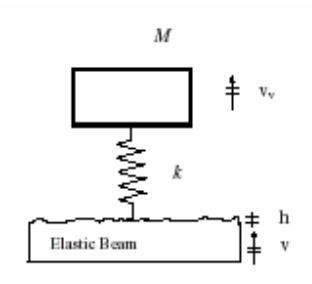


Figure 2.12: SDOF System with Linear Spring Interface with Elastic Beam

Figure 2.12 shows a single-degree-of-freedom (SDOF) system with a linear spring interface with an elastic beam. Let the dynamic displacement, v_{d_v} , be the vehicle DOF. The vehicle equilibrium equation and the modal equations of the beam are:

$$M\ddot{v}_{d_{v}}(t_{d}) + k(v_{d_{v}}(t_{d}) - v_{d_{v}}^{t}(x_{d}, t_{d})) = 0$$
 (2.38)

$$\ddot{y}_{i}(t_{d}) + 2\xi \omega_{i} \dot{y}_{i}(t_{d}) + \omega_{i}^{2} y_{i}(t_{d}) = P_{1}(x_{d}, t_{d}) \phi(Vt_{d})$$
(2.39)

in which

$$P_{1}(x_{d}, t_{d}) = k(v_{d_{v}}(t_{d}) - v_{d_{v}}^{t}(x_{d}, t_{d})) - Mg$$
(2.40)

The equations of motion of the system may be expressed in matrix form as follow:

$$M\ddot{x}(t_d) + C\dot{x}(t_d) + K(t_d)x(t_d) = F(t_d)$$
(2.41)

in which

$$x(t_d) = \begin{bmatrix} v_{d_v} & y_1 & \dots & y_n \end{bmatrix}^T$$
 (2.42)

$$M = \begin{bmatrix} M & & & & \\ & 1 & & & \\ & & 1 & & \\ & & & \ddots & \\ & & & & 1 \end{bmatrix}$$
 (2.43)

$$C = \begin{bmatrix} 0 & & & & \\ & 2\xi\omega_1 & & & \\ & & 2\xi\omega_2 & & \\ & & & \ddots & \\ & & & & 2\xi\omega_n \end{bmatrix}$$
 (2.44)

$$K(t_{d}) = \begin{bmatrix} k & -k\phi_{1}(Vt_{d}) & -k\phi_{2}(Vt_{d}) & \dots & -k\phi_{n}(Vt_{d}) \\ -k\phi_{1}(Vt_{d}) & \omega_{1}^{2} + k\phi_{1}^{2}(Vt_{d}) & k\phi_{2}(Vt_{d})\phi_{1}(Vt_{d}) & \dots & k\phi_{n}(Vt_{d})\phi_{1}(Vt_{d}) \\ -k\phi_{2}(Vt_{d}) & k\phi_{1}(Vt_{d})\phi_{2}(Vt_{d}) & \omega_{2}^{2} + k\phi_{2}^{2}(Vt_{d}) & \dots & k\phi_{n}(Vt_{d})\phi_{2}(Vt_{d}) \\ \vdots & \vdots & \vdots & \ddots & \vdots \\ -k\phi_{n}(Vt_{d}) & k\phi_{1}(Vt_{d})\phi_{n}(Vt_{d}) & k\phi_{2}(Vt_{d})\phi_{n}(Vt_{d}) & \dots & \omega_{n}^{2} + k\phi_{n}^{2}(Vt_{d}) \end{bmatrix}$$
(2.45)

$$F(t_d) = \begin{bmatrix} F_1^1 & F_1 & F_2 & \dots & F_n \end{bmatrix}^T$$
 (2.46)

in which

$$F_1^1 = kh_d\left(Vt_d\right) \tag{2.47}$$

$$F_{i} = \left[-kh_{d}\left(Vt_{d}\right) - Mg\right]\phi_{i}\left(Vt_{d}\right) \tag{2.48}$$

Note that with a linear elastic interface element, the stiffness matrix on the LHS, $K(t_d)$, is a *known* function of time. Temporally varying stiffnesses represent 'parametric' excitation terms.

Consider next a SDOF with parallel spring and dashpot interface elements [5, 30] as shown in Figure 2.13.

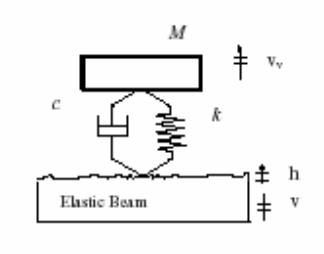


Figure 2.13: SDOF System with Parallel Spring and Dashpot Interface Elements with Elastic Beam

The governing equations are:

$$M\ddot{v}_{d_{v}}(t_{d}) + c(\dot{v}_{d_{v}}(t_{d}) - \dot{v}_{d}^{t}(x_{d}, t_{d})) + k(v_{d_{v}}(t_{d}) - v_{d}^{t}(x_{d}, t_{d})) = 0$$
(2.49)

$$\ddot{y}_{i}(t_{d}) + 2\xi \omega_{i} \dot{y}_{i}(t_{d}) + \omega_{i}^{2} y_{i}(t_{d}) = P_{2}(x_{d}, t_{d}) \phi(Vt_{d})$$
(2.50)

in which

$$P_{2}(x_{d}, t_{d}) = c(\dot{v}_{d_{v}}(t_{d}) - \dot{v}_{d}^{t}(x_{d}, t_{d})) + k(v_{d_{v}}(t_{d}) - v_{d_{v}}^{t}(x_{d}, t_{d})) - Mg$$
(2.51)

The equations of motion may be expressed in matrix form as follow:

$$M\ddot{x}(t_d) + C(t_d)\dot{x}(t_d) + K(t_d)x(t_d) = F(t_d)$$
(2.52)

in which

$$M = \begin{bmatrix} M & & & \\ & 1 & & \\ & & 1 & & \\ & & & \ddots & \\ & & & & 1 \end{bmatrix}$$
 (2.53)

$$C(t_{d}) = \begin{bmatrix} c & -c\phi_{1}(Vt_{d}) & -c\phi_{2}(Vt_{d}) & \dots & -c\phi_{n}(Vt_{d}) \\ -c\phi_{1}(Vt_{d}) & 2\xi\omega_{1} + c\phi_{1}^{2}(Vt_{d}) & c\phi_{2}(Vt_{d})\phi_{1}(Vt_{d}) & \dots & c\phi_{n}(Vt_{d})\phi_{1}(Vt_{d}) \\ -c\phi_{2}(Vt_{d}) & c\phi_{1}(Vt_{d})\phi_{2}(Vt_{d}) & 2\xi\omega_{2} + c\phi_{2}^{2}(Vt_{d}) & \dots & c\phi_{n}(Vt_{d})\phi_{2}(Vt_{d}) \\ \vdots & \vdots & \vdots & \ddots & \vdots \\ -c\phi_{n}(Vt_{d}) & c\phi_{1}(Vt_{d})\phi_{n}(Vt_{d}) & c\phi_{2}(Vt_{d})\phi_{n}(Vt_{d}) & \dots & 2\xi\omega_{n} + c\phi_{n}^{2}(Vt_{d}) \end{bmatrix}$$
(2.54)

$$K(t_{d}) = \begin{bmatrix} k & -cV\phi'_{1} - k\phi_{1} & -cV\phi'_{2} - k\phi_{2} & \dots & -cV\phi'_{n} - k\phi_{n} \\ -k\phi_{1} & \omega_{1}^{2} + cV\phi'_{1}\phi_{1} + k\phi_{1}^{2} & cV\phi'_{2}\phi_{1} + k\phi_{2}\phi_{1} & \dots & cV\phi'_{n}\phi_{1} + k\phi_{n}\phi_{1} \\ -k\phi_{2} & cV\phi'_{1}\phi_{2} + k\phi_{1}\phi_{2} & \omega_{2}^{2} + cV\phi'_{2}\phi_{2} + k\phi_{2}^{2} & \dots & cV\phi'_{n}\phi_{2} + k\phi_{n}\phi_{2} \\ \vdots & \vdots & & \ddots & \vdots \\ -k\phi_{n} & cV\phi'_{1}\phi_{n} + k\phi_{1}\phi_{n} & cV\phi'_{2}\phi_{n} + k\phi_{2}\phi_{n} & \dots & \omega_{n}^{2} + cV\phi'_{n}\phi_{n} + k\phi_{n}^{2} \end{bmatrix} (2.55)$$

$$F(t_d) = \begin{bmatrix} F_1^1 & F_1 & F_2 & \dots & F_n \end{bmatrix}^T$$
 (2.56)

in which

$$F_1^1 = cVh_d'(Vt_d) + kh_d(Vt_d)$$
(2.57)

$$F_{i} = \left[-cVh'_{d}\left(Vt_{d}\right) - kh_{d}\left(Vt_{d}\right) - Mg \right] \phi_{i}\left(Vt_{d}\right)$$
(2.58)

When a dashpot is added as an interface element the damping matrix, $C(t_d)$, becomes a known function of time. The effective forces on the RHS depend on both $h_d(t_d)$ and $h_d'(t_d)$. Therefore the roughness model must be such that both $h_d(t_d)$ and $h_d'(t_d)$ exist and have finite variances. Therefore if filtered white noise is used as a model for

roughness, the order of the filter equation must be such that the first derivative exists and has a finite variance.

Consider next a SDOF with a rigid mass in addition to the parallel spring and dashpot as interface elements, as shown in Figure 2.14. The equations of motion are:

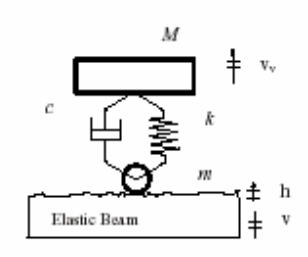


Figure 2.14: SDOF System with Rigid Mass and Parallel Spring and Dashpot as Interface

Elements with Elastic Beam

$$M\ddot{v}_{d_{v}}(t_{d}) + c(\dot{v}_{d_{v}}(t_{d}) - \dot{v}_{d}^{t}(x_{d}, t_{d})) + k(v_{d_{v}}(t_{d}) - v_{d}^{t}(x_{d}, t_{d})) = 0$$
(2.59)

$$\ddot{y}_{i}(t_{d}) + 2\xi \omega_{i}\dot{y}_{i}(t_{d}) + \omega_{i}^{2}y_{i}(t_{d}) = P_{3}(x_{d}, t_{d})\phi(Vt_{d})$$
(2.60)

in which

$$P_{3}(x_{d},t_{d}) = -m\ddot{v}_{d}^{t}(x_{d},t_{d}) + c(\dot{v}_{d_{v}}(t_{d}) - \dot{v}_{d}^{t}(x_{d},t_{d})) + k(v_{d_{v}}(t_{d}) - v_{d_{v}}^{t}(x_{d},t_{d})) - (M+m)g$$
(2.61)

The equations of motion of the system may be expressed in matrix form as follow:

$$M(t_d)\ddot{x}(t_d) + C(t_d)\dot{x}(t_d) + K(t_d)x(t_d) = F(t_d)$$
 (2.62)

in which

$$M(t_{d}) = \begin{bmatrix} M & 0 & 0 & \dots & 0 \\ 0 & m\phi_{1}^{2}(Vt_{d}) & m\phi_{2}(Vt_{d})\phi_{1}(Vt_{d}) & \dots & m\phi_{n}(Vt_{d})\phi_{1}(Vt_{d}) \\ 0 & m\phi_{1}(Vt_{d})\phi_{2}(Vt_{d}) & m\phi_{2}^{2}(Vt_{d}) & \dots & m\phi_{n}(Vt_{d})\phi_{2}(Vt_{d}) \\ \vdots & \vdots & & \vdots & \ddots & \vdots \\ 0 & m\phi_{1}(Vt_{d})\phi_{n}(Vt_{d}) & m\phi_{2}(Vt_{d})\phi_{n}(Vt_{d}) & \dots & m\phi_{n}^{2}(Vt_{d}) \end{bmatrix}$$
(2.63)

$$C(t_{d}) = \begin{bmatrix} c & -c\phi_{1} & -c\phi_{2} & \dots & -c\phi_{n} \\ -c\phi_{1} & 2\xi\alpha_{1} + 2mV\phi_{1}^{2}\phi_{1} + c\phi_{1}^{2} & 2mV\phi_{2}^{2}\phi_{1} + c\phi_{2}\phi_{1} & \dots & 2mV\phi_{n}^{2}\phi_{1} + c\phi_{n}\phi_{1} \\ -c\phi_{2} & 2mV\phi_{1}\phi_{2} + c\phi_{1}\phi_{2} & 2\xi\alpha_{2} + 2mV\phi_{2}\phi_{2} + c\phi_{2}^{2} & \dots & 2mV\phi_{n}\phi_{2} + c\phi_{n}\phi_{2} \\ \vdots & \vdots & & \vdots & \ddots & \vdots \\ -c\phi_{n} & 2mV\phi_{1}\phi_{n} + c\phi_{1}\phi_{n} & 2mV\phi_{2}\phi_{n} + c\phi_{2}\phi_{n} & \dots & 2\xi\alpha_{n} + 2mV\phi_{n}^{2}\phi_{n} + c\phi_{n}^{2} \end{bmatrix}$$
(2.64)

$$K(t_{d}) = \begin{bmatrix} k & -cV\phi_{1} - k\phi_{1} & -cV\phi_{2} - k\phi_{2} & \dots & -cV\phi_{n} - k\phi_{n} \\ -k\phi_{1} & \alpha_{1}^{2} + mV^{2}\phi_{1}^{2}\phi_{1} + cV\phi_{1}\phi_{1} + k\phi_{1}^{2} & mV^{2}\phi_{2}^{2}\phi_{1} + cV\phi_{2}\phi_{1} + k\phi_{2}\phi_{1} & \dots & mV^{2}\phi_{n}^{2}\phi_{1} + cV\phi_{n}\phi_{1} + k\phi_{n}\phi_{1} \\ -k\phi_{2} & mV^{2}\phi_{1}^{2}\phi_{2} + cV\phi_{2}\phi_{2} + k\phi_{2}\phi_{2} & \alpha_{2}^{2} + mV^{2}\phi_{2}^{2}\phi_{2} + cV\phi_{2}\phi_{2} + k\phi_{2}^{2} & \dots & mV^{2}\phi_{n}^{2}\phi_{2} + cV\phi_{n}\phi_{2} + k\phi_{n}\phi_{2} \\ \vdots & \vdots & & \vdots & & \vdots & & \vdots \\ -k\phi_{n} & mV^{2}\phi_{1}^{2}\phi_{n} + cV\phi_{1}\phi_{n} + k\phi_{n}\phi_{n} & mV^{2}\phi_{2}^{2}\phi_{n} + cV\phi_{2}\phi_{n} + k\phi_{2}\phi_{n} & \dots & \alpha_{n}^{2} + mV^{2}\phi_{n}^{2}\phi_{n} + cV\phi_{n}\phi_{n} + k\phi_{n}^{2} \end{bmatrix}$$
(2.65)

$$F(t_d) = \begin{bmatrix} F_1^1 & F_1 & F_2 & \dots & F_n \end{bmatrix}^T$$
 (2.66)

in which

$$F_1^1 = cVh_d'(Vt_d) + kh_d(Vt_d)$$
(2.67)

$$F_{i} = \left[-mV^{2}h_{d}''(Vt_{d}) - cVh_{d}'(Vt_{d}) - kh_{d}(Vt_{d}) - (M+m)g \right] \phi_{n}(Vt_{d})$$

$$(2.68)$$

When a mass, spring and dashpot are used as interface elements, all matrices are time dependent and the effective forces are functions of $h_d(Vt_d)$, $h'_d(Vt_d)$ and $h''_d(Vt_d)$. Therefore the roughness model must be such that $h_d(Vt_d)$, $h'_d(Vt_d)$ and $h''_d(Vt_d)$ exist

and have finite variances. Therefore if filtered white noise is used as a model for roughness, the order of the filter equation must be such that the second derivative exists and has a finite variance.

The vehicle model considered thus far has one contact point or axle. Realistic vehicle models have multiple axles. Therefore the effects of multiple axles are examined next.

2.5 Modeling Lags

 $h_d(Vt_d),Vt_d$ fixed, and $h_d(Vt_d-l),Vt_d-l$ fixed, are two random variables whose correlation is controlled by the filter parameter, Δ_c , and the wheelbase, l. It is proposed here to replace $h_d(Vt_d-l)$ by another process $h_{d_2}(Vt_d)$, which has the same autocovariance as $h_d(Vt_d)$ and is such that the correlation coefficient between $h_d(Vt_d)$ and $h_{d_2}(Vt_d)$ is the same as the correlation coefficient between $h_d(Vt_d-l)$. This is possible because the correlation between two filter responses can be controlled by the assumed zero-time-lag correlation between components of vector-valued white excitation. This is shown as follows: Consider two linear first order ODE's, driven by stationary white noises

$$\frac{\Delta_c}{V} \dot{h}_{d_1}(t_d) + h_{d_1}(t_d) = W_{d_1}(t_d)$$
 (2.69)

$$\frac{\Delta_{c}}{V}\dot{h}_{d_{2}}(t_{d}) + h_{d_{2}}(t_{d}) = W_{d_{2}}(t_{d})$$
(2.70)

The equations are decoupled but $W_{d_1}(t_d)$ and $W_{d_2}(t_d)$ have the following covariance matrix

$$\sum_{W_{d_1}W_{d_2}} = Q\delta(\tau) \tag{2.71}$$

in which

$$Q = q_0 \begin{bmatrix} 1 & \rho_{W_{d_1} W_{d_2}} \\ \rho_{W_{d_1} W_{d_2}} & 1 \end{bmatrix}$$
 (2.72)

 q_0 is the strength of both $W_{d_1}(t_d)$ and $W_{d_2}(t_d)$, $\rho_{W_{d_1}W_{d_2}}$ is the zero-time-lag correlation between $W_{d_1}(t_d)$ and $W_{d_2}(t_d)$. The two equations can be written in matrix, first order form, as:

$$\dot{h}_{d}(t_{d}) = Ah_{d}(t_{d}) + BW_{d}(t_{d})$$
(2.73)

in which

$$W_d\left(t_d\right) = \begin{bmatrix} W_{d_1} & W_{d_2} \end{bmatrix}^T \tag{2.74}$$

$$A = \begin{bmatrix} -\frac{1}{\Delta_c/V} & 0\\ 0 & -\frac{1}{\Delta_c/V} \end{bmatrix}$$
 (2.75)

$$B = \begin{bmatrix} \frac{1}{\Delta_c/V} & 0\\ 0 & \frac{1}{\Delta/V} \end{bmatrix}$$
 (2.76)

The expected value matrix of $h_d(t_d)$ can be obtained by solving the following equation:

$$E \left[h_d \left(t_d \right) \right] = \exp \left[A t_d \right] E \left[h_d \left(0 \right) \right] = \Phi \left(t_d \right) E \left[h_d \left(0 \right) \right] \tag{2.77}$$

in which $\Phi(t_d)$ is a transition matrix, given by:

$$\Phi(t_d) = \begin{bmatrix} \exp\left[-\frac{1}{\Delta_c/V}\right] & 0 \\ 0 & \exp\left[-\frac{1}{\Delta_c/V}\right] \end{bmatrix}$$
(2.78)

The zero-time-lag covariance matrix of h_d is given by:

$$\sum_{h_d(t_d)h_d(t_d)} = \Phi(t_d) \sum_{h_d(0)h_d(0)} \Phi^{T}(t_d) + \int_{0}^{t} \Phi(t_d - u) B\left(\int_{0}^{t} Q \delta(u - v) B^{T} \Phi^{T}(t_d - v) dv\right) du$$
(2.79)

in which u and v arbitrary times between 0 and t and $\tau_d = u - v$. Since W_{d_1} and W_{d_2} are Gaussian white noises, the double convolution integral reduces to

$$\sum_{h_d(t_d)h_d(t_d)} = \Phi(t_d) \sum_{h_d(0)h_d(0)} \Phi^T(t_d) + \int_0^t \Phi(t_d - u) BQB^T \Phi^T(t_d - u) du$$
 (2.80)

For stationary responses, the first term becomes zero. Therefore,

$$\sum_{h_d(t_d)h_d(t_d)} = \int_0^t \Phi(t_d - \tau_d) B Q B^T \Phi^T(t_d - \tau_d) d\tau_d$$
 (2.81)

Solving the integral, the zero-time-lag covariance matrix is:

$$\sum_{h_d(t_d)h_d(t_d)} = \frac{1}{4} \frac{\Delta_c}{V} q_0 \begin{bmatrix} 1 & \rho_{W_{d_1}W_{d_2}} \\ \rho_{W_{d_1}W_{d_2}} & 1 \end{bmatrix}$$
 (2.82)

Therefore,

$$\rho_{h_{d}h_{d_{0}}}(0) = \rho_{W_{d}W_{d_{0}}} \tag{2.83}$$

That is, the correlation between $h_{d_1}(t_d)$ and $h_{d_2}(t_d)$ is equal to the correlation between $W_{d_1}(t_d)$ and $W_{d_2}(t_d)$. Therefore lags are modeled as follows:

From the stationary response of a first order filter, the correlation function, $\rho_{h_d(Vt_d)h_d(Vt_d-l)}$, is known for any lag, l, then $\rho_{W_{d_1}W_{d_2}}$ is set equal to $\rho_{h_d(Vt_d)h_d(Vt_d-l)}$. Let $h_{d_1} = h_d\left(Vt_d\right)$ and $h_{d_2} = h_d\left(Vt_d-l\right)$. So, a first order filter equation is added to model $h_d\left(Vt_d-l\right)$ and both filter equations are excited by correlated white noises with $\rho_{W_{d_1}W_{d_2}} = \rho_{h_d(Vt_d)h_d(Vt_d-l)}$. Then $\rho_{h_{d_1}(Vt_d)h_{d_2}(Vt_d)} = \rho_{h_d(Vt_d)h_d(Vt_d-l)}$.

M,C and $K\left(t_{d}\right)$ for the 4DOF vehicle/guideway coupled system in Equation remain the same, $F\left(t_{d}\right)$ can be rewritten as

$$F(t_d) = \begin{bmatrix} 0 & 0 & k_2 h_{d_1}(t_d) & k_2 h_{d_2}(t_d) & F_1 & \dots & F_n \end{bmatrix}^T$$
 (2.84)

in which

$$F_{i} = -k_{2} \left[h_{d_{1}} \left(t_{d} \right) \phi_{i} \left(V t_{d} \right) + h_{d_{2}} \left(t_{d} \right) \phi_{i} \left(V t_{d} - l \right) \right]$$

$$+ \left[\phi_{i} \left(V t_{d} \right) + \phi_{i} \left(V t_{d} - l \right) \right] \left(\frac{M}{2} + m \right) g$$

$$(2.85)$$

2.6 Conclusions

- Existence of variances of derivative processes depends on the order of linear filter equations (driven by white noise).
- Appearance of higher order derivative processes, h' and h'', and parametric terms in system equations depend on type of interface between vehicle and guideway, i.e., a mass-dashpot-spring interface has h, h' and h'' (whose variances must exist) in the forcing function. It also has parametric terms in M(t), C(t) and K(t).
- Multiple axle vehicles have a kinematic filtering effect on system excitation. A
 first order filter is added to model an excitation with lag and filter equations are
 excited by correlated white noises in order to have an appropriate zero-time-lag
 cross-correlation between any two roughness processes.
- In this work, only interfaces between a vehicle and guideway are considered, therefore first order filters are sufficient.

References

- 1. Chan, T.H.T., Yu, L., and Law, S.S. Comparative studies on moving force identification from bridge strains in laboratory. *J. of Sound and Vibration* 235 (2000), 87-104.
- 2. Cheng, Y.S., Au, F.T.K., Cheung, Y.K., and Zheng, D.Y. On the separation between moving vehicles and bridge. *J. of Sound and Vibration* 222 (1999), 781-801.
- 3. Cheung, Y.K., Au, F.T.K., Zheng, D.Y., and Cheng, Y.S. Vibration of multi-span non-uniform bridges under moving vehicles nad trains by using modified beam vibration functions. *J. of Sound and Vibration* 228 (1999), 611-628.
- 4. Cho, D.S., and Lee, W.K. Modal interactions of a randomly excited hinged-clamped beam. *J. of sound and Vibration* 237 (2001), 377-393.

- 5. Dahlberg, T. Parametric optimization of a sdof vehicle travelling on a random profiles road. *J. of Sound and Vibration* 55 (1977), 245-253.
- 6. Dahlberg, T. Ride comfort and road holding of a 2dof vehicle travelling on a randomly profiled road. *J. of Sound and Vibration* 58 (1978), 179-187.
- 7. Dodds, C.J., and Robson, J.D. The description of road surface roughness. *J. of Sound and Vibration* 31 (1973), 175-183.
- 8. Gasparini, D.A., and Kanj, N. Response of vehicles movign on rough concrete floors. *ACI Structural Journal* (Sept 1989), 546-550.
- Gasparini, D.A., Petrou, M., and Ozer, M.E. Wavelength content of concrete floors and its significance for moving vehicles. *ACI Structural Journal* (1990), 706-715.
- 10. Grigoriu, M. Applied Non-Gaussian Processes. Prentice Hall, 1995.
- 11. Haldar, A., and Mahadevan, S. *Realiability Assessment Using sTochastic Finite Element Analysis*. John Wiley and Sons, 2000.
- 12. Hammond, J.K., and Harrison, R.F. Nonstationary response of vehicles on rough ground-state space approach. *J. of Dynamic Systems, Measurement and Control* 103 (1981), 245-250.
- 13. Harrison, R.F., and Hammond, J.K. Analysis of the nonstationary response of vehicles with multiple wheels. *J. of Dynamic Systems, Measurement and Control* 108 (1986), 69-73.
- 14. Henchi, K., Fafard, M., Dhatt, G., and Talbot, M. An efficient algorithm for dynamic analysis of bridges under moving vehicles using a coupled modal and physical components approach. *J. of Sound and Vibration* 212 (1998), 663-683.
- 15. Law, S.S., Chan, T.H.T., and Zeng, Q.H. Moving force identification: A time domain method. *J. of Sound and Vibration* 210 (1997), 1-22.
- 16. Law, S.S., and Zhu, X. Study on different beam models in moving force identification. *J. of Sound and Vibration*234 (2000), 661-679.
- 17. Liu, C. Vehicle-road interaction, evolution of road profiles and present service ability index. *Road Material and Pavement Design* 1 (2000), 35-51.

- 18. Marchesiello, S., Fasana, A., Garibaldi, L., and Piombo, B.A.D. dynamics of multi-span continuous straight bridges subject to mdof moving vehicle excitation. *J. of Sound and Vibration* 224 (1999), 541-561.
- 19. Muller, P.C., Popp, K., and Schiehlen, W.O. Nonlinear stochastic guideway-vehicle-systems. In *Proceeding of the Vehicles on Roads and on Tracks* (1979).
- 20. Okabayashi, T. Probabilistic structural analysis based on random differential equation. *Transactions of JSCE* 13 (1981), 360-363.
- 21. Pesterev, A.V., and Bergman, L.A. Response of elastic continuum carrying moving linear oscillator. *J. of Engineering Mechanics* (Aug 1997), 878-889.
- 22. Raju, G.V., and Narayanan, S. Optimal estimation and control of nonstationary response of a 2dof vehicle model. *J. of Sound and Vibration* 149 (1991), 413-428.
- 23. Sadiku, S., and Leipholz, E. On the dynamics of elastic systems with moving concentrated masses. *Ingenieur-Archiv* 57 (1987), 223-242.
- 24. Smith, C.C., and Wormley, D.N. Response of continuous periodic supported guideway beams to traveling vehicle loads. *J. of Dynamic Systems, Measurement and Control*(1975), 21-29.
- 25. Snyder, III, J.E., and Wormley, D.N. Dynamic interactions between vehicles and elevated, flexible randomly irregular guideways. *J. of Dynamic Systems, Measurement and Control* (1977), 23-33.
- 26. Stanisic, M. On a new theory of the dynamic behavior of the structures carrying movingmasses. *Ingenieur-Archiv* 55 (1985), 176-185.
- 27. Thompson, D.J. On the relastionship between wheel and rail surface roughness nad rolling noise. *J. of Sound and Vibration* 193 (1996), 149-160.
- 28. Wu, J.S., and Shih, P.Y. Dynamic responses of railway and carriage under the high speed moving loads. *J. of Sound and Vibration* 136 (1990), 323-342.
- 29. Xia,H., Xu, Y.L. and Chan, T.H.T. Dynamic interaciton of long suspension bridge with running trains. *J. of Sound and Vibration* 237 (2001), 263-280.
- 30. Yadav, D., and Nigam, N.C. Ground induced nostationary response of vehicles. *J. of Sound and Vibration* 61 (1978), 117-126.

CHAPTER 3

DYNAMIC RESPONSES OF A TWO-SPAN BEAM SUBJECTED TO HIGH SPEED 2DOF SPRUNG VEHICLES

3.1 Introduction

The principal objective of this work is to perform studies of coupled vehicle-structure dynamic systems to guide the design of structures for high-speed vehicles. The random roughness is modeled by filtered white noise. The structure is modeled as a two-equal-span prismatic flexure beam. The vehicle is modeled as a series of 2DOF vehicles. System parameters are nondimensionalized and the equations of motion are written in state space. Here the equations for the mean and zero-time-lag covariance matrices of the state vector are solved using modal technique. *Static* values of a set of responses are determined, the statistical moments of the dynamic responses are normalized by the corresponding maximum static values. Therefore statistical moments of all responses are expressed in terms of *dynamic amplification factors* (DAF). Extensive parametric studies are presented that identify effects of important nondimensional parameters on the behavior of coupled vehicle-structure systems. This work provides designers of structures for high-speed vehicles insights on effects of nondimensional system parameters on behavior and quantifies values of DAF that may be produced by high-speed vehicles.

3.2 Coupled vehicle-structure system equations in state space

The dynamic response of a structure traversed by a vehicle is assumed to be completely defined by a vertical displacement function, v(x,t) [1]. The vertical displacement of the structure is here expressed in the modal domain as follows:

$$v(x,t) = \sum_{i=1}^{n} y_i(t)\phi_i(x)$$
 (3.1)

in which $\phi_i(x)$ is the i^{th} mode shape and $y_i(t)$ is i^{th} modal coordinate. The total displacement at an interface of a vehicle with a structure having surface roughness, h(x), is [2]:

$$v^{t}(x,t) = v(x,t) + h(x)$$
(3.2)

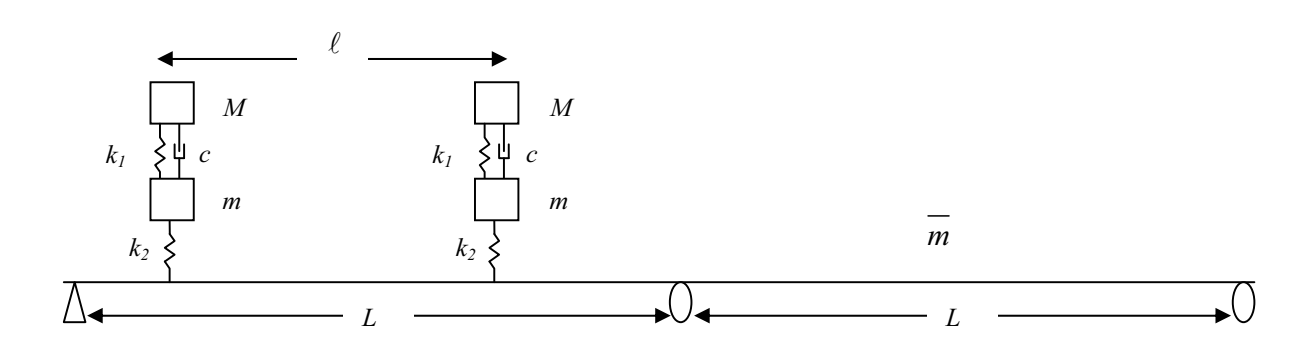
The surface profile, h(x), can be modeled as an output of a shaping filter to a white noise [3, 4] expressed by:

$$\Delta_c h'(x) + h(x) = W(x) \tag{3.3}$$

in which Δ_c is a correlation distance and W(x) is a zero-mean white process with intensity S_0 or strength q_0 .

The coupled vehicle-structure models considered in this research are shown in Fig. 3.1. Figure 3.1a) shows two of 2DOF vehicle models, each one can be considered as a half-car model [5]. Then, a distance between two models is called wheelbase, ℓ . Figure 3.1b) shows a model for eight of 2DOF vehicle models with the total length equal to the wheelbase in Fig. 3.1a). It can be used to study effects of number of vehicle axles to the system. Structure model considered here is a two-equal-span prismatic flexure beam as shown in Fig. 3.1.

a.



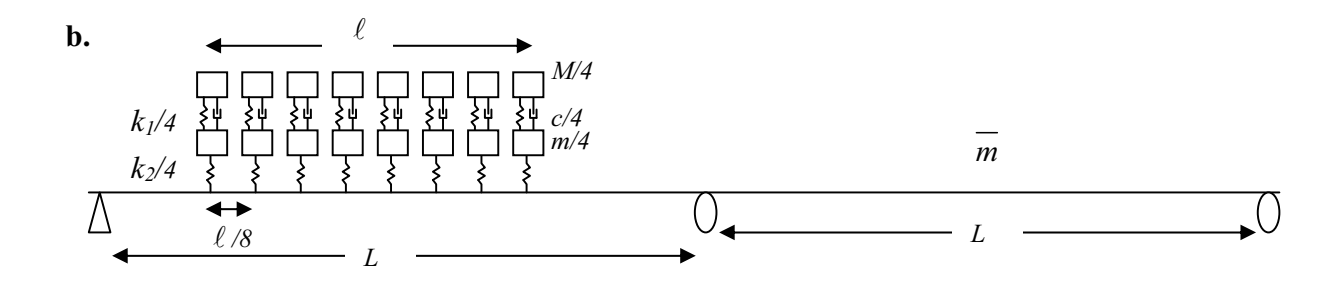


Figure 3.1 Models of coupled vehicle structure system: a. two of 2DOF vehicle model, b. eight of 2DOF vehicle model

The coupled linear system equations driven by correlated white noises are then written in state form:

$$\dot{X}(t) = A(t)X(t) + BW(t) + C(t), \qquad X(0)$$
 (3.4)

in which X(t) is a state vector, W(t) is a vector of correlated white noises, A and B are matrices of appropriate dimension, C(t) is a vector of deterministic excitation and X(0) is an initial condition of the system. Taking the expectation operator, the equation for expected value vector is:

$$E[\dot{X}(t)] = A(t)E[X(t)] + C(t), \quad E[X(0)]$$
(3.5)

in which E[X(t)] is a vector of expected values of state variables with an initial condition, E[X(0)]. The term BW(t) disappears because W(t) is a zero mean vector.

The zero-time-lag covariance matrix of the state vector, Σ_{XX} , may be solved from the well-known first order Lyapunov equation, given by:

$$\dot{\Sigma}_{XX} = A \Sigma_{XX} + \Sigma_{XX} A^T + BQB^T, \qquad \Sigma_{XX}(0)$$
(3.6)

in which $\Sigma_{XX}(0)$ is an initial condition of the covariance matrix and Q is a strength matrix for the vector white noises,

$$Q = q_0 \begin{pmatrix} 1 & \dots & \rho_{W_i W_j} \\ \vdots & \ddots & \vdots \\ \rho_{W_i W_j} & \dots & 1 \end{pmatrix}$$

$$(3.7)$$

in which q_0 is a strength of the white noise and $\rho_{W_iW_j}$ is the zero-time-lag correlation coefficient between two white noises.

3.3 Parametric study and results

The equations of motion of this coupled system are written in state space. To facilitate parametric studies, all quantities are nondimensionalized as follow,

Position - x/L, Time -Vt/L, Roughness -W/L and h/L

White noise intensity $-q_0/L^3 = 0.0625 \times 10^{-6}$ for rail roughness

Autocorrelation distance - $\Delta_c / L = 2.50$

Distance between two vehicles - ℓ/L (show in Table 4.1)

Masses -
$$\mu = M / \overline{m}L = 0.20, \ \eta = m / \overline{m}L = 0.1 \ \mu$$

Frequencies -
$$f_{k_1} = \sqrt{\frac{k_1/\overline{m}L}{\omega_1^2}} = 0.05$$
, $f_{k_2} = \sqrt{\frac{k_2/\overline{m}L}{\omega_1^2}} = 0.20$, $f_g = \sqrt{\frac{g/L}{\omega_1^2}} = 0.01$,

$$f_c = \frac{c / \overline{m}L}{\omega_1} = 0.02$$

Speed -
$$f_v = \frac{V/L}{\omega_1} = 0.06, 0.08, 0.10, 0.12$$

Fundamental frequencies of a two-span beam - $f_i = \omega_i / \omega_1$

Damping ratio, ξ , for the beam is assumed 0.01.

For design of the guideway structure, the statistical moments of the structure responses are essential. The computed beam responses are displacement and moment at midspan, moment at the middle support and the shear at 0.95L. Time histories of the expected values of beam responses are plotted in Figures 3.2 to 3.11 for $\ell/L = 0.5$, 0.6, 0.7 and $f_{\nu} = 0.06$, 0.08, 0.10, 0.12.

3.3.1 Effect of span passage rate, f_v - Span passage rate is a ratio of V/L to a first beam frequency, ω_1 . Assuming that a 20m-two-span beam has a frequency of 7 Hz,

$$f_{res.} = V/(2L)$$

7 Hz = $V/(2*20m)$
 $V = 280m/s$

A velocity of 280 m/s or 1000 km/h is impossible for a ground transportation system [6]. However, there are many other frequencies in the system, including the vehicle axle arrival rate and the fundamental frequencies of the vehicle.

3.3.2 Effect of axle arrival rate, f_a - The axle arrival rate is V/ℓ or, in terms of rad/sec, $2\pi V/\ell$. It can be nondimensionalized by ω_1 . The nondimensional arrival rate, denoted by f_a , may be written in terms of f_v and ℓ/L as shown in Table 3.1. The nondimensional frequencies of the first two modes of the two-span beam are $f_1 = 1$ and $f_2 = 1.57$.

Table 3.1 Vehicle axle arrival rate and span passage rate for high speed

f_a for L = 20 m		f_{v} (speed, km/h)				
and $f_{beam} = 7$ Hz.		0.06(190)	0.08	0.10	0.12(380)	
	0.40	<u>0.94</u>	1.26	<u>1.57</u>	1.88	
	0.50	0.75	<u>1.01</u>	1.26	<u>1.51</u>	
ℓ/L	0.60	0.63	0.84	<u>1.05</u>	1.26	
	0.70	0.54	0.72	0.90	<u>1.08</u>	

For $f_{\nu}=0.06$ to 0.12 (V=190 to 380 km/h for beam span 20 m and frequency 7 Hz) - at high velocity level - vehicle is assumed to be rail vehicle system. Thus, the roughness model for the rail system is used here. The combinations of f_{ν} and ℓ/L that cause resonance are shown in Table 3.1. If $\ell/L=0.5$ and $f_{\nu}=0.08$ the axle arrival rate equals the fundamental frequency. For typical values of ω_1 and L, $f_{\nu}=0.08$ corresponds to a velocity of 70 m/s (250 km/h). If $\ell/L=0.5$ and $f_{\nu}=0.12$, the axle arrival rate equals the second natural frequency. Therefore it is possible for the axle arrival rate to be in resonance with the first and second beam frequencies, for feasible vehicle speeds. Let ℓ/L be fixed at 0.5 and the span passage rate, f_{ν} , be 0.08 (\approx 250 km/h). Figures 3.2 and

3.3 show that the displacement and the moment at midspan have the largest amplification. The maximum expected values of dynamic amplifications are 1.32 and 1.22 respectively (recall that multiples of standard deviations of amplification factors must be added to determine *design* amplification factors). It is simply because the first mode is excited, f_a matches f_1 , and the displacement and moment at midspan are two responses dominated by this fundamental asymmetric mode. When the span passage rate increases to 0.12 (\approx 380 km/h), the moment at the interior support is amplified by as much as 1.32 (Fig. 3.4) which is more than the other responses. In this case the second mode, the symmetric mode, is excited. A response dominated by this symmetric second mode is the moment at the interior support. For $\ell/L = 0.6$ and 0.7, only the first mode is excited (Figs. 3.2 and 3.3) for realistic velocities (less than 380 km/h). If ℓ/L is greater than 0.5, the axle arrival rate is unlikely to be in resonance with the second mode since the velocity corresponding to that resonance mode is well above a practical level. If ℓ/L is greater than 1, f_a will never match f_1 and resonance due to f_a never occurs.

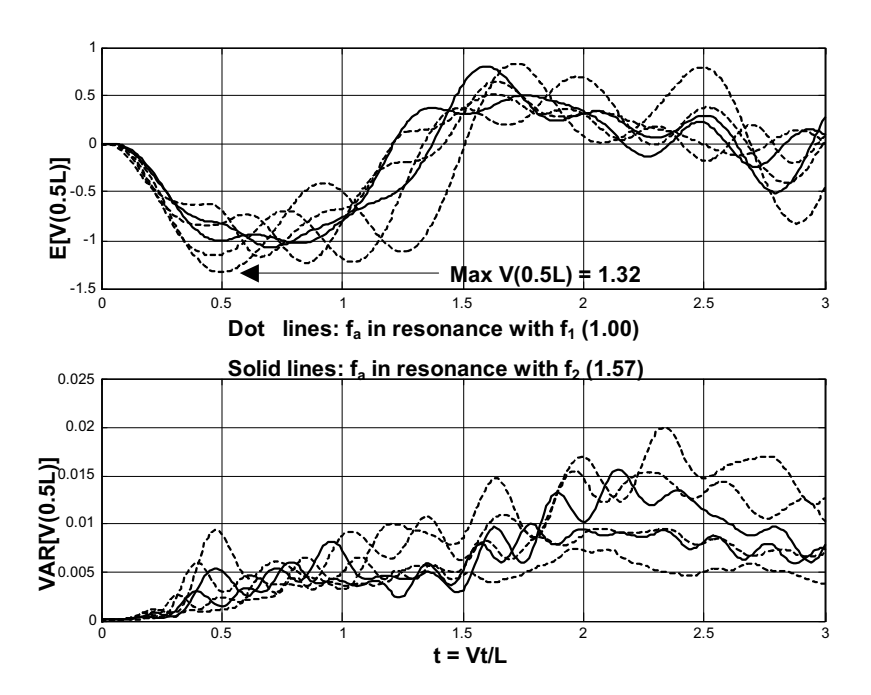


Figure 3.2 Time history of expected values and variances of displacement at midspan

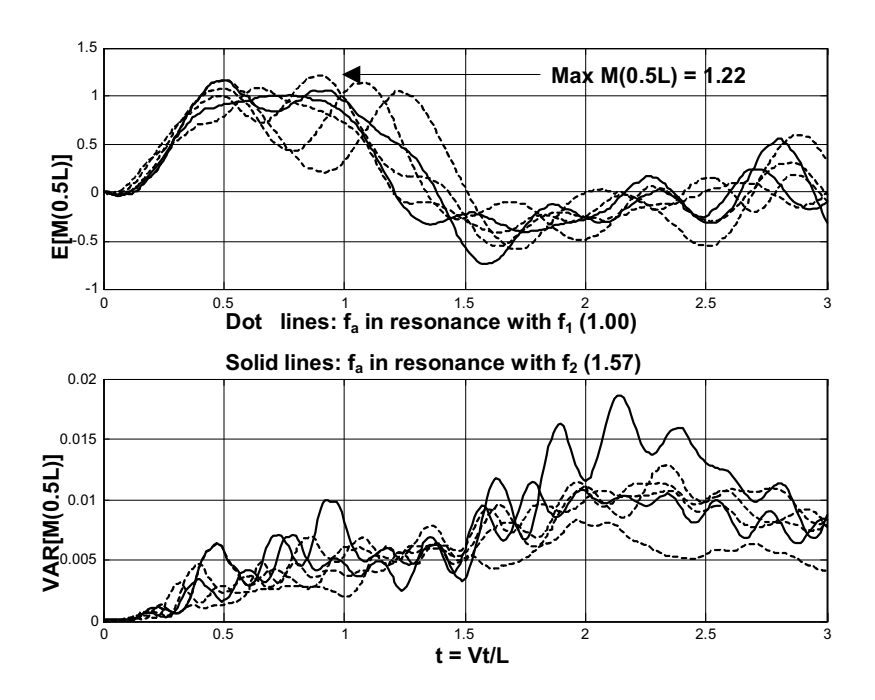


Figure 3.3 Time history of expected values and variances of moment at midspan

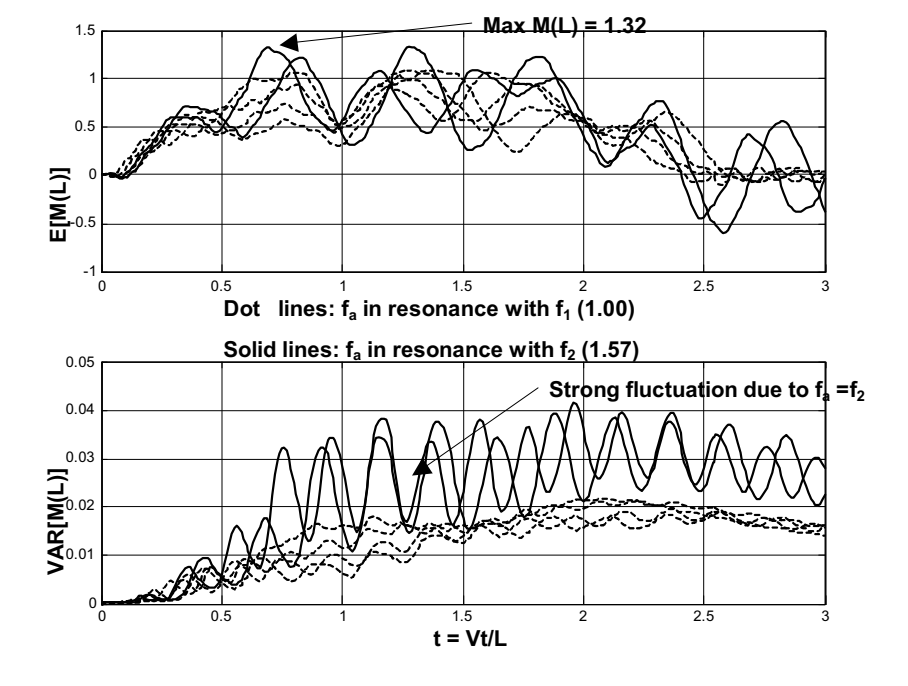


Figure 3.4 Time history of expected values and variances of moment at interior support

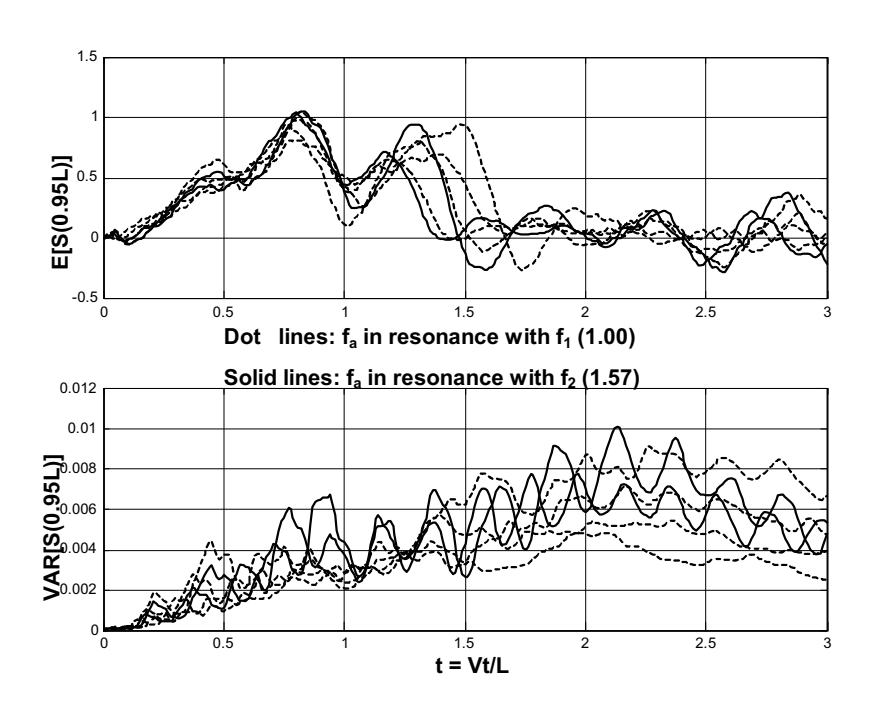


Figure 3.5 Time history of expected values and variances of shear at 0.95L

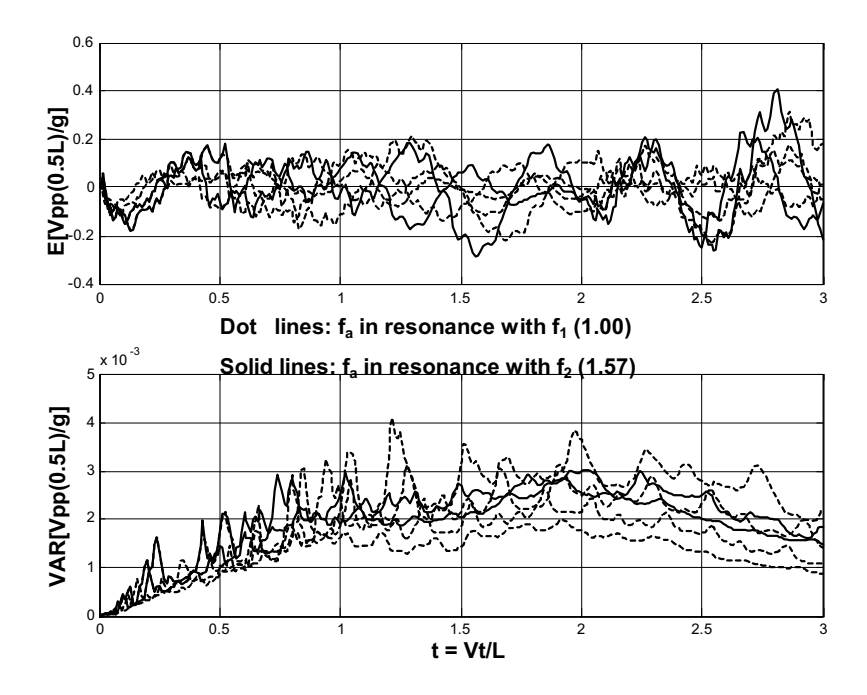


Figure 3.6 Time history of expected values and variances of beam acceleration at midspan

The shear (figure 3.5) is different from the other responses as all of the modes (both asymmetric and symmetric modes) participate in this response. Figure 3.6 shows time history of expected value and variance of beam acceleration at midspan. It is found that the maximum expected beam acceleration is 0.4g (quite high) and occurs after vehicles left the span.

For a high-speed ground transportation system there is a possibility to have resonance between the axle arrival rate and the second mode frequency. For this condition the moment at the middle support needs to be examined closely.

3.3.3 Effect of number of axles (interfaces)

For high speed vehicle, i.e. maglev (magnetic levitated vehicle), the suspension system can have more than two contact points. More contact points can benefit the design of the system. Figures 3.7 to 3.10 (also Table 3.2 and 3.3) show the expected beam responses reduce, i.e. E[M(L)] reduces from 1.32 to 1.10, when eight suspensions are used. This suspension arrangement can also reduce strong fluctuation in VAR[M(L)] dramatically (Figs. 3.4 and 3.9). Figure 3.11 shows the expected beam acceleration at midspan reduces from 0.4g in figure 4.6 to 0.16g.

Table 3.2 The maximum beam responses when f_a is in resonance with f_1 for two different suspension configurations

Y = Structural	Two contact		Eight contact	
Responses	points		points	
	E[Y]	VAR[Y]	E[Y]	VAR[Y]
v(0.5L)	1.32	0.0200	1.20	0.0105
M(0.5L)	1.22	0.0125	1.15	0.0105
M(L)	1.10	0.2100	1.10	0.0280
S(0.95L)	1.00	0.0090	1.10	0.0090
$\ddot{v}(0.5L)/g$	0.30	0.0040	0.14	0.0025

Table 3.3 The maximum beam responses when f_a is in resonance with f_2 for two different suspension configurations

Y = Structural	Two contact		Eight contact	
Responses	points		points	
	E[Y]	VAR[Y]	E[Y]	VAR[Y]
v(0.5L)	1.05	0.015	1.25	0.0100
M(0.5L)	1.20	0.019	1.20	0.0100
M(L)	1.32	0.041	1.10	0.0260
S(0.95L)	1.05	0.010	1.10	0.0085
$\ddot{v}(0.5L)/g$	0.40	0.003	0.16	0.0035

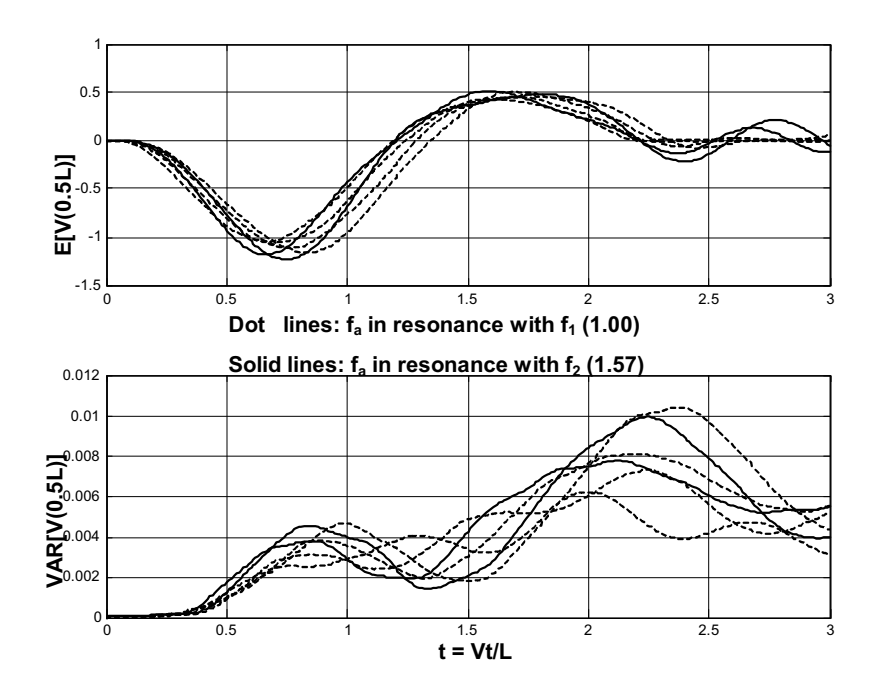


Figure 3.7 Time history of expected values and variances of displacement at midspan

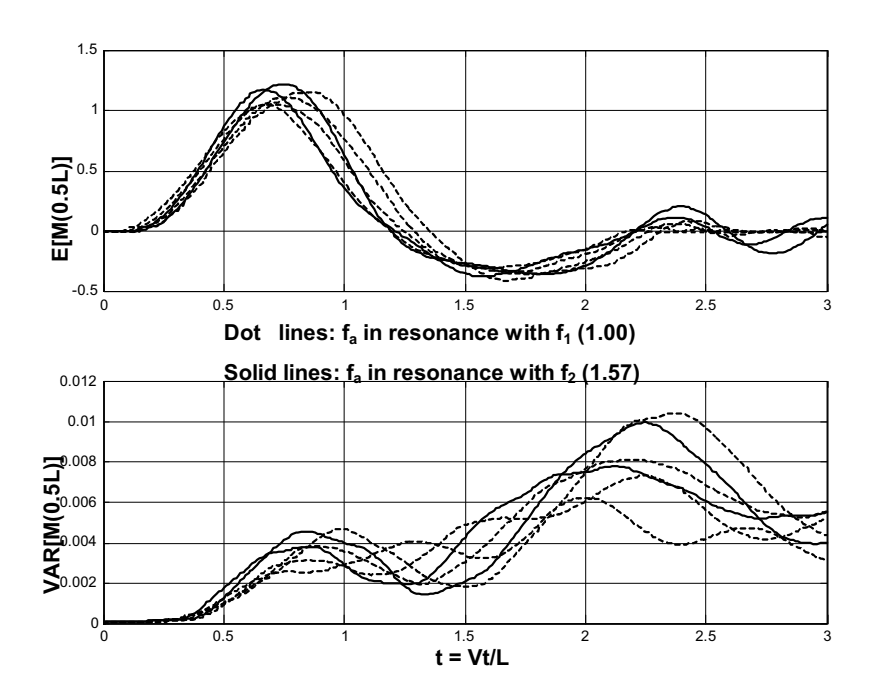


Figure 3.8 Time history of expected values and variances of moment at midspan

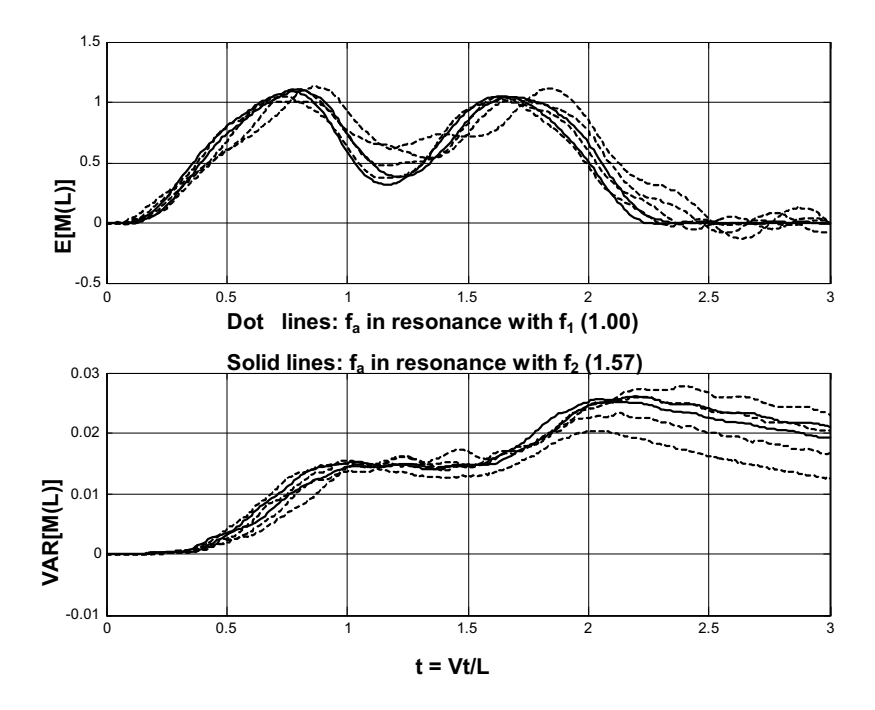


Figure 3.9 Time history of expected values and variances of moment at interior support

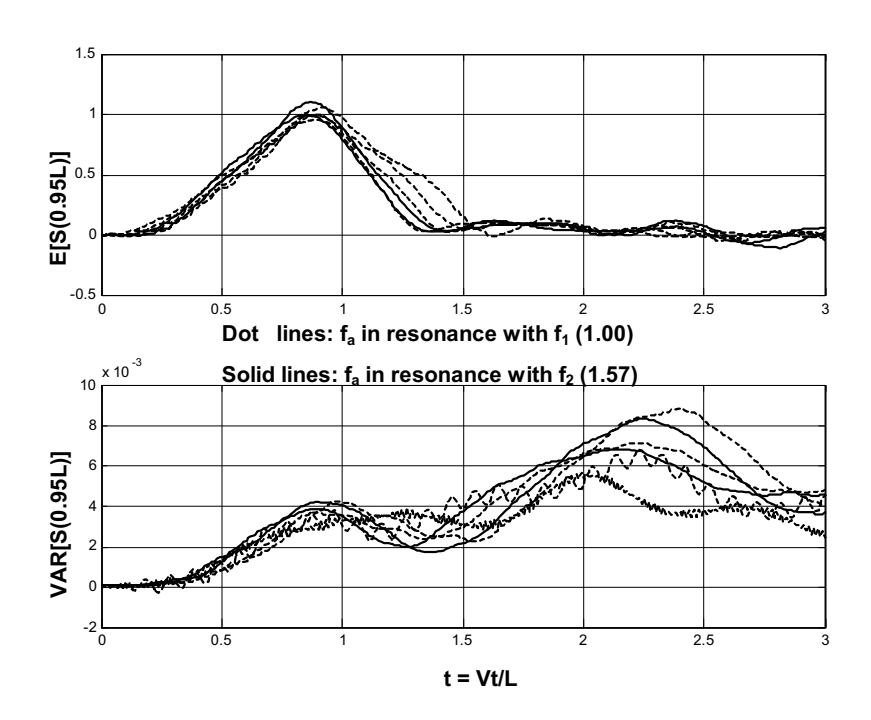


Figure 3.10 Time history of expected values and variances of shear at 0.95L

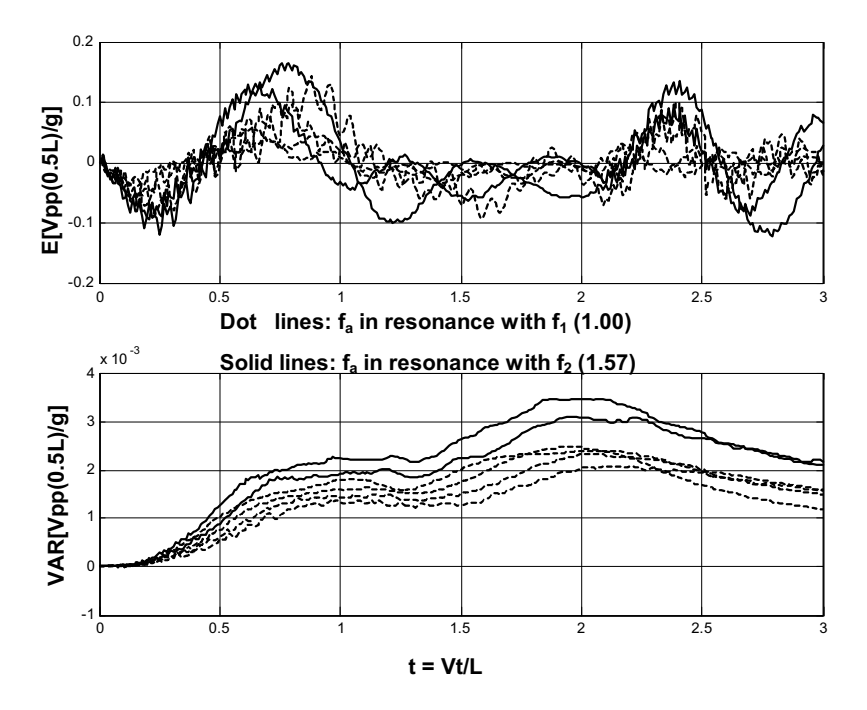


Figure 3.11 Time history of expected values and variances of beam acceleration at midspan

3.3.4 Effect of fundamental frequencies of vehicle

Natural frequencies of the car body (normally low) may not be equal to the first mode frequency of a typical short-span bridge unless the primary and secondary springs are very stiff. It is not realistic to have such a stiff suspension [7], since passenger comfort criteria may not be met. For a structure with low frequency such as a large suspension bridge [8], there is a chance of a structure frequency matching a vehicle frequency. However, the mass of the vehicle is very small compared to the mass of a suspension bridge, so significant dynamic amplification is not likely.

3.4 Conclusion

Random vibration time history analyses provide vehicle and structure responses that can define appropriate surface smoothness requirements and design amplification factors for structure for high speed vehicles. Mean value and covariance matrix of system responses can be determined.

It is found that one specific value of a nondimensional parameter may cause a maximum in one response while a different value may cause a maximum in another response. For two-span beam, the moment at the interior support can have high dynamic amplification factors when axle arrival rate matches to the second natural frequency of the beam.

For high speed rail system, an appropriate suspension configuration of vehicle can reduce the expected value and variance of DAF of beam responses.

References

- 1. Fryba, L. *Vibration of Solids and Structures under Moving Loads*. Groninggen: Noordhoff International Publishing, 1972.
- 2. Gasparini, D.A., Petrou, M., and Ozer, M.E. Wavelength content of concrete floors and its significance for moving vehicles. *ACI Structural Journal* (1990), 706-715.
- 3. Seetapan P. Dynamics of high speed traversing structures with random surfaces. Ph.D. thesis, Case Western Reserve University, USA, 2001.
- 4. Seetapan P. and Gasparini D.A. Dynamic of bridge for very high speed vehicle. In *Proceedings of the EURODYN'02*, *Structural Dynamics*, Munich, Germany (2002).
- 5. Au, F.T.K., Wang, J.J., and Cheung, Y.K. Impact study of cable-stayed bridge under railway traffic using various models. *J. of Sound and Vibration* 240 (2001), 277-283.
- 6. Marchesiello, S., Fasana, A., Garibaldi, L., and Piombo, B.A.D. dynamics of multispan continuous straight bridges subject to mdof moving vehicle excitation. *J. of Sound and Vibration* 224 (1999), 541-561.
- 7. Tamboli, J.A., and Joshi, S.G. Optimum design of a passive suspension system of a vehicle subjected to actual random road excitations. *J. of Sound and Vibration* 219 (1999), 193-205.
- 8. Xia, H., Xu, Y.L. and Chan, T.H.T. Dynamic interaction of long suspension bridge with running trains. *J. of Sound and Vibration* 237 (2001),263-280.

CHAPTER 4

CONCLUSIONS

The interface model determines which system matrices become time-dependent and whether derivatives of roughness enter the governing equations. If a simple axial spring is used as an interface model, then only the system stiffness matrix is nonautonomous and derivatives of roughness are not needed. For a linear spring interface, roughness may be modeled by the responses of cascaded linear first order differential equations driven by white noise.

Multi-axle vehicle models introduce a length parameter or wheelbase into the governing equations. This length leads to ystem equations that depend on the roughness at several positions that lag behind the leading axles. Here, roughness processes with lags are also modeled by responses of linear first order differential equations. The vector of roughness processes is driven by a vector of correlated white noises such that all roughness processes have the same autocovariance function and the appropriate zero-time-lag cross-correlation. This new formulation for the excitation, W(t), in turn allwos a Markov vector random vibration approach.

All qutities of the interface, vehicle, roughenss and structure models are nondimensionalized. The vehicle speed and its wheelbase are represented by the span crossing rate, $f_{\nu} = \frac{V/L}{\omega_{\rm l}}$, and the axle arrival rate, $f_a = \frac{V/\ell}{\omega_{\rm l}}$. Time is nondimensionalized by the time required to cross one span of a structure.

The coupled system equations are written as a linear, first order, matrix stochastic differential equaiton. The equation has *deterministic parametric excitation* in the sense that the system matrix is a *known* function of time. It has *deterministic additive excitation* from the mass of the moving vehicle entering a span and it has *random additive excitation* from the random roughness. Deterministic linear ordinary differential equations for the mean and covariance matrices of the state vector follow directly. These

moments of the state vector may in turn be used to compute corresponding moments of any structural responses.

Important system parameters include the wheelbase-to-span ratio, ℓ/L and the span crossing rate, $2\pi f_v = \frac{V/L}{f_1}$. For realizable combinations of ℓ/L and $\frac{V/L}{f_1}$, the axle arrival rate, $2\pi f_a = \frac{V/\ell}{f_1}$, can become equal to the first or second frequencies of typical structures. If this occurs, high expected values of dynamic amplification factors are likely. The number of axles also has effects to the structure. For the two-span beam, it yields the lower dynamic amplification factors for the vehicle with more axles.

Values of dynamic amplification factors are computed for a set of responses of a two-span beam traversed by a series of 2DOF vehicle model. Different parameter combinations yield the largest dynamic amplification factors for different responses. For the two-span beam, the moment at the interior support can have high dynamic amplification factors.

This work considers only planar systems and passive vehicle models. For design, it may be necessary to use three-dimensional models and, possibly, vehicle model with variable speed.

Output

Outputs of this research are as follows;

- 1. Pritsathat Seetapan and Somchai Chucheepsakul, Dynamic Responses of A Two-Span Beam Subjected to High Speed 2DOF Sprung Vehicles, *International Journal of Structural Stability and Dynamics*, submitted.
- 2. Pritsathat Seetapan, Akesit Maiwattana, and Somchai Chucheepsakul, Significance of Surface Roughness to Moving Vehicles and Infrastructures, *Proceeding in the Tenth National Covention on Civil Engineering*, 2-4 May 2548, SIE 40-45.
- 3. Pritsathat Seetapan, Akesit Maiwattana, and Somchai Chucheepsakul, Dynamic Responses of A Two-Span Beam Subjected to 2DOF Sprung Vehicles, *Proceeding in the Tenth National Covention on Civil Engineering*, 2-4 May 2548, STR 52-57.

Appendix

DYNAMIC RESPONSES OF A TWO-SPAN BEAM SUBJECTED TO HIGH SPEED 2DOF SPRUNG VEHICLES

Pritsathat Seetapan[†],* Somchai Chucheepsakul[‡]

[†]Department of Civil Engineering, Naresuan University, Phitsanulok 65000, Thailand pseetapan@hotmail.com

*Department of Civil Engineering, King Mongkut's University of Technology Thonburi, Bangkok 10140, Thailand somchai.chu@kmutt.ac.th

*To whom all correspondence should be addressed

ABSTRACT: The deflection-, bending moment-, shear- and acceleration-time histories of a two-span beam subjected to moving sprung vehicles are presented. The vehicle model is a 2DOF system with a constant velocity. The two-span beam with rough surface is used as structure model. It is defined in modal domain by natural frequencies, mode shapes and modal damping values. The rough surface is modeled by filtered white noise. The equations of motion for the coupled vehicle-structure system are formulated. All variables in the system equation are nondimensionalized. The first order linear stochastic differential equations are solved. The effects of the span passage rate and other important parameters are studied.

Keywords: Coupled vehicle-structure system; Random roughness; Dynamic response; Two-span beam.

1. Introduction

The problem of vehicle-structure interaction has been the subject of study during the last few years. Early work adopted to model vehicle-bridge system by Biggs¹, Fryba² and Timoshenko, *et*

al.,³ considered simply supported beam with a moving point load/sprung mass at constant speed along its span. Since guideway structures are getting lighter and more flexible, while the speed and the weight of vehicular loads tend to be higher, other detailed models were developed. Multiple axle, multiple degree of freedom models were used for vehicle models,⁴⁻⁶ and different kinds of structures such as simply supported beam, multiple-span beam or nonprismatic beam were analyzed.⁷⁻¹⁰ Most of these studies have solved equations of motion by numerical integration. Many researchers, Lin, et al.,¹¹ Henchi, et al.,¹² and Hino, et al.¹³ used the finite element method to model and analyze structures. Several others employed Fourier series and Fourier Transforms.⁸ Later, more studies have concentrated on analyses of dynamic responses of the vehicle and structure coupling system with random roughness surface. Power spectral density technique of representing random surface roughness have been developed. ¹⁴⁻¹⁹

The principal objective of this work is to perform studies of coupled vehicle-structure dynamic systems to guide the design of structures for high-speed vehicles. The random roughness is modeled by filtered white noise. The structure is modeled as a two-equal-span prismatic flexure beam. The vehicle is modeled as a series of 2DOF vehicles. System parameters are nondimensionalized and the equations of motion are written in state space. Here the equations for the mean and zero-time-lag covariance matrices of the state vector are solved using modal technique. *Static* values of a set of responses are determined, the statistical moments of the dynamic responses are normalized by the corresponding maximum static values. Therefore statistical moments of all responses are expressed in terms of *dynamic amplification factors* (DAF). Extensive parametric studies are presented that identify effects of important nondimensional parameters on the behavior of coupled vehicle-structure systems. This work provides designers of structures for high-speed vehicles insights on effects of nondimensional system parameters on behavior and quantifies values of DAF that may be produced by high-speed vehicles.

2. Coupled vehicle-structure system equations in state space

The dynamic response of a structure traversed by a vehicle is assumed to be completely defined by a vertical displacement function, v(x,t). The vertical displacement of the structure is here expressed in the modal domain as follows:

$$v(x,t) = \sum_{i=1}^{n} y_i(t)\phi_i(x)$$
 (1)

in which $\phi_i(x)$ is the i^{th} mode shape and $y_i(t)$ is i^{th} modal coordinate. The total displacement at an interface of a vehicle with a structure having surface roughness, h(x), is: 14-19

$$v^{t}(x,t) = v(x,t) + h(x) \tag{2}$$

The surface profile, h(x), can be modeled as an output of a shaping filter to a white noise $^{15, 20-22}$ expressed by:

$$\Delta_{\circ}h'(x) + h(x) = W(x) \tag{3}$$

in which Δ_c is a correlation distance and W(x) is a zero-mean white process with intensity S_0 or strength q_0 .

The coupled vehicle-structure models considered in this research are shown in Fig. 1. Figure 1a) shows two of 2DOF vehicle models, each one can be considered as a half-car model.⁵ Then, a distance between two models is called wheelbase, ℓ . Figure 1b) shows a model for eight of 2DOF vehicle models with the total length equal to the wheelbase in Fig. 1a). It can be used to

study effects of number of vehicle axles to the system. The 2DOF vehicle model has two vertical DOFs denoted by v_v and v_1 located at the center of mass of the car and the suspension mass. Each vehicle axle has primary and secondary suspensions. The primary suspension is a linear spring, k_2 . This spring may represent a tyre stiffness or a magnetic force in the case of magnetic levitated vehicle (maglev). The secondary suspension which attached between mass M and m is a kelvin type of interface; i.e. a linear spring, k_1 , and dashpot, c, in parallel. Note that M represents mass of car, m represents a suspension mass, and vehicle speed, V, is assumed constant. Other parameters in the vehicle-structure system are: span length, L, unit mass of a two-equal-span prismatic flexure beam, \overline{m} .

The coupled linear system equations driven by correlated white noises are then written in state form:

$$\dot{X}(t) = A(t)X(t) + BW(t) + C(t), \qquad X(0)$$
 (4)

in which X(t) is a state vector, W(t) is a vector of correlated white noises, A and B are matrices of appropriate dimension, C(t) is a vector of deterministic excitation and X(0) is an initial condition of the system. Taking the expectation operator, the equation for expected value vector is:

$$E[\dot{X}(t)] = A(t)E[X(t)] + C(t), \quad E[X(0)]$$
 (5)

in which E[X(t)] is a vector of expected values of state variables with an initial condition, E[X(0)]. The term BW(t) disappears because W(t) is a zero mean vector.

The zero-time-lag covariance matrix of the state vector, Σ_{XX} , may be solved from the well-known first order Lyapunov equation, given by:

$$\dot{\Sigma}_{XX} = A \Sigma_{XX} + \Sigma_{XX} A^T + BQB^T, \qquad \Sigma_{XX}(0)$$
(6)

in which $\Sigma_{XX}(0)$ is an initial condition of the covariance matrix and \boldsymbol{Q} is a strength matrix for the vector white noises,

$$Q = q_0 \begin{pmatrix} 1 & \dots & \rho_{w_i w_j} \\ \vdots & \ddots & \vdots \\ \rho_{w_i w_j} & \dots & 1 \end{pmatrix}$$
 (7)

in which q_0 is a strength of the white noise and $\rho_{W_iW_j}$ is the zero-time-lag correlation coefficient between two white noises.

3. Parametric study and results

The equations of motion of this coupled system are written in state space. To facilitate parametric studies, all quantities are nondimensionalized as follow,

Position - x/L, Time - Vt/L, Roughness - W/L and h/L

White noise intensity $-q_0/L^3 = 0.0625 \times 10^{-6}$ for rail roughness

Autocorrelation distance - $\Delta_c / L = 2.50$

Distance between two vehicles - ℓ/L (show in Table 1)

Masses -
$$\mu = M / \overline{m}L = 0.20$$
, $\eta = m / \overline{m}L = 0.1 \mu$

Frequencies -
$$f_{k_1} = \sqrt{\frac{k_1/\overline{m}L}{\omega_l^2}} = 0.05$$
, $f_{k_2} = \sqrt{\frac{k_2/\overline{m}L}{\omega_l^2}} = 0.20$, $f_g = \sqrt{\frac{g/L}{\omega_l^2}} = 0.01$,

$$f_c = \frac{c / \overline{m}L}{\omega_1} = 0.02$$

Speed -
$$f_v = \frac{V/L}{\omega_1} = 0.06, 0.08, 0.10, 0.12$$

Fundamental frequencies of a two-span beam - $f_i = \omega_i / \omega_l$

Damping ratio, ξ , for the beam is assumed 0.01.

For design of the guideway structure, the statistical moments of the structure responses are essential. The computed beam responses are displacement and moment at midspan, moment at the middle support and the shear at 0.95L. Time histories of the expected values of beam responses are plotted in Figures 2 to 11 for $\ell/L = 0.5$, 0.6, 0.7 and $f_{\nu} = 0.06$, 0.08, 0.10, 0.12.

3.1 Effect of span passage rate, f_{ν} - Span passage rate is a ratio of V/L to a first beam frequency, $\omega_{\rm l}$. Assuming that a 20m-two-span beam has a frequency of 7 Hz,

$$f_{res.} = V/(2L)$$

7 Hz = $V/(2*20m)$
 $V = 280m/s$

A velocity of 280 m/s or 1000 km/h is impossible for a ground transportation system.⁶ However, there are many other frequencies in the system, including the vehicle axle arrival rate and the fundamental frequencies of the vehicle.

3.2 Effect of axle arrival rate, f_a - The axle arrival rate is V/ℓ or, in terms of rad/sec, $2\pi V/\ell$. It can be nondimensionalized by ω_1 . The nondimensional arrival rate, denoted by f_a , may be written in terms of f_v and ℓ/L as shown in Table 1. The nondimensional frequencies of the first two modes of the two-span beam are f_1 = 1 and f_2 = 1.57.

For $f_{\nu}=0.06$ to 0.12 (V=190 to 380 km/h for beam span 20 m and frequency 7 Hz) - at high velocity level - vehicle is assumed to be rail vehicle system. Thus, the roughness model for the rail system is used here. The combinations of f_{ν} and ℓ/L that cause resonance are shown in Table 1. If $\ell/L=0.5$ and $f_{\nu}=0.08$ the axle arrival rate equals the fundamental frequency. For typical values of ω_1 and L, $f_{\nu}=0.08$ corresponds to a velocity of 70 m/s (250 km/h). If $\ell/L=0.5$ and $f_{\nu}=0.12$, the axle arrival rate equals the second natural frequency. Therefore it is possible for the axle arrival rate to be in resonance with the first and second beam frequencies, for feasible vehicle speeds. Let ℓ/L be fixed at 0.5 and the span passage rate, f_{ν} , be 0.08 (\approx 250 km/h). Figures 2 and 3 show that the displacement and the moment at midspan have the largest

amplification. The maximum expected values of dynamic amplifications are 1.32 and 1.22 respectively (recall that multiples of standard deviations of amplification factors must be added to determine design amplification factors). It is simply because the first mode is excited, f_a matches f_1 , and the displacement and moment at midspan are two responses dominated by this fundamental asymmetric mode. When the span passage rate increases to 0.12 (≈ 380 km/h), the moment at the interior support is amplified by as much as 1.32 (Fig. 4) which is more than the other responses. In this case the second mode, the symmetric mode, is excited. A response dominated by this symmetric second mode is the moment at the interior support. For ℓ/L =0.6 and 0.7, only the first mode is excited (Figs. 2 and 3) for realistic velocities (less than 380 km/h). If ℓ/L is greater than 0.5, the axle arrival rate is unlikely to be in resonance with the second mode since the velocity corresponding to that resonance mode is well above a practical level. If ℓ/L is greater than 1, f_a will never match f_1 and resonance due to f_a never occurs. The shear (figure 5) is different from the other responses as all of the modes (both asymmetric and symmetric modes) participate in this response. Figure 6 shows time history of expected value and variance of beam acceleration at midspan. It is found that the maximum expected beam acceleration is 0.4g (quite high) and occurs after vehicles left the span.

For a high-speed ground transportation system there is a possibility to have resonance between the axle arrival rate and the second mode frequency. For this condition the moment at the middle support needs to be examined closely.

3.3 Effect of number of axles (interfaces)

For high speed vehicle, i.e. maglev (magnetic levitated vehicle), the suspension system can have more than two contact points. More contact points can benefit the design of the system. Figures 7 to 10 (also Table 2 and 3) show the expected beam responses reduce, i.e. E[M(L)] reduces from 1.32 to 1.10, when eight suspensions are used. This suspension arrangement can also reduce strong fluctuation in VAR[M(L)] dramatically (Figs. 4 and 9). Figure 11 shows the expected beam acceleration at midspan reduces from 0.4g in figure 6 to 0.16g.

3.4 Effect of fundamental frequencies of vehicle

Natural frequencies of the car body (normally low) may not be equal to the first mode frequency of a typical short-span bridge unless the primary and secondary springs are very stiff. It is not realistic to have such a stiff suspension ²³, since passenger comfort criteria may not be met. For a structure with low frequency such as a large suspension bridge ⁵, there is a chance of a structure frequency matching a vehicle frequency. However, the mass of the vehicle is very small compared to the mass of a suspension bridge, so significant dynamic amplification is not likely.

4. Conclusion

Random vibration time history analyses provide vehicle and structure responses that can define appropriate surface smoothness requirements and design amplification factors for structure for high speed vehicles. Mean value and covariance matrix of system responses can be determined.

It is found that one specific value of a nondimensional parameter may cause a maximum in one response while a different value may cause a maximum in another response. For two-span beam, the moment at the interior support can have high dynamic amplification factors when axle arrival rate matches to the second natural frequency of the beam.

For high speed rail system, an appropriate suspension configuration of vehicle can reduce the expected value and variance of DAF of beam responses.

Acknowledgements

This research was supported by the Office of Higher Education Commission and the Thai Research Fund (TRF) under Grant No. MRG4680169. This support is gratefully acknowledged.

References

- 1. J.M. Biggs. Introduction to structural dynamics (McGraw-Hill, New York, 1964).
- L. Fryba, Vibration of solid and structures under moving load. (Noordhoff International Publishing, Groningen, 1972).
- 3. S. Timoshenko, D.H. Young and W. Weaver, *Vibration problems in engineering*. (Wiley, New York, 1974).
- S. Marchesiello, A. Fasana, L. Garibaldi and B.A.D. Piombo, Dynamics of multi span continuous straight bridges subjected to MDOF moving vehicle excitation, *J. Sound Vib.*, 224 (1999) 541-561.
- 5. H. Xia, Y.L. Xu and T.H.T. Chan, Dynamic interaction of long suspension bridge with running trains, *J. Sound Vib.*, 237 (2001) 263-280.
- 6. F.T.K. Au, J.J. Wang and Y.K. Cheung, Impact study of cable-stayed bridge under railway traffic using various models, *J. Sound Vib.*, 240 (2001) 447-465.
- G. Michaltsos, D. Sophianopoulos and A.N. Kounadis, The effect of a moving mass and other parameters on the dynamic response of a simply supported beam, *J. Sound Vib.*, 191 (1996) 357-362.
- 8. K. Henchi, M. Fafard, G. Dhatt and M. Talbot, Dynamic behaviour of multi-span beams under moving loads, *J. Sound Vib.*, 199 (1997) 33-50.
- 9. G. Michaltsos, Dynamic behviour of a single-span beam subjected to loads moving with variable speeds, *J. Sound Vib.*, 258 (2002) 359-372.

- 10 F.T.K. Au, R.J. Jiang and Y.K. Cheung, Parameter identification of vehicles moving on continuous bridges, *J. Sound Vib.*, 269 (2004) 91-111.
- 11. Y.H. Lin, and M.W. Trethewey, Finite element analysis of elastic beams subjected to moving dynamic loads, *J. Sound Vib.*, 236 (2000) 61-87.
- 12. K. Henchi, M. Fafard, G. Dhatt, and M. Talbot, An efficient algorithm for dynamic analysis of bridges under moving vehicles using a coupled modal and physical components approach, J. Sound. Vib., 212 (1998) 663-683.
- J. Hino, T. Yoshimura, K. Konishi, and N. Ananthanarayana, A finite element method prediction of the vibration of a bridge subjected to a moving vehicle load, *J. Sound Vib.*, 96 (1984) 45-53.
- 14. J.E. Snyder, III and D.N. Wormley, Dynamic interactions between vehicle and elevated, flexible, randomly irregular guideways, *J. Dyn. Syst. Meas. Control*, (1977) 23-33.
- 15. R.F. Harrison and J.K. Hammond, Analysis of the nonstationary response of vehicles with multiple wheel, *J. Dyn. Syst. Meas. Control*, 108 (1986) 69-73.
- N.C. Nigam and S. Narayanan, Applications of random vibrations (Springer-Verlag, Delhi, 1994).
- 17. X. Lei and N.-A. Noda, Analyses of dynamic response of vehicle and track coupling system with random irregularity of track vertical profile, *J. Sound Vib.*, 258 (2002) 147-165.
- 18. R.J. Jiang, F.T.K. Au and Y.K. Cheung, Identification of vehicles moving on continuous bridges with rough surface, *J. Sound Vib.*, 274 (2004) 1045-1063.
- 19. S.S. Law and X.Q. Zhu, Bridge dynamic responses due to road surface roughness and braking of vehicle, *J. Sound Vib.*, 282 (2005) 805-830.
- D.A. Gasparini, M. Petrou and M.E. Ozer, Wavelength content of Concrete floors, ACI Struct. J., (1990) 706-715.

- P. Seetapan, Dynamics of high speed vehivles traversing structures with random surfaces,
 Ph.D. Thesis, Case Western Reserve University, USA (2002).
- P. Seetapan and D.A. Gasparini, Dynamic of bridge for very high speed vehicle, in EuroDyn2002 (Munich, Germany, 2002).
- 23. J.A. Tamboli and S.G. Joshi, Optimum design of a passive suspension system of a vehicle subjected to actual random road excitations, *J. Sound Vib.*, 219 (1999) 193-205.

Table 1 Vehicle axle arrival rate and span passage rate for high speed

f_a for L = 20 m		f_{ν} (speed, km/h)			
and $f_{beam} = 7$ Hz.		0.06(190)	0.08	0.10	0.12(380)
	0.40	<u>0.94</u>	1.26	<u>1.57</u>	1.88
	0.50	0.75	<u>1.01</u>	1.26	<u>1.51</u>
ℓ/L	0.60	0.63	0.84	<u>1.05</u>	1.26
	0.70	0.54	0.72	0.90	<u>1.08</u>

Table 2 The maximum beam responses when f_a is in resonance with f_1 for two different suspension configurations

Y = Structural	Two contact		Eight contact	
Responses	pe	oints	points	
	E[Y]	VAR[Y]	E[Y]	VAR[Y]
v(0.5L)	1.32	0.0200	1.20	0.0105
M(0.5L)	1.22	0.0125	1.15	0.0105
M(L)	1.10	0.2100	1.10	0.0280
S(0.95L)	1.00	0.0090	1.10	0.0090
$\ddot{v}(0.5L)/g$	0.30	0.0040	0.14	0.0025

Table 3 The maximum beam responses when f_a is in resonance with f_2 for two different suspension configurations

Y = Structural	Two contact		Eight contact	
Responses	points		points	
	E[Y]	VAR[Y]	E[Y]	VAR[Y]
v(0.5L)	1.05	0.015	1.25	0.0100
M(0.5L)	1.20	0.019	1.20	0.0100
M(L)	1.32	0.041	1.10	0.0260
S(0.95L)	1.05	0.010	1.10	0.0085
$\ddot{v}(0.5L)/g$	0.40	0.003	0.16	0.0035

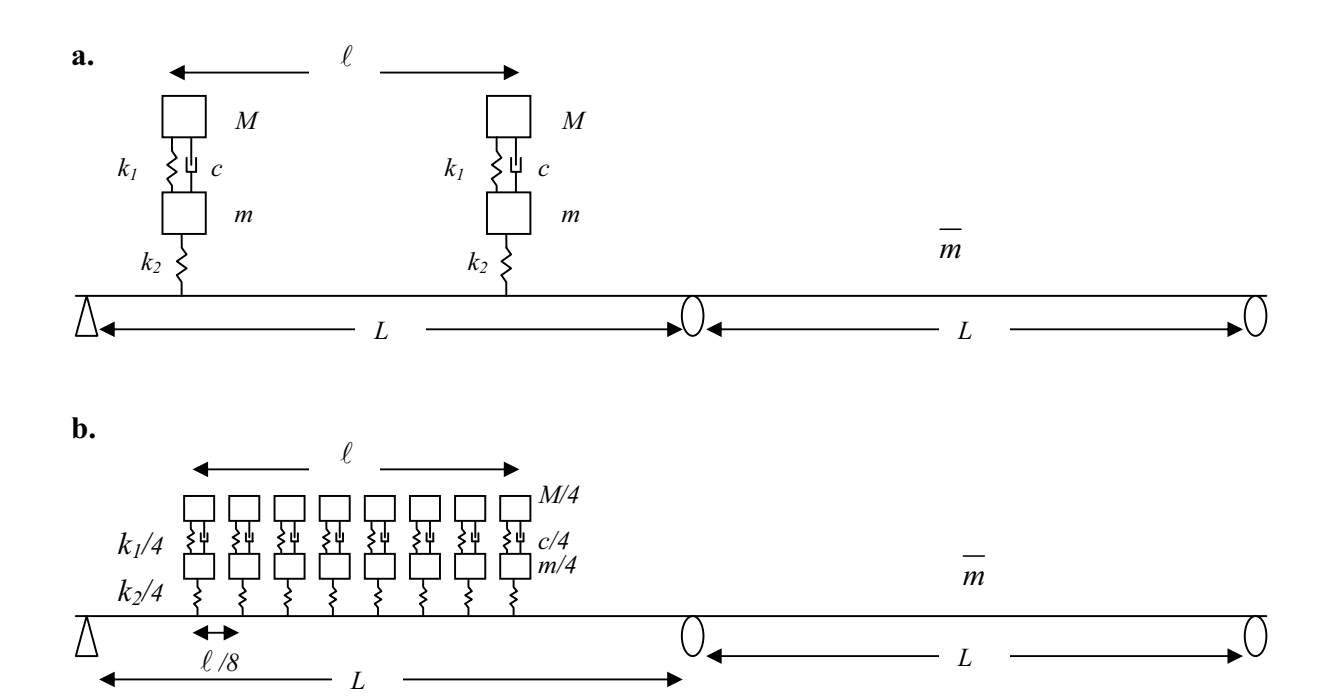


Figure 1 Models of coupled vehicle structure system: a. two of 2DOF vehicle model, b. eight of 2DOF vehicle model

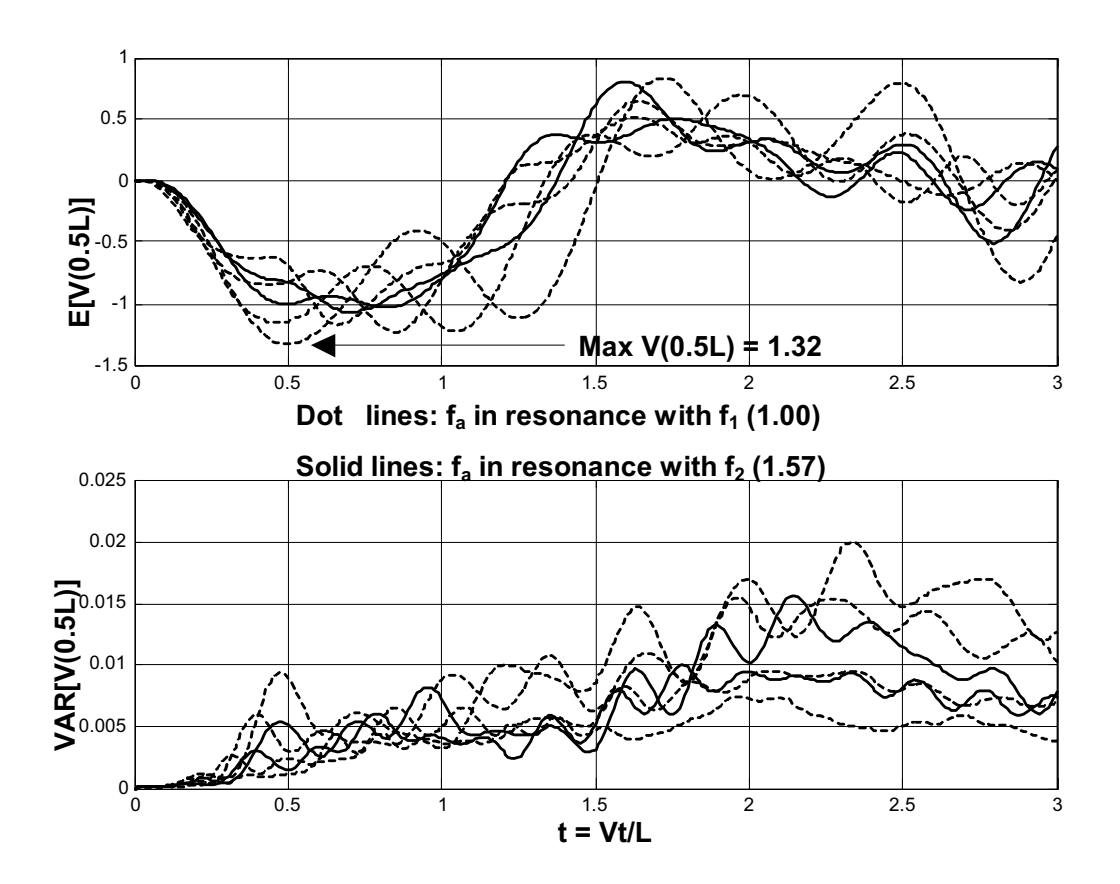


Figure 2 Time history of expected values and variances of displacement at midspan

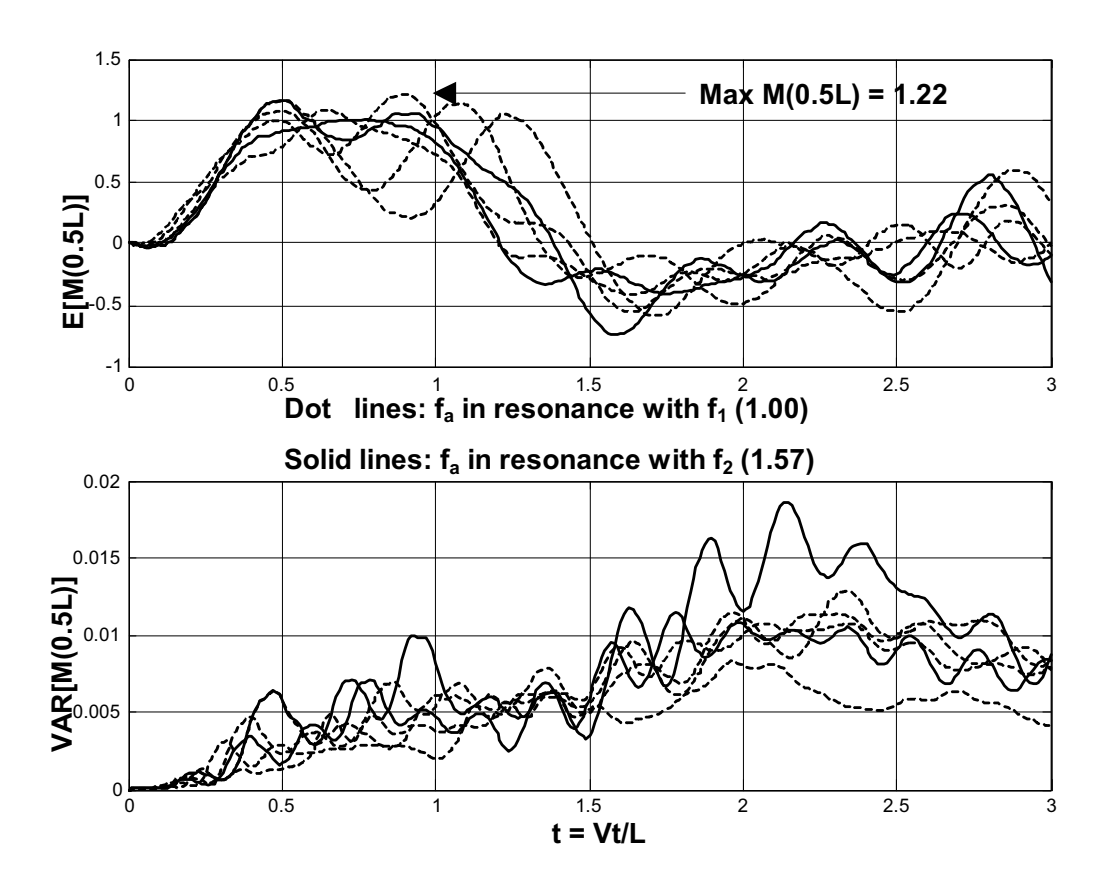


Figure 3 Time history of expected values and variances of moment at midspan

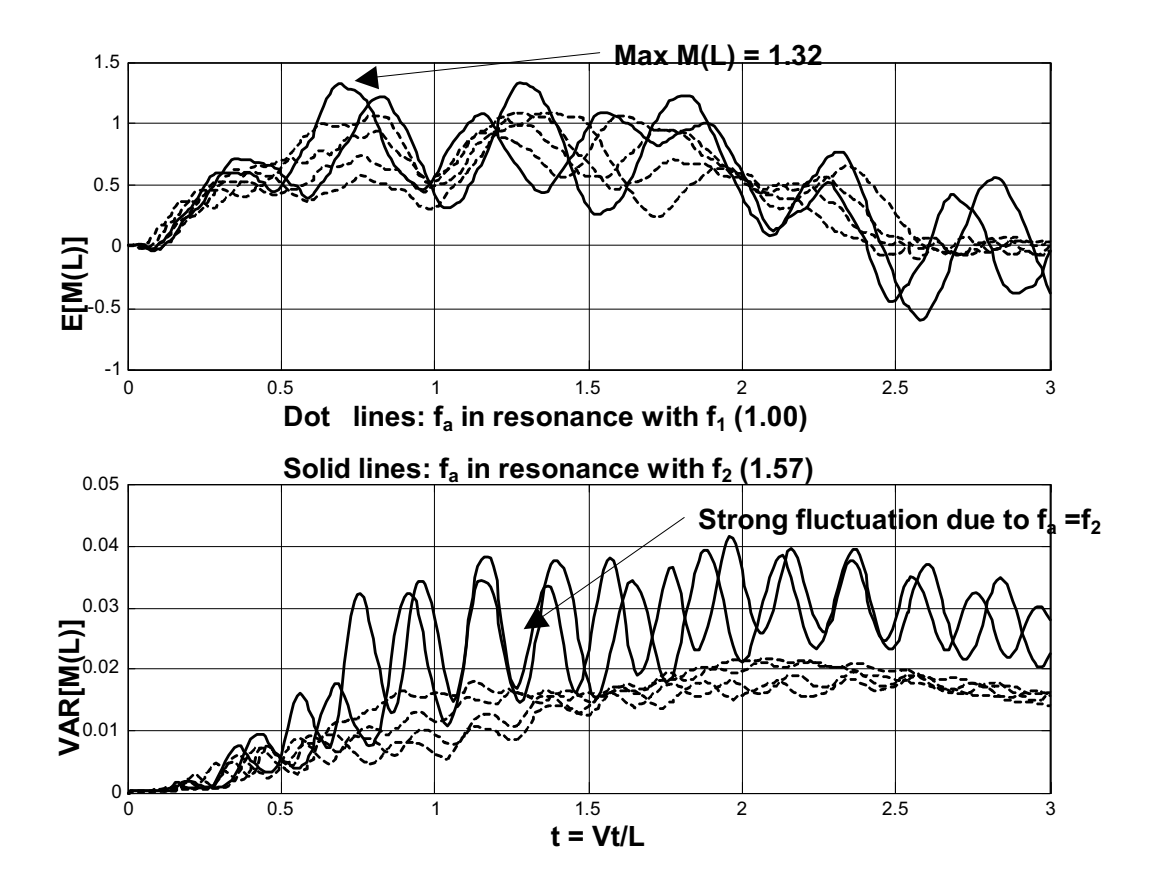


Figure 4 Time history of expected values and variances of moment at interior support

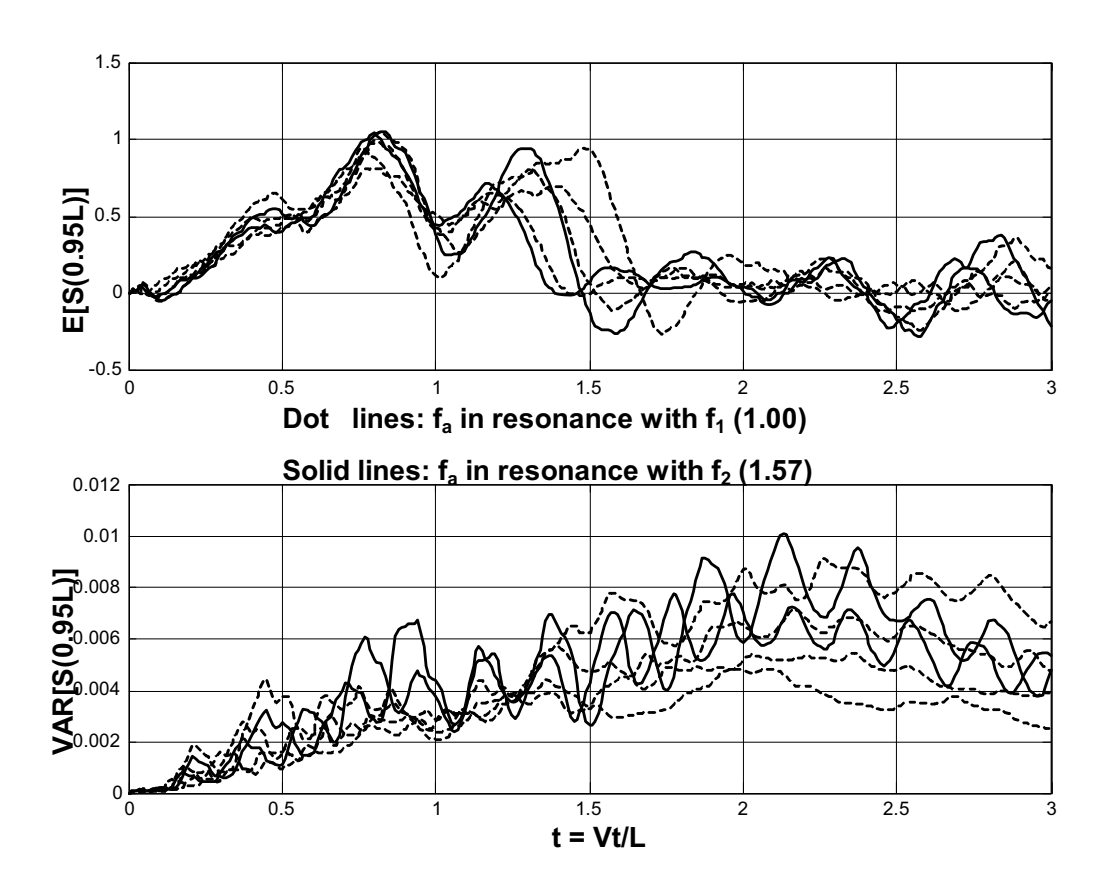


Figure 5 Time history of expected values and variances of shear at 0.95L

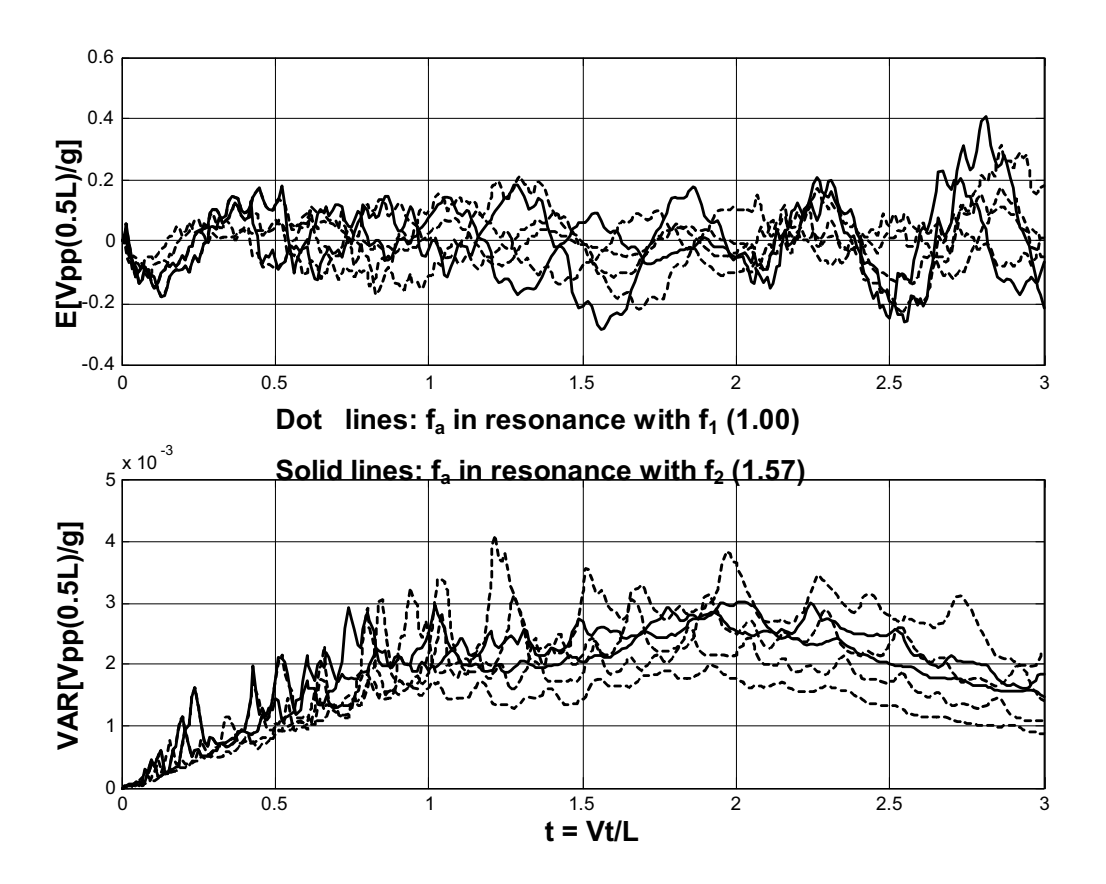


Figure 6 Time history of expected values and variances of beam acceleration at midspan

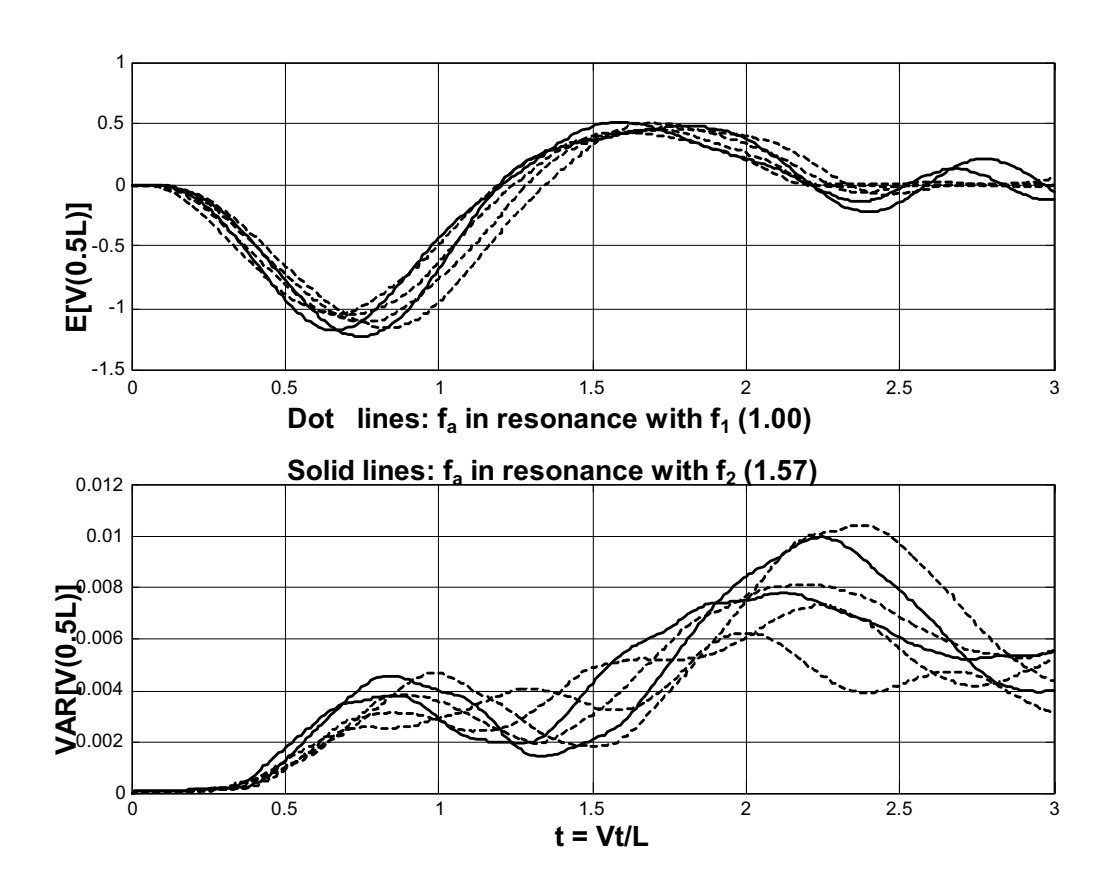


Figure 7 Time history of expected values and variances of displacement at midspan

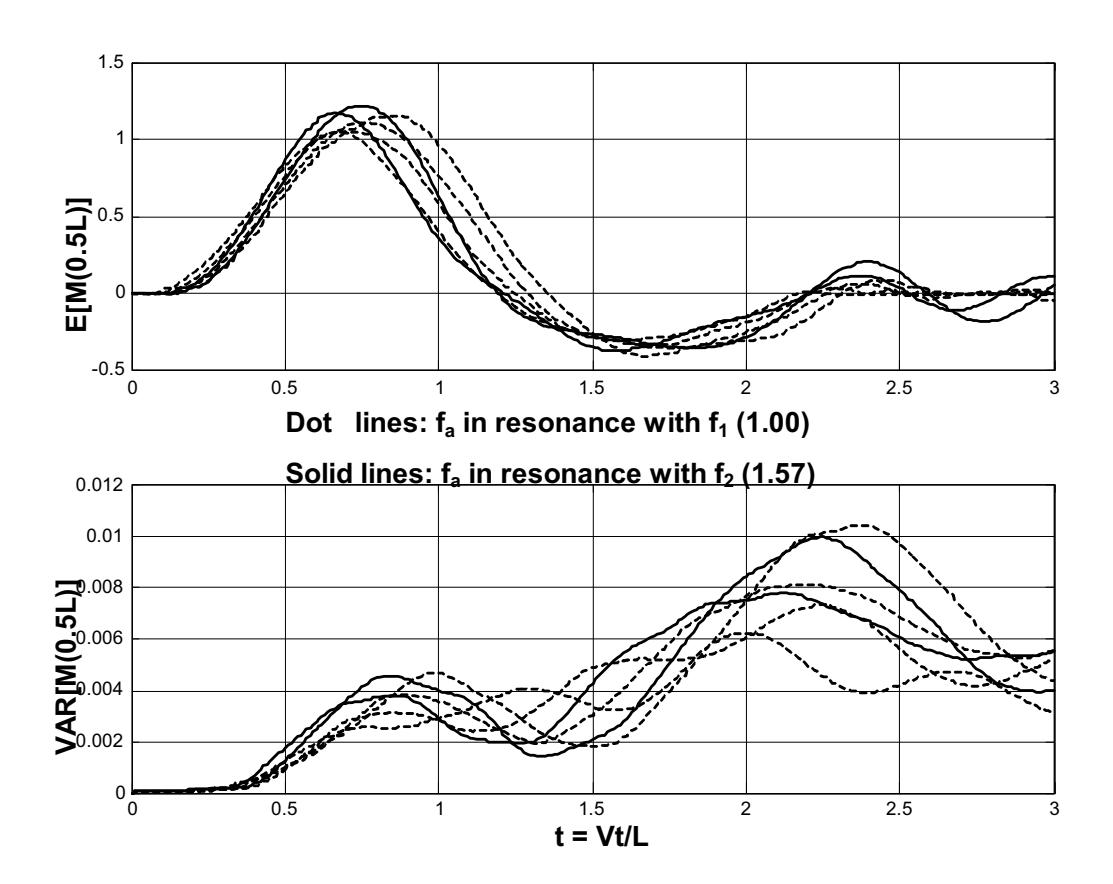


Figure 8 Time history of expected values and variances of moment at midspan

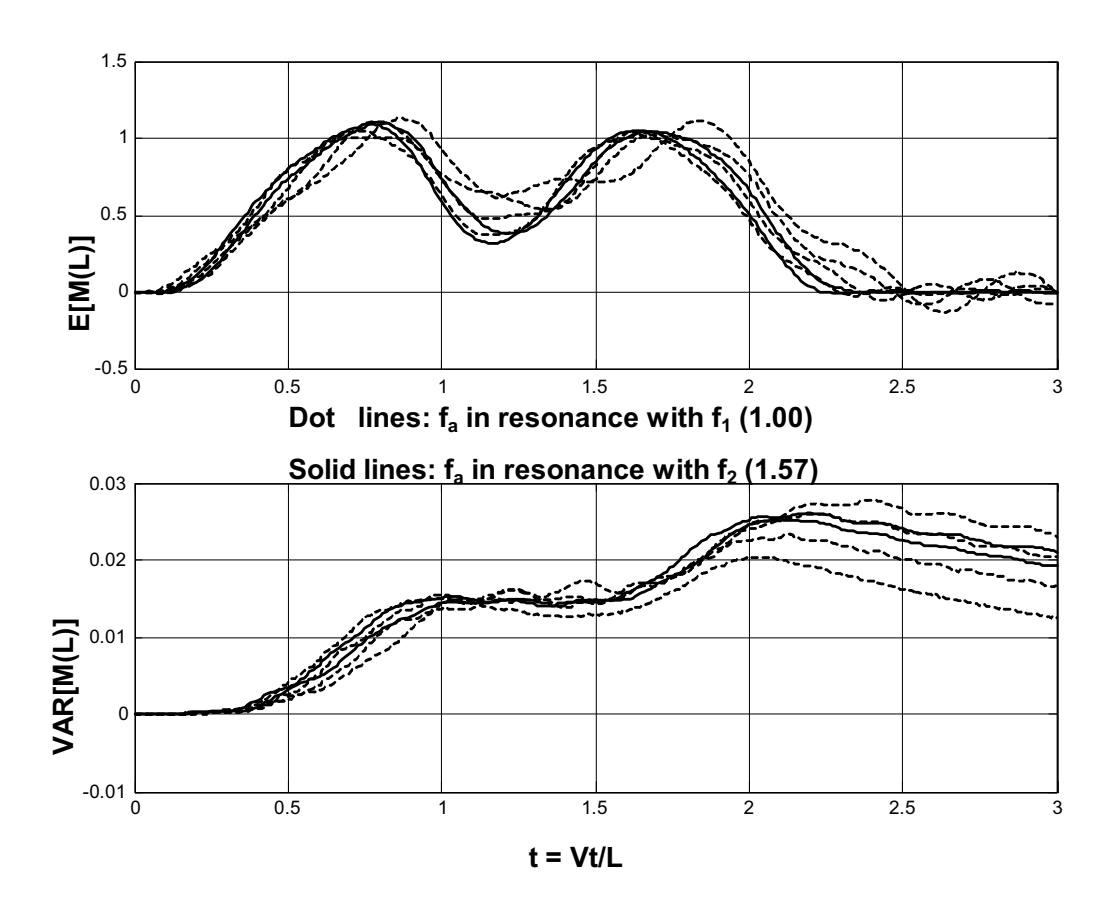


Figure 9 Time history of expected values and variances of moment at interior support

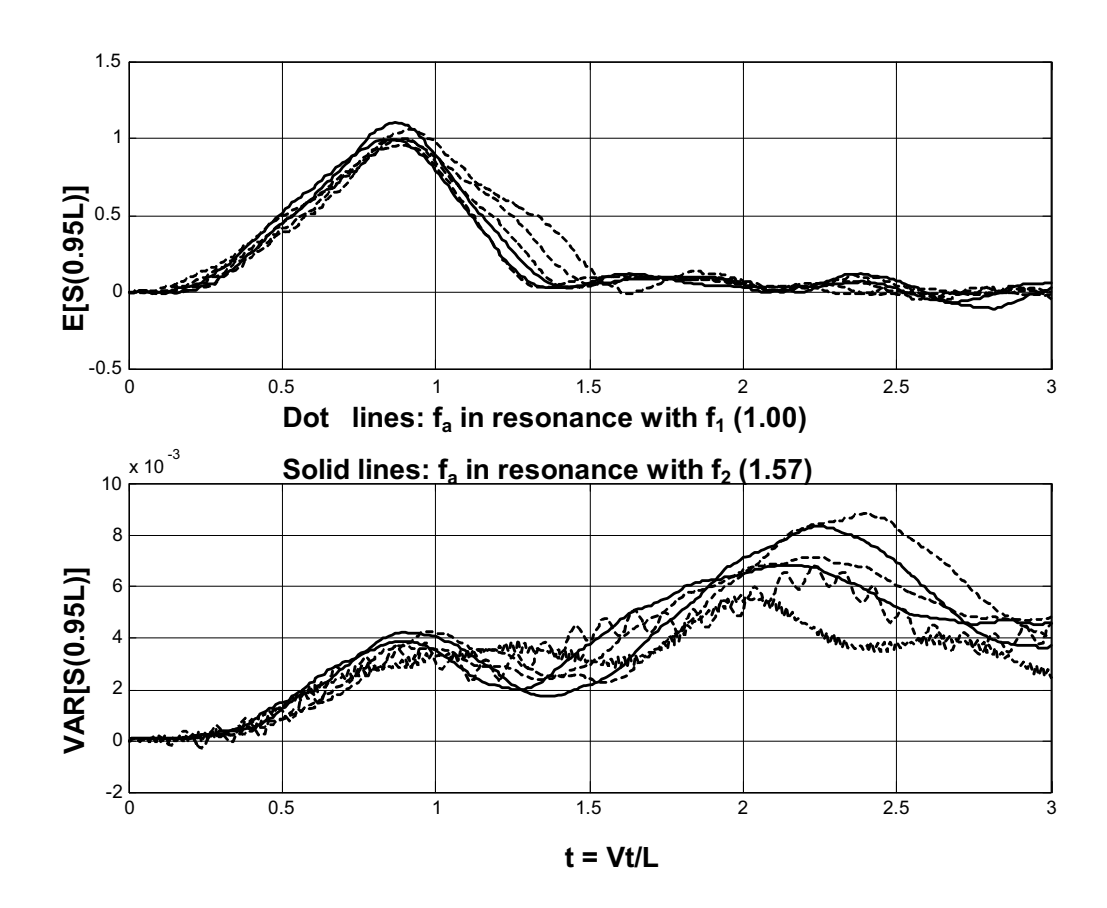


Figure 10 Time history of expected values and variances of shear at 0.95L

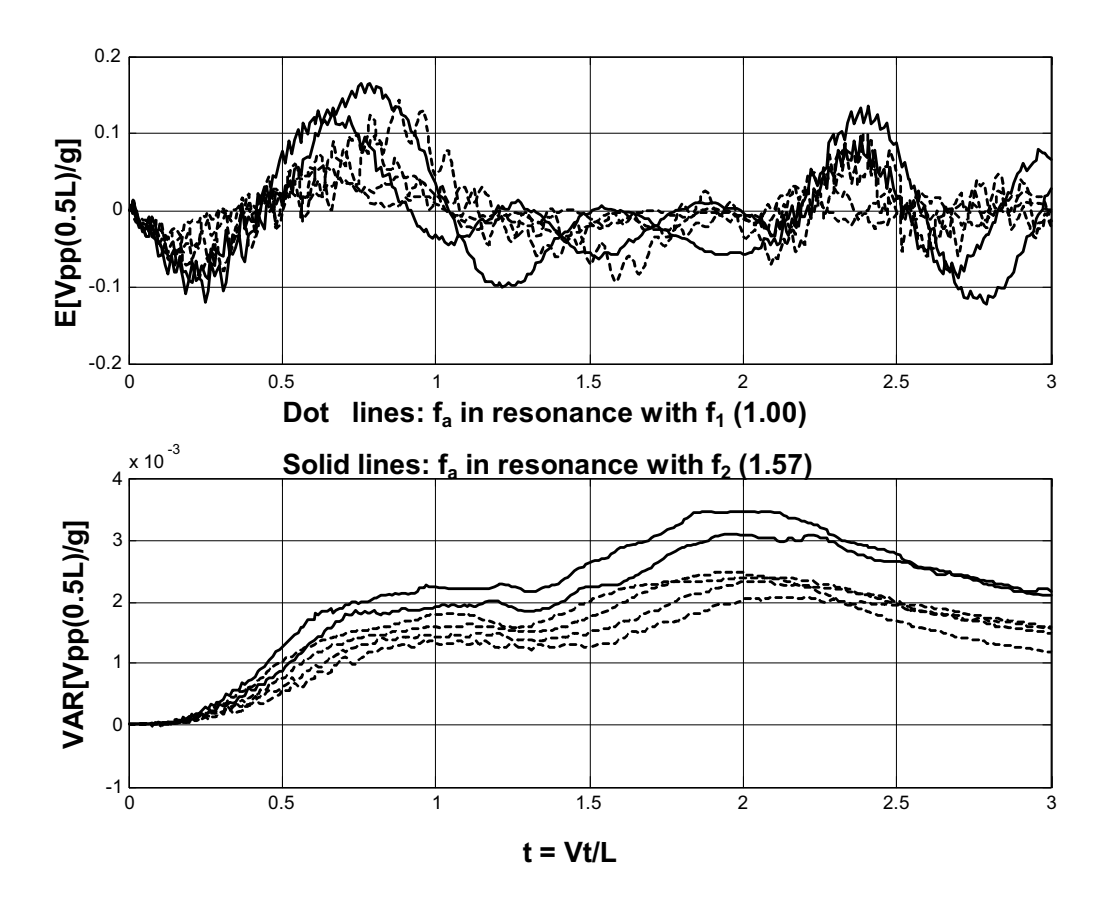


Figure 11 Time history of expected values and variances of beam acceleration at midspan

ความสำคัญของความขรุขระพื้นผิวต่อยานพาหนะและโครงสร้างพื้นฐาน SIGNIFICANCE OF SURFACE ROUGHNESS TO MOVING VEHICLES AND INFRASTRUCTURES

ปฤษทัศว์ ศีตะปันย์ (Pritsathat Seetapan)¹ เอกสิทธิ์ ใม้วัฒนา (Akesit Maiwattana)² สมชาย ชูชีพสกุล (Somchai Chucheepsakul)³

¹อาจารย์ ภาควิชาวิศวกรรมโยธา คณะวิศวกรรมศาสตร์ มหาวิทยาลัยนเรศวร ²นิสิตปริญญาโท ภาควิชาวิศวกรรมโยธา คณะวิศวกรรมศาสตร์ มหาวิทยาลัยนเรศวร ³ศาสตราจารย์ ภาควิชาวิศวกรรมโยธา คณะวิศวกรรมศาสตร์ มหาวิทยาลัยเทคโนโลยีพระจอมเกล้าธนบุรี

บทคัดย่อ: บทความนี้นำเสนอตัวอย่างข้อมูลระดับพื้นผิวถนนในประเทศไทย ซึ่งถูกเก็บด้วยวิธีบั๊ม อินทิเกรเตอร์ ฟังก์ชันความ หนาแน่นกำลังสเปกตรัล (Power Spectral Density function) ของข้อมูลพื้นผิว กำนวนได้จากการแปลงรูปฟูเรียร์ PSD จะเป็นตัวแสดง การกระจายตัวของกำลังที่ความยาวคลื่นต่าง ๆ ของโปรไฟล์พื้นผิว โดยทั่วไปพื้นผิวถนนอาจถูกพิจารณาเป็นชุดข้อมูลของ สเตชั่นนารี่ เกาส์เซียน แรนดอม โพรเซส ดังนั้นการสร้างแบบจำลองเชิงวิเคราะห์ของพื้นผิวสามารถทำได้ โดยการใช้ฟิวล์เตอร์ไวท์นอยซ์ แบบจำลองของยานพาหนะ 2DOF เคลื่อนที่บนถนนซึ่งมีการสึกกร่อนแบบแรนดอมถูกใช้เป็นตัวอย่างในการสรุปประเด็นเกี่ยวกับ ค่าที่ ยอมให้ของความขรุจระพื้นผิวซึ่งใช้ควบคุมผลตอบสนองของยานพาหนะ และการจจัดของโครงสร้างพื้นฐาน

ABSTRACT: Actual road surface elevation data in Thailand collected by using Bump Integrater are presented. Power Spectral Density (PSD) function of the surface roughness can be computed by Fourier Transform. It shows the wavelength content of surface profile. Typical road surfaces may be considered as realizations of stationary Gaussian random processes. Analytical model of random surface can be constructed by using filtered white noise. An example of a 2DOF vehicle travelling on a randomly corrugated road is presented. The issue of specifying surface roughness tolerances to control vehicular response and displacement of the infrastructure is discussed.

KEYWORDS: Road surface, Power spectral density, Bump integrater, Vehicle response

1. บทนำ

ถนนทางหลวงเป็นการคมนาคมหลักที่สำคัญของประเทศ ในแต่ ละวัน ถนนทางหลวงรับแรงกระทำพลวัตซ้ำ ๆ หลายครั้ง จาก การเคลื่อนที่ของยานพาหนะ นำไปสู่ความเสียหายต่อโครงสร้าง พื้นผิวทาง เพื่อให้การตรวจสอบและประเมินสภาพถนนเป็นไป อย่างมีประสิทธิภาพ จึงทำการเก็บรวบรวมข้อมูลความขรุขระ ของพื้นผิวทางด้วยเครื่องมือบั๊มอินทิเกรเตอร์ (Bump Integrator) และ แปลงรูปฟูเรียร์ หาฟังก์ชันความหนาแน่นกำลังสเปคตรัล (Power Spectral Density function, PSD) และเปรียบเทียบค่าที่ ยอมให้ของความขรุขระพื้นผิวทางตามมาตรฐานสากล จากนั้น ทำการสร้างแบบจำลองพื้นผิวทางด้วยฟิวล์เตอร์ไวท์นอยซ์ เพื่อ ศึกษาผลของความขรุขระพื้นผิวทางที่มีต่อ ความสะดวกสบาย ของผู้ใช้ยานพาหนะ และผลตอบสนองของโครงสร้างพื้นฐาน ในแต่ละช่วงความเร็วของยานพาหนะ

2. หลักการพื้นฐานที่ใช้ในงานวิจัย

2.1 การเก็บรวบรวมข้อมูลความขรุขระของพื้นผิวทาง
บั๊ม อินทิเกรเตอร์ (Bump Integrater, BI) เป็นเครื่องมือทดสอบที่
มีความคล่องตัวสูง สามารถวัดรายละเอียดส่วนย่อยติดต่อกัน ได้
อย่างอัต โนมัติ ทุกสภาวะการใช้งานของทางหลวง โดยเริ่มทำ
การบันทึกข้อมูล เมื่อรถยนต์เคลื่อนที่ออกจากจุดเริ่มต้น และทำ
การเก็บค่าการขึ้น-ลงของเพลาหลังสะสม ส่งผ่านไปที่ฮาร์ดแวร์
ROMDAS ทำการแปลงสัญญาณส่งไปที่คอมพิวเตอร์
ลอมพิวเตอร์ทำการบันทึกข้อมูล ค่าความขรุขระบั๊มอินทิเกรเตอร์
ระยะทาง ความเร็วรถยนต์ ไว้ในไฟล์งาน ทุก ๆ 1,000 เมตร โดย
ไม่ต้องทำการจอดรถยนต์ที่บันทึก เมื่อถึงช่วงที่เป็นสะพานหรือ
บริเวณที่มีการก่อสร้าง ผลที่ได้จากการวัด คือดัชนีชี้วัดความ
ขรุขระผิวทาง (International Roughness Index) หน่วยเป็น
มิลลิเมตรต่อกิโลเมตร ดังตารางที่ 1

ตารางที่ 1 ดัชนีชี้วัดความขรขระผิวทาง

สภาพทาง	คัชนีชี้วัดความขรุขระผิวทาง (IRI)
ดี	0 - 3
ปานกลาง	3 - 4
rra _,	4 - 5
แย่มาก	> 5

2.2 การแปลงรูปฟูเรียร์ (Fourier Transform)

นิยมใช้กันอย่างกว้างขวางในการคำนวณทางวิศวกรรม เป็นการ แปลงรูปฟังก์ชันในโดเมนเวลา(หรือระยะทาง) ให้ เป็นฟังก์ชัน ในโดเมนความถี่ หรือที่เรียกว่า ฟังก์ชันความหนาแน่น กำลังสเปกตรัล (Power Spectral Density function, PSD) ดัง แสดงในสมการที่ (1) ในรูปจำนวนเชิงซ้อน และจำนวนคลื่น (wave number, r)

$$Y(r) = \int_{-\infty}^{\infty} y(x)e^{-2\pi i rx} dx \tag{1}$$

2.3 การคำนวณค่าเฉลี่ย Root-Mean-Square, RMS การหาค่าเฉลี่ยสำหรับ แรนดอมโพรเซสนั้น นิยมหาจากค่า rootmean-square ในโคเมนความถี่หาได้จาก

$$RMS = \sqrt{\frac{1}{S} \int_{0}^{S} y^{2}(x) dx} = \sqrt{\frac{1}{S} \int_{-\infty}^{\infty} |Y(r)|^{2} dr}$$
 (2)

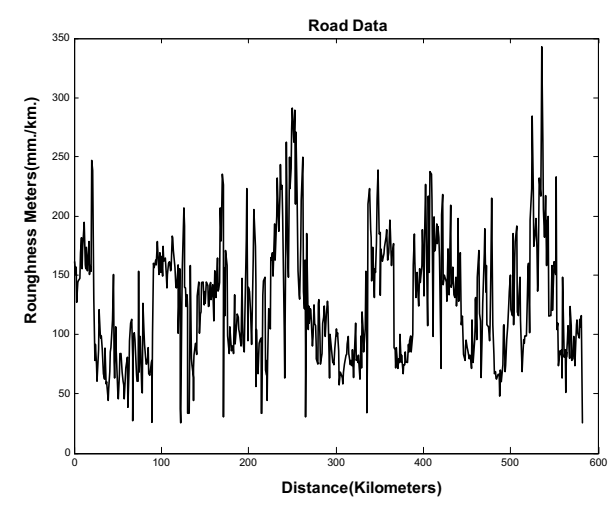
โดย **S** คือความยาวของข้อมูล หรือ ถ้าทราบค่าทางสถิติของข้อมูล ค่า *RMS* อาจหาได้จากสมการที่ (3)

$$RMS = \sqrt{E^2[x] + VAR[x]}$$
 (3)

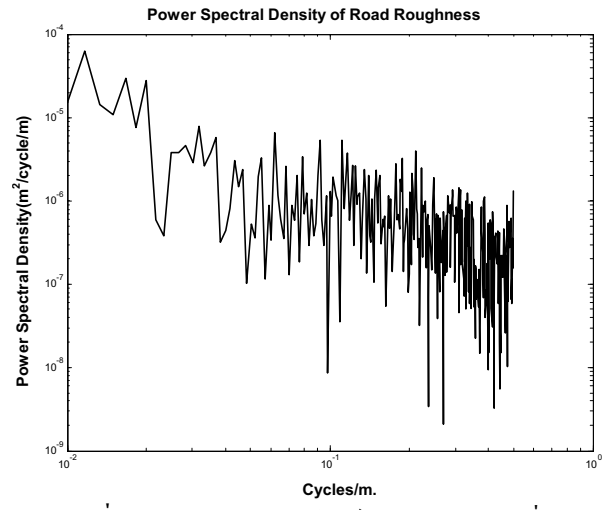
โดย E[x] คือ ค่าเฉลี่ย หรือ ค่าที่คาดหมาย ของ x (mean or expected value of x), VAR[x] คือ ค่าความแปรปรวนของ x (variance of x)

3. ข้อมูลความขรุขระของถนนในประเทศไทย

ตัวอย่างโปรไฟล์ของถนนหลวงหมายเลขหนึ่ง เก็บข้อมูลด้วยวิธี บั๊ม อินทิเกรเตอร์ แสดงในรูปที่ 1 ข้อมูลมีรูปร่างสม่ำเสมอ คล้าย สเตชั่นนารี่ เกาส์เซียน แรนคอม โพรเซส (homogenous random process)[1,4]



รูปที่ 1 แสดงตัวอย่างโปรไฟล์ของผิวถนนหมายเลขหนึ่งในประเทศไทย



รูปที่ 2 แสดง PSD ของโปรไฟล์ของผิวถนนในรูปที่ 1 รูปที่ 2 แสดง PSD ของความขรุขระของผิวถนนในรูปที่ 1 บน แกน y แสดงค่ากำลังของ PSD ส่วนแกน x แสดงค่าจำนวนคลื่น (wave number, r) ในความเป็นจริง PSD จะมีสองค้านมี ลักษณะสมมาตรทั้งทางค้านบวกและลบ (ในรูปที่ 2 แสดงค้าน

บวกเท่านั้น)โดยจะแสดงค่ากำลังของ PSD ที่จำนวนคลื่น (ความถี่) ต่าง ๆ จาก $-\infty$ ถึง ∞ โดยทั่วไปจะมีค่ากำลังของ PSD สูงที่จำนวนคลื่นต่ำ ๆ (low wave number) และจะมีค่ากำลังของ PSD ต่ำลงที่จำนวนคลื่นสูงขึ้น (high wave number) ค่าจำนวน คลื่นเท่ากับส่วนกลับของความยาวคลื่น $(r=1/\lambda)$ ดังนั้น r=0 จะได้ว่า $\lambda \to \infty$ ซึ่งพิจารณาได้ว่าเป็นค่าออฟเซทจาก สูนย์ (offset) และที่ r=0 จะได้ค่าแอมปริจูดสูงสุดของโพรเซส ความขรุงระ[3]

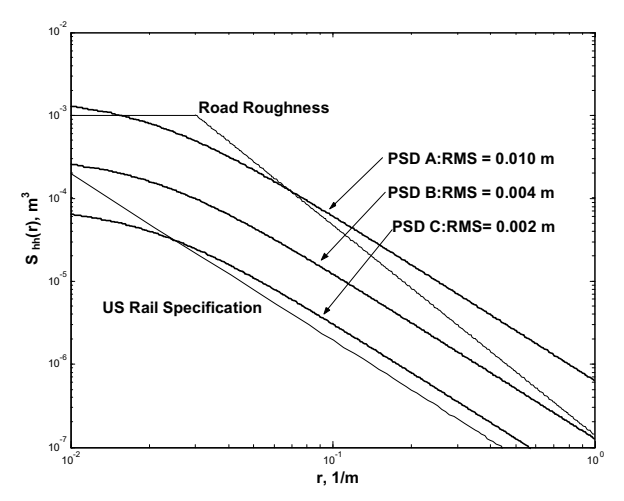
PSD ของข้อมูลนี้ นำไปใช้เป็นแบบจำลองเป้าหมายที่จะสร้าง ขึ้นเพื่อใช้เป็น อินพุทให้กับ ระบบยานพาหนะ-โครงสร้าง พื้นฐาน

4. แบบจำลองพื้นผิวทาง ยานพาหนะ และ โครงสร้างพื้นฐาน

4.1 แบบจำลองความขรุ*งระพื้นผิวทาง* ถูกสร้างขึ้นจาก สมการ ฟิวล์เตอร์ ซึ่งเป็นสมการอนุพันธ์ที่มีไวท์นอยซ์ (white noise, **W**) เป็น อินพุท (input) และมีค่าความขรุงระพื้นผิว (**h**) เป็น เอาพุท (output) ดังสมการที่ (4)

$$\Delta_c h'(x) + h(x) = W(x) \tag{4}$$

โดย Δ_c คือ ระยะคอร์รีเลชั่น (correlation distance) และ S_0 คือ ความเข้มของไวท์นอยซ์ (white noise intensity) นำมาใช้ในการ ปรับค่าเพื่อให้ได้ PSD ของความขรุขระที่ต้องการ ในงานวิจัยนี้ ได้สร้างแบบจำลอง PSD ของความขรุขระพื้นผิวสำหรับ PSD เป้าหมายในรูปที่ 2 (ซึ่งอยู่ในเกณฑ์มาตรฐานสากลสำหรับถนน (PSD A) คังรูปที่ 3), และ PSD C สำหรับระบบขนส่งแบบราง (rail) โดยใช้ข้อกำหนดของทางสหรัฐอเมริกา เป็นเป้าหมาย

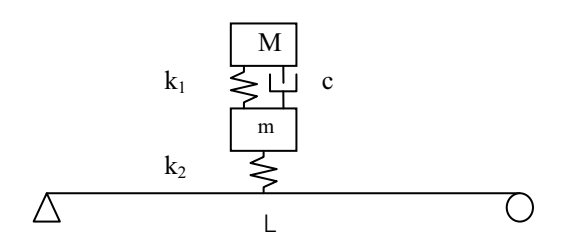


รูปที่ 3 แสดง PSD ของแบบจำลอง โปร ไฟล์ของผิวถนน (PSD A), พื้นผิว ระบบราง (PSD C) และ PSD B

สำหรับค่า PSD B เป็น PSD ที่มีความขรุขระอยู่ระหว่างถนนและ ระบบขนส่งแบบราง โดยปรับค่าตัวแปรให้ แบบจำลอง PSD มี รูปร่างที่ใกล้เคียง และมีค่า *RMS* ที่สอดคล้องกับเป้าหมายที่มีอยู่

4.2 แบบจำลองยานพาหนะ อาจใช้เป็น SDOF หรือ MDOF ที่มี สปริง ตัวหน่วง มวลหรือตัวควบคุม ประกอบเป็นตัวเชื่อม ใน งานวิจัยนี้เลือกใช้ 2DOF ที่มีสปริงเป็นตัวเชื่อม เพื่อที่จะไม่ทำให้ เกิดปัญหาในการคำนวณค่าความแปรปรวน ดังรูปที่ 4

4.3 แบบจำลองโครงสร้างพื้นฐาน อาจเป็นสะพานช่วงเคียวหรือ หลายช่วง หรือ คานพื้นวางบนฐานรองรับแบบยืดหยุ่น[2,7] ใน งานวิจัยนี้ใช้คานช่วงเคียว ดังรูปที่ 4 และใช้เทคนิคการวิเคราะห์ โมดอล (modal analysis)



รูปที่ 4 แสดงแบบจำลองยานพาหนะและ โครงสร้างที่ใช้ในงานวิจัย สมการอนุพันธ์ของระบบจำลองใน สเตทสเปซ (state space) แสดงในสมการที่ (5)

$$\dot{X} = AX + BW + C \tag{5}$$

โดย X คือ สเตทเวคเตอร์ (state vector), W คือ ไวท์นอยซ์ เวคเตอร์ (vector of white noise), A B และ C เป็นเมตริกซ์ แสดงความสัมพันธ์ระหว่างความขรุขระ ยานพาหนะ และ โครงสร้างพื้นฐาน ในการวิเคราะห์ระบบ ตัวแปรต่าง ๆ จะถูกจัด อยู่ในรูป ตัวแปรไร้หน่วย (dimensionless parameter) ดังนั้นตัว แปรไร้หน่วยแต่ละตัวจะเป็นอิสระต่อกัน[5,6]

$$\begin{split} f_{v} &= \frac{V/L}{\omega_{l}}, f_{k_{l}} = \sqrt{\frac{k_{l}/\overline{m}L}{\omega_{l}^{2}}}, f_{k_{2}} = \sqrt{\frac{k_{2}/\overline{m}L}{\omega_{l}^{2}}} \\ f_{c} &= \frac{c/\overline{m}L}{\omega_{l}}, f_{g} = \sqrt{\frac{g/L}{\omega_{l}^{2}}}, \mu = M/\overline{m}L, \eta = m/\overline{m}L \end{split}$$

อัตราส่วนของความถี่พื้นฐานของสะพานโหมดที่ $m{i}$ ต่อโหมดที่ $m{i}$ - $f_i = \omega_i \, / \, \omega_1$, โดย $f_1 = 1.00$ และ $f_2 = 4.00$ พารามิเตอร์ของแบบจำลองความขรุขระ - $\Delta_c \, / \, L$, $\, S_0 \, / \, L^3$

5. ผลการวิเคราะห์

 $f_{_{\scriptscriptstyle V}} \! = \, 0.02, 0.03, 0.04, 0.05$ สำหรับช่วงความเร็วปกติ

= 0.06, 0.08, 0.10, 0.12 สำหรับช่วงความเร็วสูง สำหรับสะพานที่มีช่วงคานยาว 20 เมตร และ มีความถี่พื้นฐาน 7 เฮิรทซ์ ช่วงความเร็วปกติหมายถึง 60 ถึง 160 กม.ต่อ ชม. และ ช่วงความเร็วสูง หมายถึง 190 ถึง 380 กม.ต่อ ชม.

 $f_{k_1} = 0.05, \ f_{k_2} = 0.2, \ f_c = 0.02, \ f_g = 0.01$ ค่า $f_{k_1} \ f_{k_2} \ f_c$ และ f_g ถูกคำนวณจากข้อมูล ค่าคงที่สปริง ตัว หน่วงและแรงโน้มถ่วงโลกจากระบบ suspension ยานพาหนะ อัตราส่วนของมวลของยานพาหนะต่อมวลของสะพาน,

 $\mu=0.2$, $\eta=0.02$, ความหน่วงของโครงสร้าง - $\xi=0.01$, $\Delta_c/L=2.50,~S_0/L^3=0.0625\mathrm{x}10^{-6}\mathrm{(PSD~C)}~0.25\mathrm{x}10^{-6}\mathrm{(PSD~B)}$ และ $1.25\mathrm{x}10^{-6}\mathrm{(PSD~A)}$

ค่าเฉลี่ย และค่าความแปรปรวน ของผลตอบสนองของระบบ สามารถคำนวณได้โดย วิธีเชิงตัวเลขด้วยโปรแกรม MATLAB

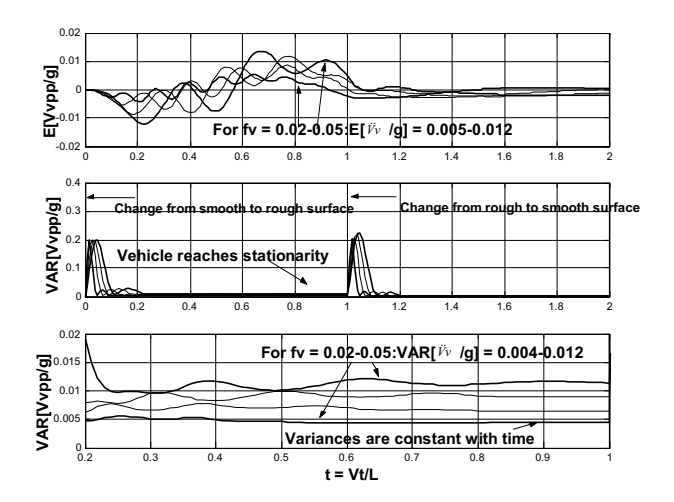
5.1 ผลตอบสนองของยานพาหนะ

โดยทั่วไปผลตอบสนองของยานพาหนะที่สนใจคือความเร่งใน ห้องโดยสาร ซึ่งบ่งบอกความรู้สึกของผู้ใช้ยานพาหนะ ตามค่า มาตรฐาน ISO 2631 แสดงในตารางที่ 2

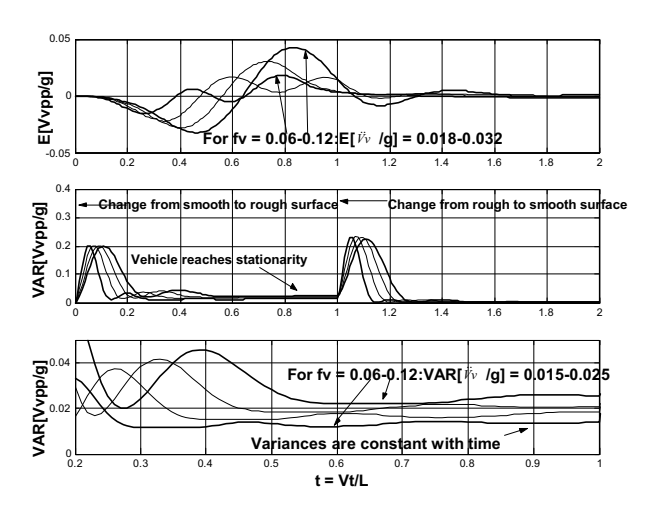
ตารางที่ 2 แสดงค่าอัตราเร่งสูงสุดที่มีผลต่อความรู้สึกของผู้ใช้ยานพาหนะ ตามมาตรฐาน ISO 2631

อัตราเร่งสูงสุด	ความรู้สึกของผู้ใช้ยานพาหนะ
< 0.032 g	สะควกสบาย
0.032 g to 0.064 g	ไม่สะควกสบายบ้าง เล็กน้อย
0.051 g to 0.102 g	เกือบจะไม่สะควกสบาย
0.082 g to 0.160 g	ไม่สะควกสบาย
0.127 g to 0.255 g	ไม่สะควกสบาย มาก
> 0.200 g	ไม่สะควกสบาย ที่สุค

จากรูปที่ 5 และ 6 ค่าเฉลี่ยของความเร่งแนวคิ่งของยานพาหนะ ในช่วงความเร็วปกติ บนพื้นผิวที่มีความขรุขระจำลองด้วย PSD A จะมีค่าอยู่ในช่วง 0.005g ถึง 0.012g อยู่ในช่วงที่ผู้ใช้ ยานพาหนะยอมรับได้ แต่มีค่าความแปรปรวนสูง 0.004 ถึง 0.012 สำหรับยานพาหนะความเร็วสูงถ้าพื้นผิวมีความขรุขระ เท่ากับ PSD A จะให้ค่าเฉลี่ย ในช่วง 0.018g ถึง 0.032g ซึ่งก็ยังคง อยู่ในเกณฑ์ที่ ผู้ใช้ยานพาหนะรู้สึกสะควกสบาย แต่ค่าความ แปรปรวนมีค่าสูงมาก ในช่วง 0.015 ถึง 0.025



รูปที่ 5 แสดง time history ของค่าเฉลี่ยและค่าความแปรปรวนของความเร่ง ของยานพาหนะ ในช่วงความเร็วปกติ ค่าความขรขระ PSD A

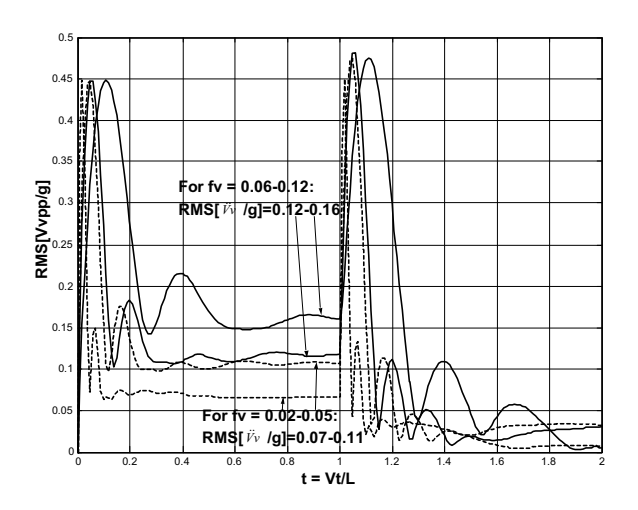


รูปที่ 6 แสดง time history ของค่าเฉลี่ยและค่าความแปรปรวนของความเร่ง

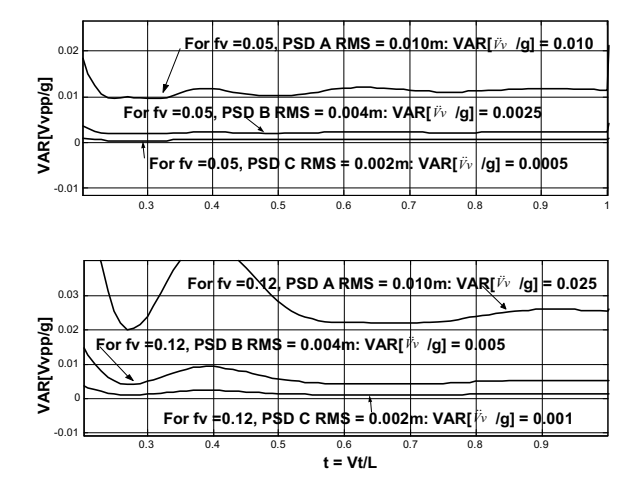
ของยานพาหนะ ในช่วงความเร็วสูง ค่าความขรุขระ PSD A รูปที่ 7 แสดงค่าเฉลี่ย RMS ของความเร่งแนวคิ่งในยานพาหนะ มี ค่า 0.07g ถึง 0.11g สำหรับยานพาหนะความเร็วปกติ และมีค่า 0.12g ถึง 0.16g สำหรับยานพาหนะความเร็วสูง จะเห็นได้ว่า เมื่อ รวมค่าความแปรปรวนเข้าในการคำนวณค่าเฉลี่ย RMS แล้ว ความเร่งแนวคิ่งในยานพาหนะ มีค่าสูง จะทำให้ผู้โดยสารใน ยานพาหนะรู้สึกไม่สะควกสบาย จึงควรที่จะปรับลดความขรุขระ ของพื้นผิว ซึ่งผลของการเปลี่ยนมาใช้ความขรุขระพื้นผิวที่ลดลง (PSD B และ C) แสดงอยู่ในรูปที่ 8 พบว่าค่าความแปรปรวน ลดลงอย่างมากเมื่อนำไปคำนวณ ค่าเฉลี่ย RMS จะได้ค่าที่น้อยลง โดย กรณี $f_v = 0.05$ ค่าเฉลี่ย RMS ของความเร่งแนวคิ่งใน ยานพาหนะ มีค่าลดลงจาก 0.11g (สำหรับ PSD A) เป็น 0.051g และ 0.025g สำหรับ PSD B และ C ตามลำดับ ส่วนกรณี $f_v = 0.12$ ค่าเฉลี่ย RMS ของความเร่งแนวคิ่งในยานพาหนะ มีค่า

ลดลงจาก 0.16g (สำหรับ PSD A) เป็น 0.078g และ 0.045g สำหรับ PSD B และ C ตามลำดับ

นอกจากนี้ กรณีที่มีการเปลี่ยนแปลงความขรุขระพื้นผิวแบบ ฉับพลัน จะทำให้เกิดค่าความแปรปรวนที่สูงเกินปกติ (overshoot) ในความเร่งแนวคิ่งของยานพาหนะ และ ในกรณี ยานพาหนะเคลื่อนที่ด้วยความเร็วสูง ความเร่งแนวคิ่งจะเข้าสู่ สเตชั่นนารี่(stationary) ได้ช้ากว่า กรณีความเร็วต่ำ



รูปที่ 7 แสดง time history ของ RMS ของความเร่งของยานพาหนะ



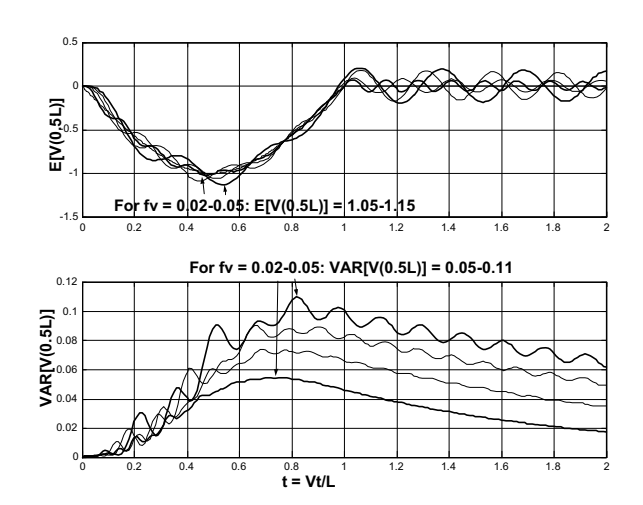
รูปที่ ${f 8}$ แสดง time history ของค่าความแปรปรวนของความเร่งของ ยานพาหนะ เมื่อ $f_v=0.05$ และ 0.12 ที่ระดับความขรุขระต่าง ๆ

5.2 ผลตอบสนองของโครงสร้าง

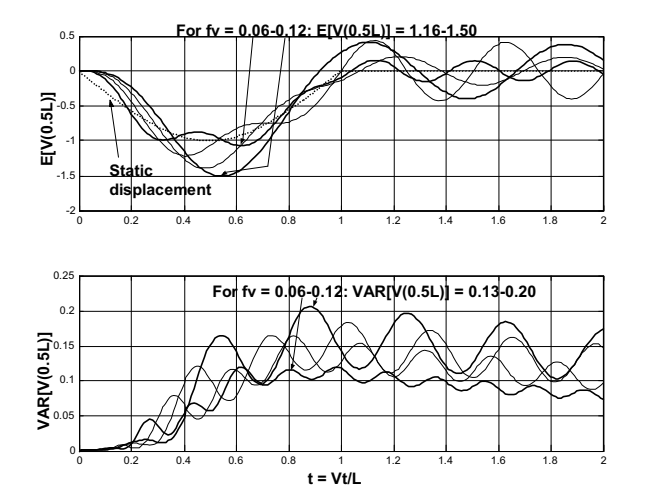
จากรูปที่ 9 และ 10 ในช่วงความเร็วปกติของยานพาหนะ ค่าเฉลี่ย ของ DAF (Dynamic Amplification Factor) ของระยะโก่งที่ กึ่งกลางของสะพานช่วงเดียวอยู่ในช่วง 1.05 ถึง 1.15 และเพิ่มขึ้น ได้ถึง 1.50 สำหรับยานพาหนะความเร็วสูง

ค่าความแปรปรวน (variance) ของ DAF ของระยะโก่งที่ กึ่งกลางสะพานช่วงเคียว กรณีความเร็วปกติและความขรุขระ PSD A มีค่าอยู่ในช่วง 0.05 ถึง 0.11 (หรือมีค่าเบี่ยงเบนมาตรฐาน (standard deviation) ในช่วง 0.22 ถึง 0.33) และมีค่าสูงขึ้นได้ถึง 0.20 (ค่าเบี่ยงเบนมาตรฐานเท่ากับ 0.45)สำหรับยานพาหนะ ความเร็วสูงและความขรุงระ PSD A

เมื่อค่า f_{ν} สูงขึ้น ค่าความแปรปรวนของระยะโก่งที่กึ่งกลาง สะพานมีการขยับขึ้นลงที่รุนแรงมากขึ้น (strongly fluctuated)



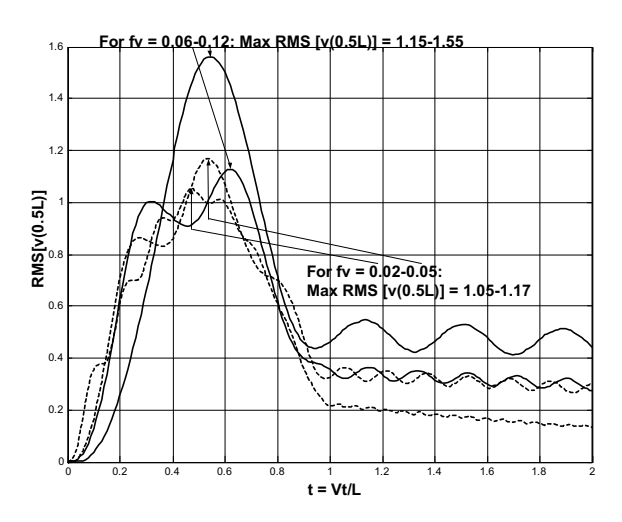
ร**ูปที่ 9** แสดง time history ของค่าเฉลี่ยและค่าความแปรปรวนของระยะ โก่งกึ่งกลางคาน เมื่อ $f_v = 0.02$ -0.05



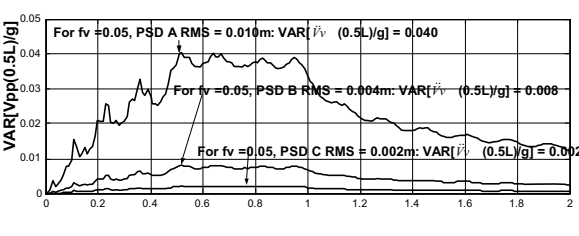
รูปที่ 10 แสคง time history ของค่าเฉลี่ยและค่าความแปรปรวนของระยะ โก่งกึ่งกลางคาน เมื่อ $f_{_{V}}=0.06$ -0.12

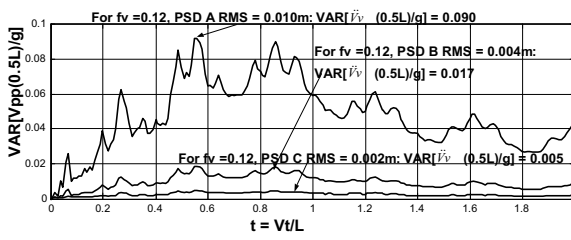
ค่าเฉลี่ย RMS (ในรูปที่ 11) ของ DAF ของระยะ โก่งที่กึ่งกลาง สะพานมีค่า 1.05 ถึง 1.17 เมื่อ $f_v = 0.02$ ถึง 0.05 และมีค่าเพิ่ม เป็น 1.15 ถึง 1.55 เมื่อ $f_v = 0.06$ ถึง 0.12

ค่า f_{V} ไม่ก่อให้เกิดการสั่นพ้อง (resonance) เพราะค่า f_{V} จะเท่ากับ 1 ก็ต่อเมื่อยานพาหนะเคลื่อนที่ด้วยความเร็วที่สูงมาก เกินที่ยานพาหนะบนดินจะเคลื่อนที่ได้ (สำหรับสะพานที่มี ค่าความถี่พื้นฐานอยู่ในเกณฑ์ปกติ)



รูปที่ 11 แสดงค่าสูงสุดของค่า RMS ของระยะ โก่งกึ่งกลางคาน





รูปที่ 12 แสดง time history ของค่าความแปรปรวนของความเร่งที่กึ่งกลาง คาน ที่ระดับความขรุขระต่าง ๆ

รูปที่ 12 พบว่าค่าความแปรปรวนสูงสุดของความเร่งแนวคิ่งที่ กึ่งกลางสะพานลดลงอย่างมาก โดยกรณี $f_{\nu}=0.05$ ค่าความ แปรปรวนสูงสุดของความเร่งแนวคิ่งที่กึ่งกลางสะพาน มีค่าลดลง จาก 0.04 (สำหรับ PSD A) เป็น 0.008 และ 0.002 สำหรับ PSD B และ C ตามลำดับ ส่วนกรณี $f_{\nu}=0.12$ ค่าความแปรปรวนสูงสุด ของความเร่งแนวคิ่งที่กึ่งกลางสะพาน มีค่าลดลงจาก 0.09 (สำหรับ PSD A) เป็น 0.017 และ 0.005 สำหรับ PSD B และ C ตามลำดับ

6. สรุปผลการวิจัย

จากข้อมูลความขรุงระพื้นผิวถนน สามารถสร้างแบบจำลอง โดยใช้สมการฟิวล์เตอร์แบบ low-passed ซึ่งมีพารามิเตอร์สองตัว คือ ระยะคอร์รีเลชั่น (correlation distance, Δ_c) และความเข้ม ของไวท์นอยซ์ (white noise intensity, S_0) จะเป็นตัวกำหน รูปร่างของแบบจำลอง PSD นอกจากนี้ ค่าเฉลี่ย RMS ควรมีค่า ใกล้เคียง กับความขรุงระจริง

ความขรุงระมีผลต่อความแปรปรวน แต่ไม่มีผลต่อค่าเฉลี่ย
ของผลตอบสนองของระบบ เนื่องจาก ไวท์นอยซ์ เป็น โพรเซสที่
มีค่าเฉลี่ยเป็นศูนย์ ดังนั้นในสมการที่ (5) พจน์ BW จะหายไปเมื่อ
ทำการหาค่าเฉลี่ย แต่ค่า RMS คำนวณจากทั้งค่าเฉลี่ยและค่าความ
แปรปรวน ดังนั้น ถ้าพื้นผิวขรุงระมาก จะทำให้ ค่าความ
แปรปรวนสูง ส่งผลให้ค่า RMS สูงตาม

โดยทั่วไป ผลตอบสนองของยานพาหนะจะเข้าสู่ สเตชั่นนารื่ นั่นคือ ความแปรปรวนจะคงที่หลังจากยานพาหนะเคลื่อนที่บน พื้นผิวขรุขระไปช่วงเวลาหนึ่ง แต่สำหรับผลตอบสนองของ โครงสร้างนั้น กลับตรงข้ามค่าความแปรปรวนไม่เข้าสู่ สเตชั่น นารี่

การวิเคราะห์ข้อมูลเวลาการสั่นสะเทือนแบบสุ่ม(random vibration time history)ของระบบความขรุขระ-ยานพาหนะโครงสร้าง สามารถบ่งบอกข้อกำหนดสำหรับความเรียบของ พื้นผิว และ ค่าตัวเลขเชิงสถิติ ของทั้งผลตอบสนองต่อ ยานพาหนะและแฟคเตอร์กำลังขยายเชิงพลศาสตร์ของ โครงสร้างพื้นฐานต่อผู้ออกแบบได้

กิตติกรรมประกาศ

งานวิจัยนี้ได้รับทุนอุดหนุนจากสำนักงานคณะกรรมการ อุดมศึกษาและ สำนักงานกองทุนสนับสนุนการวิจัย สัญญาเลขที่ MRG4680169

เอกสารอ้างอิง

- [1] Dodds, C..J. and Robson, J.D., The description of road surface roughness. J. of Sound and Vibration, 31(1973): pp175-183.
- [2] Fryba, L., 1972. Vibration of solid and structures under moving loads. Groningen: Noordhoff International Publishing.
- [3] Gasparini, D.A., Petrou, M. and Ozer, M.E., Wavelength content of Concrete floors. ACI Structural Journal, 1990: pp706-715.
- [4] Hullender, D.A., Analytical models for certain guideway irregularities. J. of Dynamic Systems, Measurement and Control, 1975: pp417-423.
- [5] Seetapan P., 2002. Dynamics of high speed traversing structures with random surfaces. Ph.D. Thesis, Case Western Reserve University.
- [6] Seetapan P. and Gasparini D.A., 2002. Dynamic of bridge for very high speed vehicle. EuroDyn2002, Munich, Germany.
- [7]Xia, H., Xu, Y.L. and Chan, T.H.T., Dynamic interaction of long suspension bridge with running trains. J. of Sound and Vibration, 237(2001): pp263-280.

DYNAMIC RESPONSES OF A TWO-SPAN BEAM SUBJECTED TO 2DOF SPRUNG VEHICLES

Pritsathat Seetapan¹ Akesit Maiwattana² Somchai Chucheepsakul³

¹ Lecturer, Department of Civil Engineering, Naresuan University
² Graduate Student, Department of Civil Engineering, Naresuan University
³ Professor, Department of Civil Engineering, King Mongkut's University of Technology Thonburi

ABSTRACT: The deflection-, bending moment-, shear- and acceleration-time histories of a two-span beam subjected to moving sprung vehicles are presented. The vehicle model is a 2DOF system with a constant velocity. The two-span beam with rough surface is used as structure model. It is defined in modal domain by natural frequencies, mode shapes and modal damping values. The rough surface is modeled by filtered white noise. The equations of motion for the coupled vehicle-structure system are formulated. All variables in the system equation are nondimensionalized. The first order linear stochastic differential equations are solved. The effects of the span passage rate and other important parameters are studied.

KEYWORDS: Coupled vehicle-structure system, Random roughness, Dynamic response, Two-span beam.

1. Introduction

The principal objective of this work is to perform studies of coupled vehicle-structure dynamic systems to guide the design of structures for high-speed vehicles. A new formulation for modeling random roughness at the interfaces between a structure and a series of 2DOF vehicles is presented therein. System parameters are nondimensionalized and the equations of motion are written in state space. Here the equations for the mean and zero-time-lag covariance matrices of the state vector are solved using MATLAB. Static values of a set of responses are determined the statistical moments of the dynamic responses are normalized by the corresponding maximum static values. Therefore statistical moments of all responses are expressed in terms of dynamic amplification factors (DAF). Extensive parametric studies are presented that identify effects of important nondimensional parameters on the behavior of coupled vehicle-structure systems. This work provides designers of structures for high-speed vehicles insights on effects of nondimensional system parameters on behavior and quantifies values of DAF that may be produced by highspeed vehicles.

2. Coupled vehicle-structure system equations in state space

The dynamic response of a structure traversed by a vehicle is assumed to be completely defined by a vertical displacement function, v(x,t). The vertical displacement of the structure is here expressed in the modal domain as follows:

$$v(x,t) = \sum_{i=1}^{n} y_{i}(t)\phi_{i}(x)$$
 (1)

in which $\phi_i(x)$ is the i^{th} mode shape and $y_i(t)$ is i^{th} modal coordinate. The total displacement at an interface of a vehicle with a structure having surface roughness, h(x), is:

$$v'(x,t) = v(x,t) + h(x)$$
a)
$$\sum_{k} \psi_{k}$$

$$\sum_{k} \psi_{k}$$

$$\sum_{k} \psi_{k}$$

$$\sum_{k} \psi_{k}$$

Figure 1 shows models of coupled vehicle structure system

The surface profile, h(x), can be modeled as an output of a shaping filter to a white noise expressed by:

$$\Delta_c h'(x) + h(x) = W(x) \tag{3}$$

in which Δ_c is a correlation distance and W(x) is a zero-mean white process with intensity S_0 or strength q_0 . The covariance matrix of two white noise is

$$\sum_{W_1 W_2} = Q \delta(x_1 - x_2) \tag{4}$$

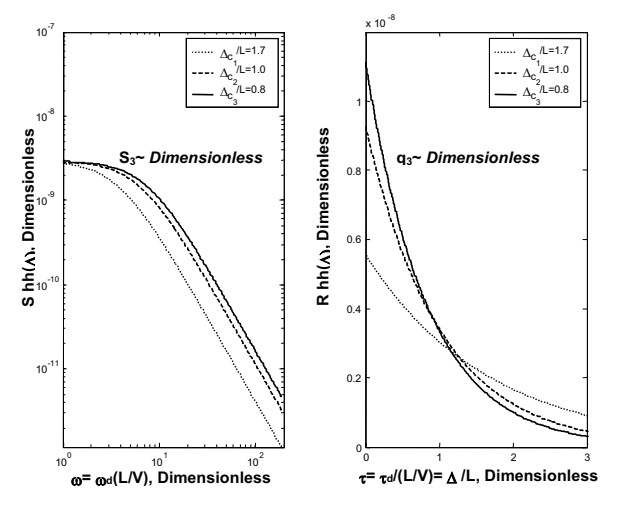


Figure 2 shows power spectral density (PSD) and correlation functions of rough surface

The coupled vehicle-structure models considered in this research are shown in Fig. 1. Figure 1a) shows two of 2DOF vehicle models, each one can be considered as a half-car model. Then, a distance between two models is called wheelbase, ℓ . Figure 1b) shows a model for eight of 2DOF vehicle models with the total length equal to the wheelbase in Fig 1a), it can be used to study effects of number of vehicle axles to the system. Structure model considered here is a two-equal-span prismatic flexure beam as shown in Fig. 1.

The coupled linear system equations driven by correlated white noises are then writen in state form:

$$\dot{X}(t) = A(t)X(t) + BW(t) + C(t), X(0)$$
(5)

in which X is a state vector, W is a vector of correlated white noises, A and B are matrices of appropriate dimension, and C is a vector of deterministic excitation. Taking the expectation operator, the equation for expected value vector is:

$$E[\dot{X}(t)] = A(t)E[X(t)] + C(t), E[X(0)]$$
(6)

The term BW(t) disappears because W(t) is a zero mean vector.

The zero-time-lag covariance matrix of the state vector, \sum_{XX} , may be solved from the well-known first order Lyapunov equation, given by:

$$\dot{\Sigma}_{XX} = A \Sigma_{XX} + \Sigma_{XX} A^T + BQB^T, \Sigma_{XX}(0)$$

in which Q is a strength matrix for the vector white noises,

$$Q = q_0 \begin{pmatrix} 1 & \dots & \rho_{W_i W_j} \\ \vdots & \ddots & \vdots \\ \rho_{W_i W_j} & \dots & 1 \end{pmatrix}$$

(8)

in which q_0 is a strength of the white noise and $\rho_{W_iW_j}$ is the zero-time-lag correlation coefficient between two white noises

3. Parametric study and results

Position -x/L, Time -Vt/L, Roughness W/L and h/L

White noise intensity $-q_0/L^3 = 1.250 \times 10^{-6}$ for road roughness

 $= 0.0625 \times 10^{-6}$ for rail

roughness

Autocorrelation distance - $\Delta_c / L = 2.50$

Distance between two vehicles - ℓ/L (show in Table 1 and 2)

Masses -
$$\mu = M / \overline{m}L = 0.20, \ \eta = m / \overline{m}L = 0.1 \ \mu$$

Frequencies -
$$f_{k_1} = \sqrt{\frac{k_1/\overline{m}L}{\omega_1^2}} = 0.05$$
, $f_{k_2} = \sqrt{\frac{k_2/\overline{m}L}{\omega_1^2}} = \sqrt{\frac{k_2/\overline{m}L}{\omega_1^2}}$

0.20,
$$f_g = \sqrt{\frac{g/L}{\omega_1^2}} = 0.01$$
, $f_c = \frac{c/\overline{m}L}{\omega_1} = 0.02$

Speed -
$$f_v = \frac{V/L}{\omega_1} = 0.02$$
, 0.03, 0.04, 0.05 for normal

velocity

= 0.06, 0.08, 0.10, 0.12 for high

velocity

Fundamental frequencies of a two-span beam -

$$f_i = \omega_i / \omega_1$$

Damping ratio, ξ , for the beam is assumed 0.01.

Effect of span passage rate, f_v - Span passage rate is a ratio of V/L to a first beam frequency, ω_l . Assuming that a 20m-two-span beam has a frequency of 7 Hz,

$$f_{res.} = V/(2L)$$

7 Hz. =
$$V/(2*20m)$$

$$V = 280 \text{m/s}$$

A velocity of 280 m/s or 1000 km/h is impossible for a ground transportation system [4]. However, there are many other frequencies in the system, including the vehicle axle arrival rate and the fundamental frequencies of the vehicle.

Effect of axle arrival rate, f_a - The axle arrival rate is V/ℓ or, in terms of rad/sec, $2\pi V/\ell$. It can be nondimensionalized by $\omega_{\rm l}$. The nondimensional arrival rate, denoted by f_a , may be written in terms of f_{ν} and ℓ/L as shown in Table 1 and 2.

Table 1 Vehicle axle arrival rate and span passage rate for normal speed

f_a for L = 20 m		f_{ν} (speed, km/h)				
and	$f_{beam} =$	0.02(60)	0.03	0.04	0.05(160)	
7Hz.						
	0.08	<u>1.57</u>	2.36	3.14	3.93	
	0.12	<u>1.05</u>	<u>1.57</u>	2.09	2.62	
	0.16	0.79	1.18	<u>1.57</u>	1.96	
ℓ / L						
	0.18	0.70	<u>1.05</u>	1.40	1.75	
	0.20	0.63	0.94	1.26	<u>1.57</u>	
	0.24	0.52	0.79	<u>1.05</u>	1.31	
	0.30	0.42	0.63	0.84	<u>1.05</u>	

Table 2 Vehicle axle arrival rate and span passage rate

for high speed

101 IIIgi	ioi iiigii speed						
f_a for L = 20		f_{ν} (speed, km/h)					
m							
and $f_{beam} =$		0.06(190)	0.08	0.10	0.12(380)		
7Hz.							
	0.40	<u>0.94</u>	1.26	<u>1.57</u>	1.88		
	0.50	0.75	<u>1.01</u>	1.26	<u>1.51</u>		
	0.60	0.63	0.84	<u>1.05</u>	1.26		
ℓ/L							
	0.70	0.54	0.72	0.90	<u>1.08</u>		

The nondimensional frequencies of the first two modes of the two-span beam are $f_1 = 1$ and $f_2 = 1.57$.

<u>At normal speed</u> ($f_v = 0.02$ to 0.05)

The vehicle model in Fig.1a) is considered here. Roughness model with parameters $q_0/L^3=0.0625\mathrm{x}10^{-6}$ and $\Delta_c/L=2.50$ is used, it is the model of a road with RMS roughness = 0.01 m.

Figures 3 and 4 show the expected value and variance of moments at midspan and at interior support for $f_a = f_1$ and $f_a = f_2$. The behaviors of expected beam responses are similar (displacement at midspan and shear at 0.95L are not shown here), DAF of those are between 1.05 to 1.10. Variances of beam responses in Figs. 3 and 4 can be separated into four pairs for each value of f_v (0.02, 0.03, 0.04, 0.05). In each pair it is clearly that $f_a = f_2$ causes strong fluctuation in variances, especially in VAR[M(L)]. Note that variances in the case of $f_a = f_1$ are slightly higher than those $f_a = f_2$ for the moment at midspan, and vice versa for the moment at interior support.

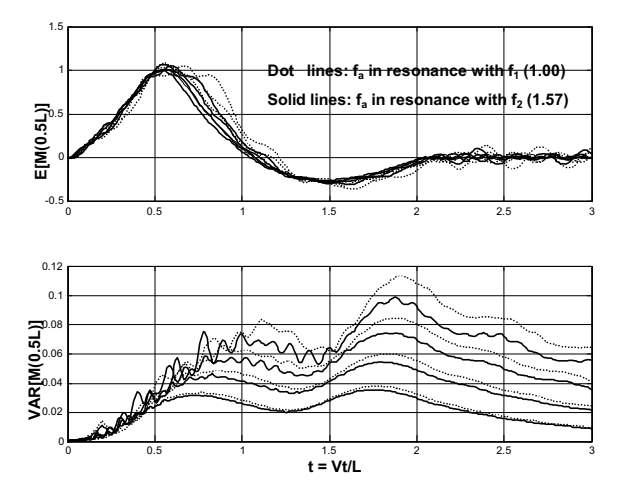


Figure 3 shows time history of expected values and variances of moment at midspan for $f_a = 1$ and 1.57

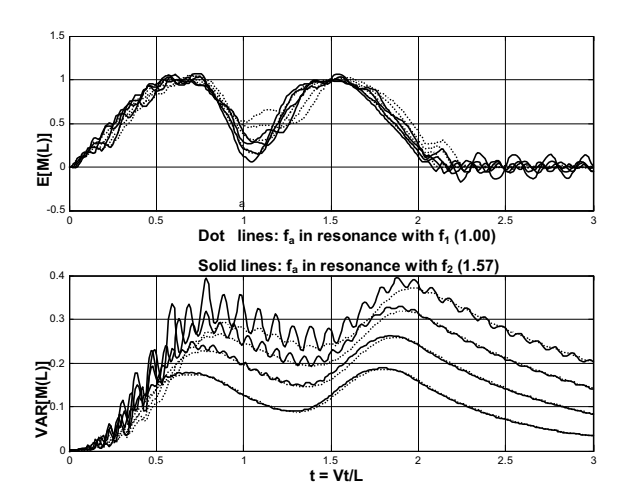


Figure 4 shows time history of expected values and variances of moment at interior support for $f_a = 1$ and

Figure 5 shows the mean values and variances of midspan acceleration. The maximum midspan acceleration in this velocity range is 0.1g which is the level that people on the bridge can feel uncomfortable. Moreover, the variances are quite high, 0.02 to 0.045.

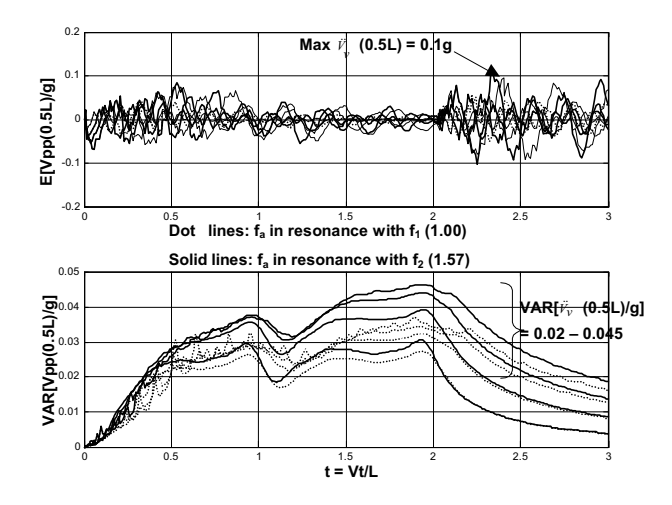


Figure 5 shows time history of expected values and variances of beam acceleration at midspan for $f_a = 1$ and

At high speed $(f_v = 0.06 \text{ to } 0.12)$

For $f_{\nu}=0.06$ to 0.12 (V=190 to 380 km/h for beam span 20 m and frequency 7 Hz). At this high velocity level vehicle is assumed to be rail vehicle system. Thus, the roughness model for the rail system is used here. The combinations of f_{ν} and ℓ/L that cause resonance are shown in Table 2. If $\ell/L=0.5$ and $f_{\nu}=0.08$ the axle arrival rate equals the fundamental frequency. For typical values of ω_1 and L, $f_{\nu}=0.08$ corresponds to a velocity of 70 m/s (250 km/h). If $\ell/L=0.5$ and $f_{\nu}=0.12$, the axle arrival rate equals the second natural frequency. Therefore it is possible for the axle arrival rate to be in resonance with the first and second beam frequencies, for feasible vehicle speeds. Let ℓ/L be fixed at 0.5 and the span passage rate, f_{ν} , be 0.08 (\approx 250 km/h). Figures 6

and 7 show that the displacement and the moment at midspan have the largest amplification. The maximum expected values of dynamic amplifications are 1.32 and 1.22 respectively (recall that multiples of standard deviations of amplification factors must be added to determine design amplification factors). It is simply because the first mode is excited, f_a matches f_1 , and the displacement and moment at midspan are two responses dominated by this fundamental asymmetric mode. When the span passage rate increases to 0.12 (\approx 380 km/h), the moment at the interior support is amplified by as much as 1.32 (Fig. 8) which is more than the other responses. In this case the second mode, the symmetric mode, is excited. A response dominated by this symmetric second mode is the moment at the interior support. For $\ell/L =$ 0.6 and 0.7, only the first mode is excited (Figs. 6 and 7) for realistic velocities (less than 380 km/h). If ℓ/L is greater than 0.5 the axle arrival rate is unlikely to be in resonance with the second mode since the velocity corresponding to that resonance mode is well above a practical level. If ℓ/L is greater than 1, f_a will never match f_1 and resonance due to f_a never occurs. The shear (Fig. 9) is different from the other responses as all of the modes (both asymmetric and symmetric modes) participate in this response.

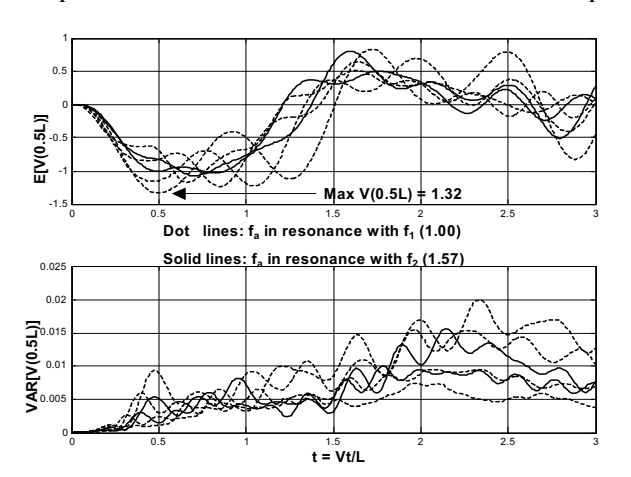


Figure 6 shows time history of expected values and variances of displacement at midspan for $f_a = 1$ and 1.57

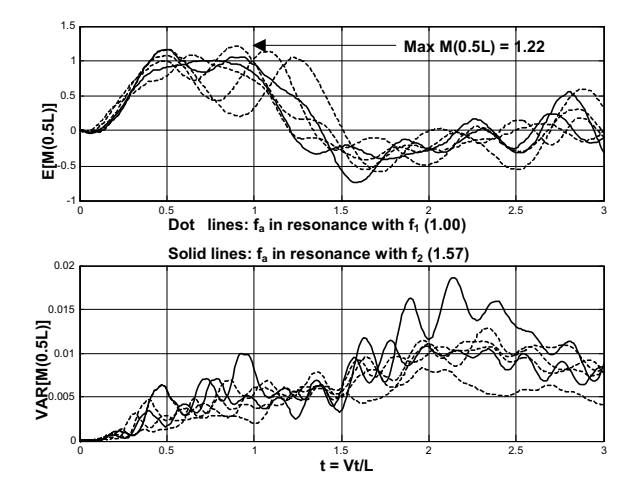


Figure 7 shows time history of expected values and variances of moment at midspan for $f_a = 1$ and 1.57

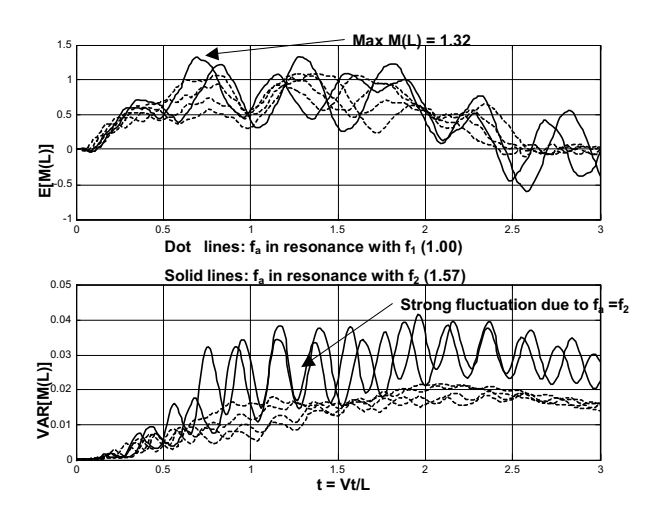


Figure 8 shows time history of expected values and variances of moment at interior support for $f_a = 1$ and

1.57

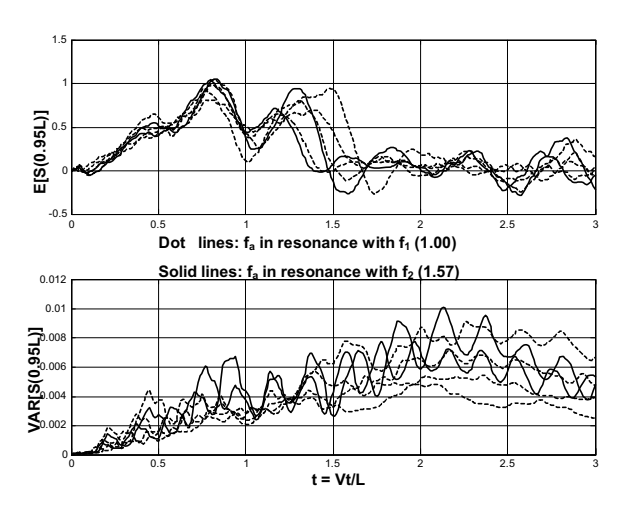


Figure 9 shows time history of expected values and variances of shear at 0.95L for $f_a = 1$ and 1.57

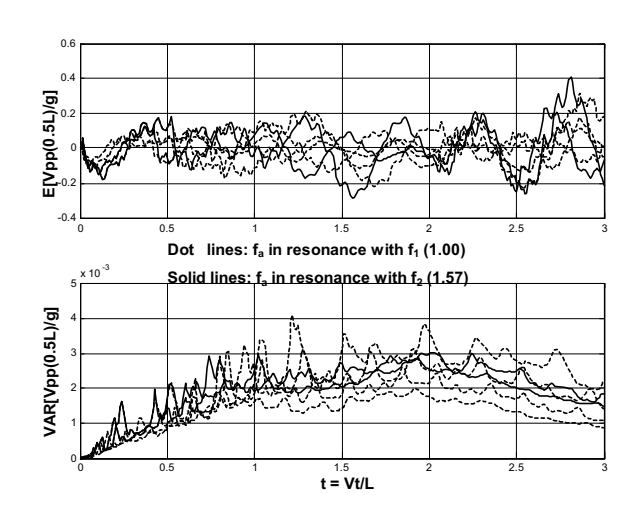


Figure 10 shows time history of expected values and variances of beam acceleration at midspan for $f_a = 1$ and 1.57

STR - 55

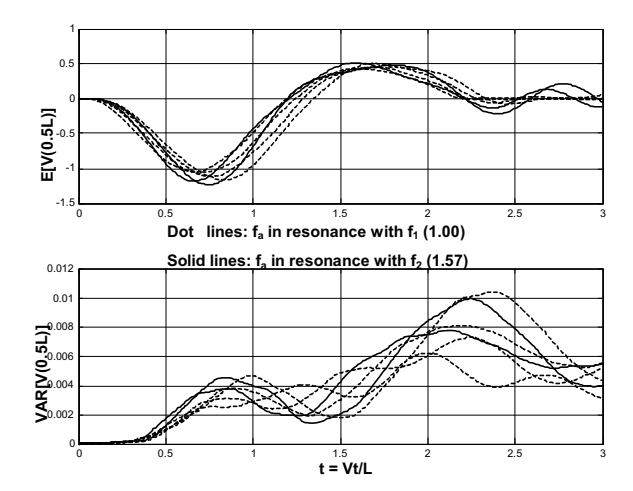


Figure 11 shows time history of expected values and variances of displacement at midspan for $f_a = 1$ and 1.57

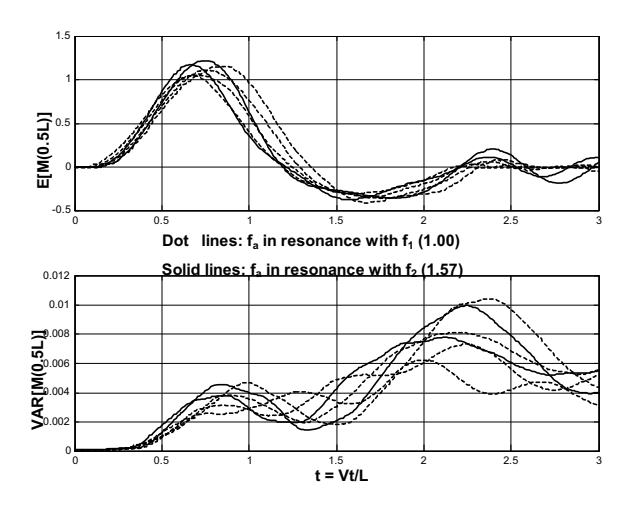


Figure 12 shows time history of expected values and variances of moment at midspan for $f_a = 1$ and 1.57

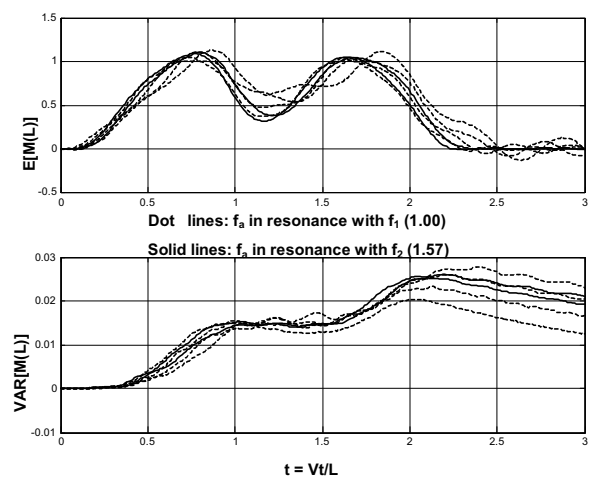


Figure 13 shows time history of expected values and variances of moment at interior support for $f_a = 1$ and

Figure 10 shows time history of expected value and variance of beam acceleration at midspan. It is found that the maximum expected beam acceleration is 0.4g (quite high) and occurs after vehicles left the span.

For a high-speed ground transportation system there is a possibility to have resonance between the axle arrival rate and the second mode frequency. For this condition the moment at the middle support needs to be examined closely

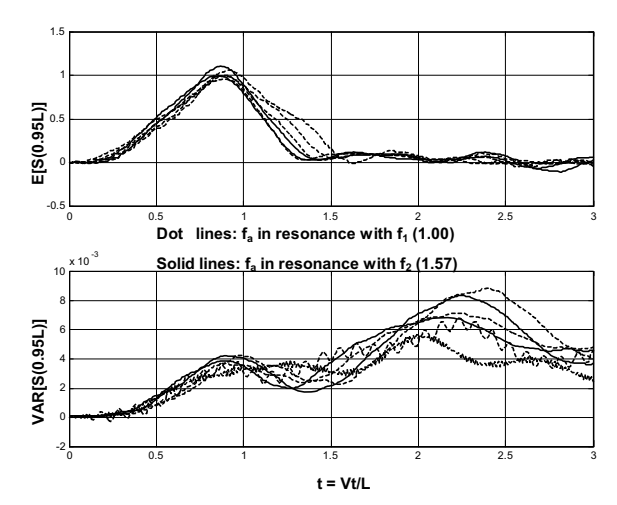


Figure 14 shows time history of expected values and variances of shear at 0.95L for $f_a = 1$ and 1.57

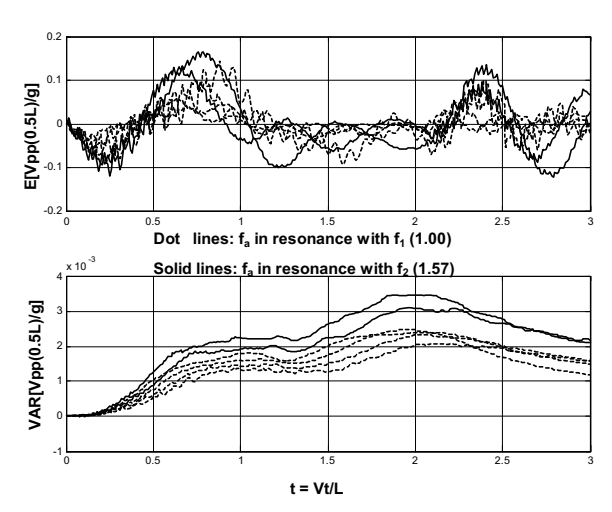


Figure 15 shows time history of expected values and variances of beam acceleration at midspan for $f_a = 1$ and

Effect of number of axles (interfaces)

For high speed vehicle, i.e. maglev, the suspension system can have more than two contact points. More contact points can benefit the design of the system. Figures 11 to 14 (also Table 3 and 4) show the expected beam responses reduce, i.e. E[M(L)] reduces from 1.32 to 1.10, when eight suspensions are used. This suspension arrangement can also reduce strong fluctuation in VAR[M(L)] dramatically (Figs. 8 and 13). Figure 15 shows the expected beam acceleration at midspan reduces from 0.4g in Fig. 10 to 0.16g.

Table 3 shows the maximum beam responses when f_a is in resonance with f_1 for two different suspension

configurations

	Verifigations.							
Y = Structural	Two contact		Eight contact					
	points		points					
Responses	E[Y]	VAR[Y]	E[Y]	VAR[Y]				
v(0.5L)	1.32	0.0200	1.20	0.0105				
M(0.5L)	1.22	0.0125	1.15	0.0105				
M(L)	1.10	0.2100	1.10	0.0280				
S(0.95L)	1.00	0.0090	1.10	0.0090				
$\ddot{v}(0.5L)/g$	0.30	0.0040	0.14	0.0025				

Table 4 shows the maximum beam responses when f_a is in resonance with f_2 for two different suspension configurations

Y = Structural	Two contact		Eight contact	
	points		points	
Responses	E[Y]	VAR[Y]	E[Y]	VAR[Y]
v(0.5L)	1.05	0.015	1.25	0.0100
M(0.5L)	1.20	0.019	1.20	0.0100
M(L)	1.32	0.041	1.10	0.0260
S(0.95L)	1.05	0.010	1.10	0.0085
$\ddot{v}(0.5L)/g$	0.40	0.003	0.16	0.0035

Effect of fundamental frequencies of vehicle - Natural frequencies of the car body (normally low) may not be equal to the first mode frequency of a typical short-span bridge unless the primary and secondary springs are very stiff. It is not realistic to have such a stiff suspension [7], since passenger comfort criteria may not be met. For a structure with low frequency such as a large suspension bridge, there is a chance of a structure frequency matching a vehicle frequency. However, the mass of the vehicle is very small compared to the mass of a suspension bridge, so significant dynamic amplification is not likely.

4. Conclusion

Random vibration time history analyses provide vehicle and structure responses that can define appropriate surface smoothness requirements and design amplification factors for structure for high speed vehicles. Mean value and covariance matrix of system responses can be determined.

It is found that one specific value of a nondimensional parameter may cause a maximum in one response while a different value may cause a maximum in another response. For two-span beam, the moment at the interior support can have high dynamic amplification factors when axle arrival rate matches to the second natural frequency of the beam.

For high speed rail system, an appropriate suspension configuration of vehicle can reduce the expected value and variance of DAF of beam responses.

Acknowledgements

This research was supported by the Office of Higher Education Commission and the Thai Research Fund (TRF) under Grant No. MRG4680169. This support is gratefully acknowledged.

Reference

[1]Au, F.T.K., Wang, J.J. and Cheung, Y.K., Impact study of cable-stayed bridge under railway traffic using various models. J. of Sound and Vibration, 240(2001): pp277-283.

[2]Fryba, L., 1972. Vibration of solid and structures under moving loads. Groningen: Noordhoff International Publishing.

[3] Gasparini, D.A., Petrou, M. and Ozer, M.E. Wavelength content of Concrete floors. ACI Structural Journal, 1990: pp706-715.

[4]Marchesiello, S., Fasana, A., Garibaldi, L. and Piombo, B.A.D., Dynamics of multi span continuous straight bridges subjected to mdof moving vehicle excitation. J. of Sound and Vibration, 224(1999): pp541-561

[5] Seetapan, P., 2002. Dynamics of high speed traversing structures with random surfaces. Ph.D. Thesis, Case Western Reserve University.

[6] Seetapan, P. and Gasparini, D.A., 2002. Dynamic of bridge for very high speed vehicle. EuroDyn2002, Munich, Germany.

[7]Tamboli, J.A., and Joshi, S.G., Optimum design of a passive suspension system of a vehicle subjected to actual random road excitations. J. of Sound and Vibration, 219(1999): pp193-205.

[8]Xia, H., Xu, Y.L. and Chan, T.H.T., Dynamic interaction of long suspension bridge with running trains. J. of Sound and Vibration, 237(2001): pp263-280.